AN EXPERIMENTAL AND ANALYTICAL INVESTIGATION OF FLOOR VIBRATIONS

By

Steven R. Alvis

Thesis submitted to the faculty of the
Virginia Polytechnic Institute and State University
For the partial fulfillment of the degree of

MASTER OF SCIENCE

in

Civil Engineering

APPROVED:

THOMAS M. MURRAY, CHAIRMAN

Raymond H. Plaut | **Mehdi Setareh**

APRIL 2001

BLACKSBURG, VA

Keywords: Structural Engineering, Floor Vibrations, Civil Engineering

AN EXPERIMENTAL AND ANALYTICAL INVESTIGATION OF FLOOR VIBRATIONS

by
Steven R. Alvis
Thomas M. Murray, Chairman
Civil Engineering

(ABSTRACT)

Several areas of research regarding floor vibrations were studied during the process of this research. A basic literature review of previous work in the field of floor vibrations is presented along with a summary of the study.

The first area of study involved a comparison of finite element models with field tests for a suspended floor system. The suspended floor system underwent several retrofits to determine which retrofit reduced annoying vibrations the most. Comparisons were also made to see how well a finite element model could be used to predict the effectiveness of the retrofits. The attempt to make accurate finite element models was successful.

The second area of study involved an experimental modal analysis (EMA). The experimental mode shape was compared with that from the finite element model (FEM). The research done in this area of study also involved measuring damping for a suspended floor system. The floor system was also subjected to a known input force and the response of the system was compared to the theoretical response based on the finite element model and the hand calculations prescribed by AISC Design Guide 11—Floor Vibrations Due to Human Activity (Murray et al., 1997). The findings helped provide useful information for the third area of study.

The third area of this study focused on finding a method for performing a quick and inexpensive field test on a floor system to determine its acceptability. No good method found.

The fourth area of this study was to find a way to accurately model complex floor systems with finite element modeling programs. Previous research yielded good results in

the area of frequency prediction. However, the main focus of this study was to find a way to accurately predict peak acceleration of a complex floor system. This portion of research did not find a way to model complex floor systems in a finite element program for producing accurate peak accelerations. However, the source of error between the finite element program and the hand calculations was accurately defined.

ACKNOWLEDGEMENTS

I'd like to thank my committee members for their support and advice. Dr. Murray has been a great source of help in my process of learning, research, writing, and especially editing. The staff at Virginia Tech has been great to work with and learn from as well. I would also like to recognize the great lab technicians Brett, Dennis, and Ricky. They have helped me a lot in setting up my tests and helping me with things that I could not even do by myself with an unlimited amount of time. I would also like to thank Joe Howard for helping me with my experimental modal analysis testing and for briefing me on the theory behind the test.

I also thank Nucor Research and Development who sponsored this research.

I also thank all of my fellow classmates here at VT and the many friends whom I met during my stay here. They have been a great blessing as well. I also thank my undergraduate professor, Dr. Leftwich, from West Virginia Tech. Without his excellent instruction I wouldn't have made it to graduate school. He also talked me into taking a mechanical vibrations class in my undergraduate level, which helped me get a good start in this enjoyable field of research.

Special thanks goes to my parents and sister for being there and keeping in touch and being home when I visit. Also to dad especially who helped with a lot of other things.

Finally and most of all, I would like to thank the Lord Jesus Christ for finding and saving me while I was at VT. I am not the same person as I was when I came to Tech because of Him. He is the One who has provided the most support. Also I thank my brothers and sisters in Christ. God bless you all.

TABLE OF CONTENTS

LIST OF FIGURES

LIST OF TABLES

CHAPTER I
FLOOR VIBRATIONS:
INTRODUCTION AND LITERATURE REVIEW

1.1 INTRODUCTION

Throughout the history of structural engineering, many advances have increased efficiency of design and construction. Such increases in technology ranging from new materials, design codes, and construction techniques have allowed the completion of great monumental structures. Although these advancements may allow completion of lightweight systems with higher strength than their ancestral predecessors, serviceability problems can still arise in these more efficient products. A common serviceability issue that arises is the problem of floor vibrations.

Floor vibrations are a serviceability issue that can occur in a system that is perfectly sound from a strength standpoint. This issue is primarily caused by the combined use of lightweight concrete and high-strength materials that are used to fabricate flexible, long-span floor systems. In extreme cases, issues of floor vibrations can render a facility totally unusable by the occupants based solely on levels of personal comfort. Accurate prediction is not an easy goal because of the human-based factor. Everyone has a different tolerance level based on his or her own idea of personal comfort.

If a system is found to be a "problem-system," it can be rather expensive to correct. If a situation arises with only one or two individuals on the floor, relocation of the affected people closer to a structural support can solve the problem easily. However, if a number of occupants are annoyed because of a neglected design consideration, a more expensive solution will be required. It is much easier and less expensive to design the floor against such vibrations. If the appropriate design actions are taken, the building owner can save considerable expense.

Current methods of vibration prediction in floor systems range from hand calculations of a simplified model to complex finite element models. The variety of techniques usually yield different results due to the different simplifying assumptions in each method and because of the general complex nature of the floor vibrations. This study looks into several aspects of floor vibration to achieve a greater understanding of the phenomenon in general. This chapter presents the scope of study, related terminology, background information and history, current research, and the need for research, followed by a summary of the following chapters.

1.2 SCOPE OF RESEARCH

The general goal of this research is to gain a better understanding of vibration phenomena in order to apply it to a better prediction than what exists for real systems. This study includes four main areas of research. The first area involves comparisons between test data and finite element models of simple systems. Secondly, comparisons are made between dynamic loading tests on a one-bay system and finite element model results. This second area of research is an attempt to excite a real system with the specified excitation in the American Institute of Steel Construction Design Guide 11--Floor Vibrations Due to Human Activity (1997). These test results are compared with results from a finite element model using the corresponding dynamic load. The third area of study attempts to find a good field test that will yield immediate results on the quality of a floor without requiring expensive testing equipment. Test data taken from several floors around the United States are analyzed, compared, evaluated, and ranked. The fourth and final area of this study is to accurately predict the peak acceleration for complex framing. This portion of the study is purely analytical and involves the use of finite element models with the Design Guide excitation force. The following section defines relevant terminology for this area of study.

1.3 TERMINOLOGY

Several definitions of the terminology critical to this study are contained within this section.

Wave – a disturbance traveling through a medium by which energy is transferred from one particle of the medium to another without causing any permanent displacement of the medium itself. In this case the energy input is due to a dynamic force.

Dynamic Force – a force that changes with respect to time (not static).

Vibration – Oscillation of a system in alternately opposite directions from its position of equilibrium, when that equilibrium position has been disturbed. Two types are free vibration and forced vibration. Forced vibration takes place when a dynamic force disturbs equilibrium in the system. Free vibration takes place after the dynamic force becomes static (or zero).

Amplitude – The offset of equilibrium of the system at a given time. Also known as the magnitude of the wave when plotting displacement, velocity, or acceleration against time. (see Figure 1.1).

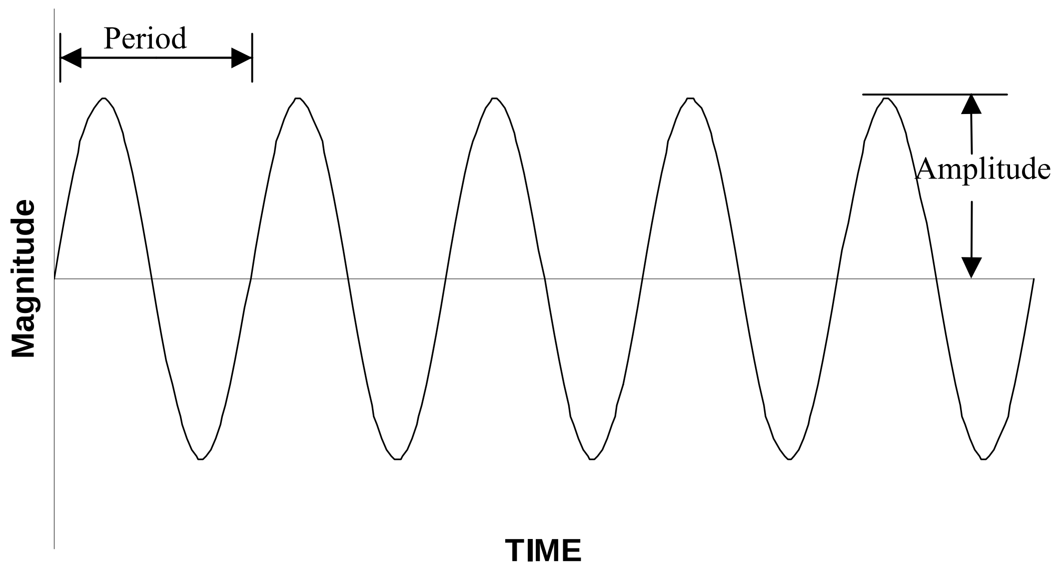

Figure 1.1 – Basic Sine Wave

Period – The amount of time it takes for one cycle (see Figure 1.1).

Cycle – A complete motion of a system starting at any given point of magnitude and direction that ends with the same magnitude and direction (i.e., the motion over a full period).

Frequency – number of cycles over a given time, usually cycles per second (also called Hz).

Natural Frequency – A frequency at which the system will vibrate freely when excited by a sudden force.

Fundamental Natural Frequency – the lowest natural frequency for the system at which a system will vibrate.

Resonance – a condition where a system is excited at one of its natural frequencies.

Damping – a property of energy dissipation within the system. More damping results in a quicker decay of amplitude in free vibration. When less damping is present, the system retains its energy for a longer amount of time.

Viscous Damping – the form of damping that is proportional to velocity. This is the easiest type of damping to model mathematically.

Fast Fourier Transform (FFT)- An algorithm for computing the Fourier transform of a set of discrete data values. The FFT expresses the data in terms of its component frequencies.

FFT Spectrum – The relative contribution of frequencies in a trace of amplitude over a time range. This is obtained by performing an FFT of the data.

Mode shapes – The shape of a system showing relative displacements when undergoing vibration.

Node – The point location on a mode shape that undergoes zero relative displacement.

Anti-node – The point location on a mode shape that undergoes maximum relative deflection.

Node-line – The line on a mode shape that undergoes zero deflection. Node-lines occur on surfaces.

1.4 LITERATURE REVIEW

The first known stiffness criterion for floors was proposed by Treadgold (1828). He indicated that timber beams should be made deeper to reduce the vibration caused by people moving on the floors of houses. Most of the recent design criteria can be found in the *AISC Steel Design Guide Series 11—Floor Vibrations Due to Human Activity* (Murray et al. 1997). Design criteria are based on levels of human comfort; levels of comfort can depend on both the environment and the individual.

Reiher and Meister (1931) did a study to determine exactly what combinations of frequency and amplitude affect humans. Subjects of the research were placed on shaking tables and subjected to steady state motion. The frequencies varied from 5 to 70 Hz and the amplitude ranged from 0.001 to 0.04 in. Classifications of "slightly perceptible", "distinctly perceptible", "strongly perceptible", "disturbing", and "very disturbing" were used to describe the vibration conditions. Lenzen (1966) proposed that the amplitudes of the Reiher-Meister scale be lowered by a factor of ten to account for the transient nature of floor vibrations. The Lenzen modified Reiher-Meister scale is shown in Figure 1.2.

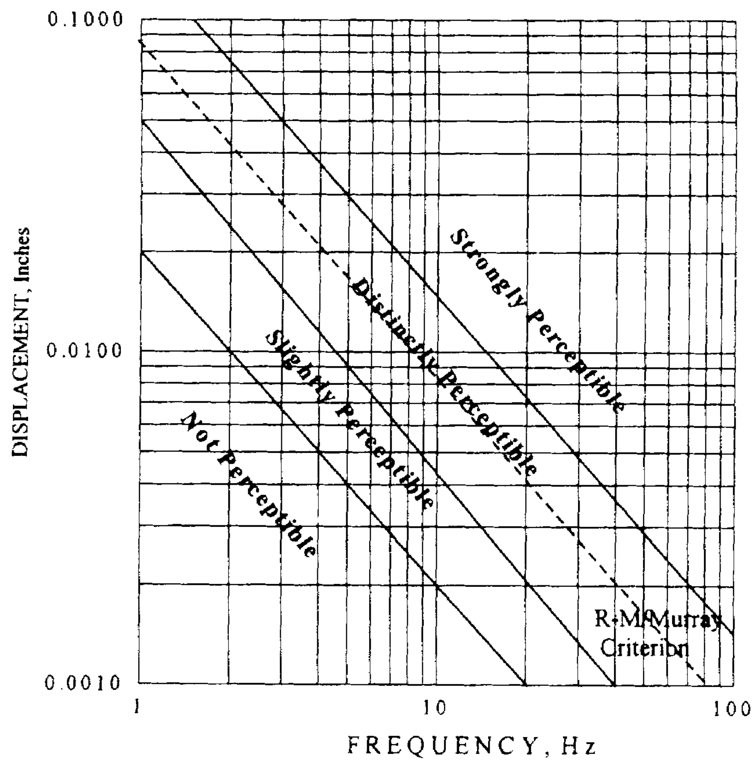

Figure 1.2 - Modified Reiher-Meister Scale (Band 1996)

In 1975, Murray suggested "steel beam, concrete slab systems, with relatively open areas free of partitions and damping between 4 and 10 percent, which plot above the upper one-half of the distinctly perceptible range, will result in complaints from the occupants". Figure 1.2 shows this acceptability criterion and is called the Reiher-Meister/Murray criterion. Everything below the dotted line in the figure is considered acceptable by the criterion.

In 1981, Murray established an acceptability criterion based on the required damping of a floor system. The required damping is a function of the amplitude of a system due to a heel-drop impact and its natural frequency. Ninety-one systems with varying properties were statistically analyzed for Murray (1981) to determine the amount of damping required for an acceptable system as described in Equation 1.1:

$$D > 35 A_o f + 2.5 \qquad \textbf{(1.1)}$$

where D = percent of critical damping, A_o = initial amplitude from a heel-drop impact, in., and f = first natural frequency of the floor system, Hz. This equation is valid for systems with natural frequencies less than 10Hz and spans less than 40ft.

Figure 1.3 is a set of recommended acceleration tolerances for humans (Murray et al. 1997). It can be seen in this figure how different environments have different acceptance levels for vibrations.

According to Murray (1991), common values for first natural frequency range between 5 and 8 Hz. Comfort studies for automobiles and aircraft have found that, in this range, humans are especially sensitive to the vibration. Murray (1991) explains that this is due to many of the major organs in the human body resonating at these frequencies. It is for this reason that the lowest tolerance level is within this frequency range (the flat portion of the curve).

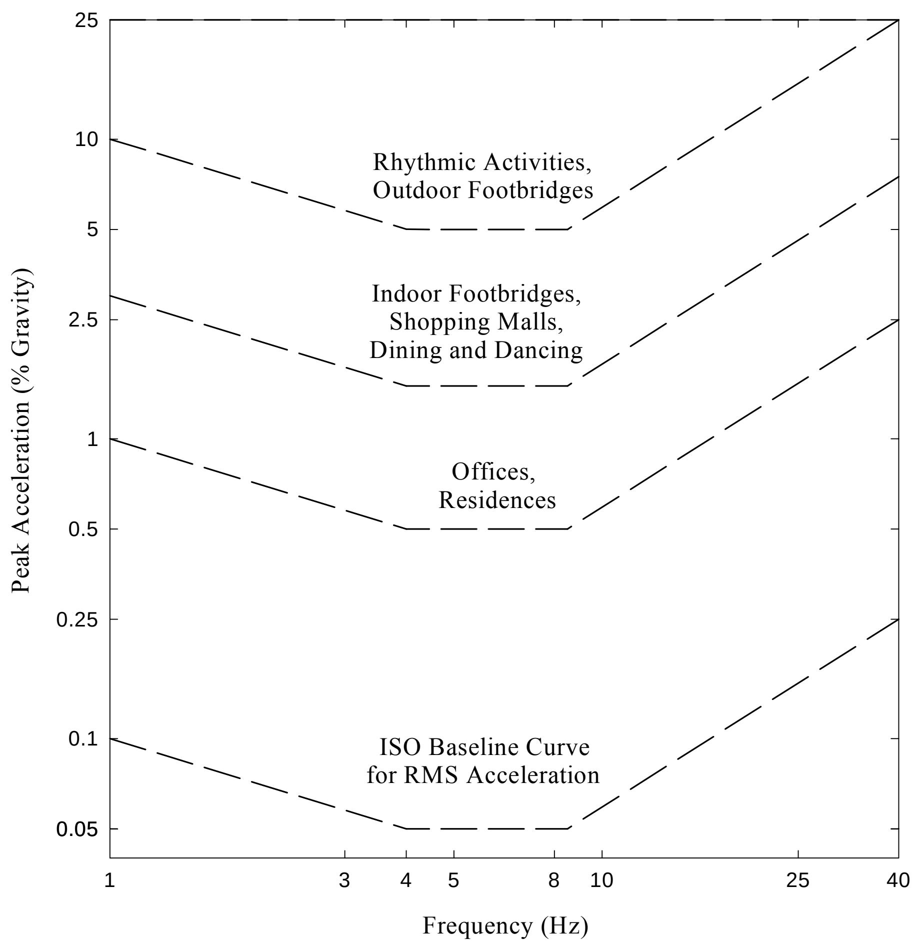

Figure 1.3 – Recommended Peak Accelerations (Allen and Murray 1993)

The primary method for determining the fundamental natural frequency of a floor system is by hand calculations. Hand calculation methods are found in the AISC Steel Design Guide Series 11 provisions. Experimental testing and finite element modeling are two other methods for determining the fundamental natural frequency and frequencies for higher modes.

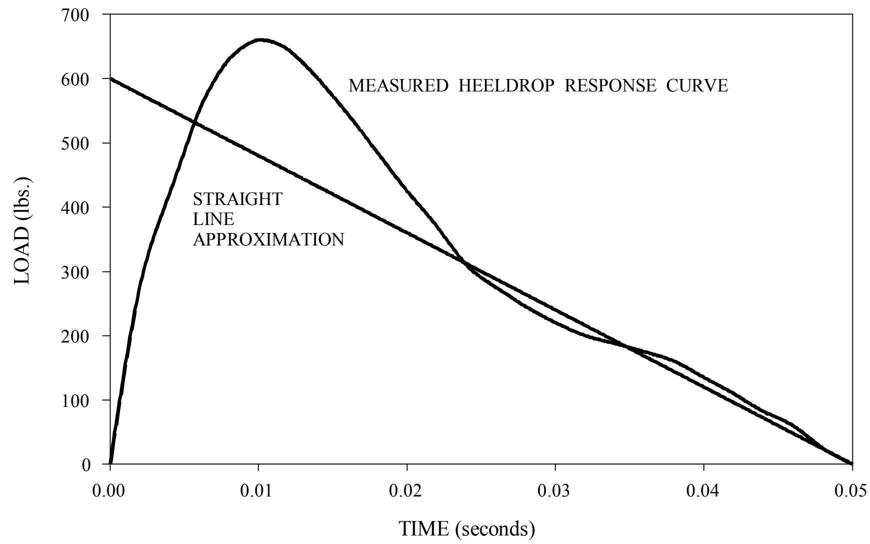

Figure 1.4 – Heel-Drop Impact and Approximation

Experimental testing is done using an accelerometer and a data collector. The accelerometer is placed in an area of interest and the floor system is subjected to a dynamic load. The standard heel drop function is applied to a system by having a 170-lb person rocking up on the balls of his feet with his heels about 2.5 in. off the floor, and then relaxing and allowing his heels to impact the floor (Murray 1981). One such loading is a heel-drop test as measured by Ohmart (1968). He also came up with a reasonably accurate approximation for the impact as described in Figure 1.4. Other methods of loading the system include walking in various directions or doing a bounce test. A bounce test is where a person will try to bounce at a multiple of the natural frequency of the floor system in an attempt to excite the system at its natural frequency. For all tests,

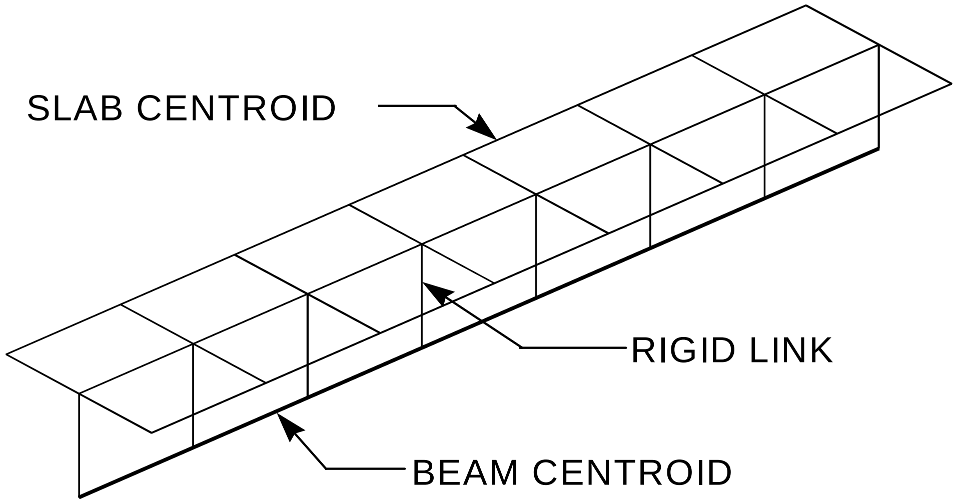

Figure 1.5 – Slab and Beam FEM (Beavers 1998)

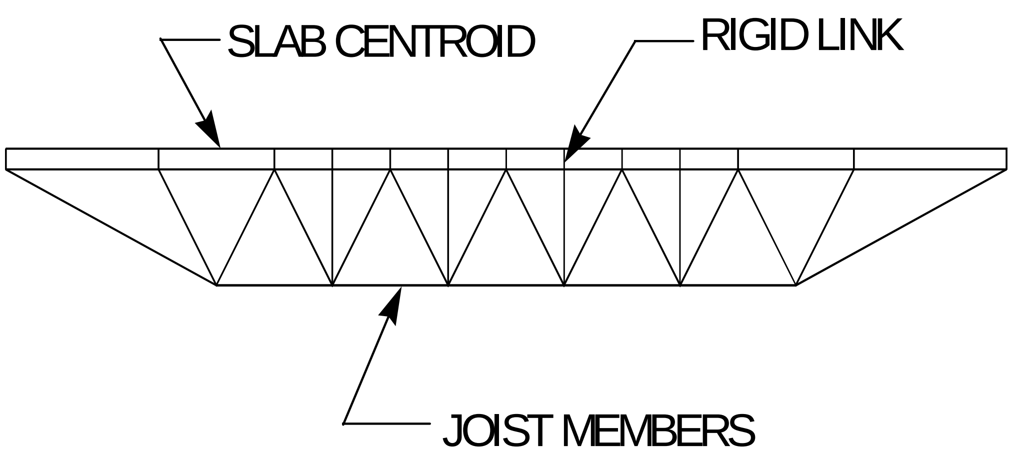

Figure 1.6 – Full Joist Model (Beavers 1998)

the dynamic response is measured with the accelerometer and a Fast Fourier Transform then is used to determine the frequency spectrum.

Finite element modeling of floor systems requires several considerations. Figures 1.5 and 1.6 show finite element modeling techniques for steel and concrete composite floor systems (Beavers 1998). Beavers also determined that, in terms of accuracy and simplicity, the most efficient way to model a joist girder system is to use at least eight plate elements for each section of a beam. The work of Gibbings (1993) showed that eccentricities should be included when modeling joists. The actual eccentricities were not as important as long as there was eccentricity included in the finite element model (Gibbings 1993). Gibbings also stated that about 2-in. of eccentricity provides accurate stiffness for joists.

Some of the most recent research which used complex finite element models was performed by Sladki (1999). This research concluded that the finite element methods gave a better prediction for the lowest natural frequency of floor systems than the Design Guide criteria. However, for peak acceleration the analytical methods did not compare well with the actual test results (Sladki 1999).

Once a floor system has been built and it is found to have poor serviceability due to excessive vibrations, there are several solutions. Tuned Mass Dampers (TMD) may be used to reduce vibrations. Research in this area was performed by Rottmann (1996). She concluded that TMDs could successfully control floor vibrations if there is initially a low relative damping in the system. She further states that, although it is possible, there are difficulties in using TMDs to control multiple modes of vibration with closely spaced frequencies and high damping. Rottmann also noted that the true effectiveness of TMDs is dependent on the perceptivity of occupants of the structure.

Another solution to overcome annoying floor vibrations is through active control. Active control uses an actively controlled mass to dampen vibration (Hanagan 1994). Hanagan stated that the method is very effective, and it also provides much less disruption in the building function than most other methods of repair. High initial and maintenance costs are regarded as serious disadvantages to using this system, according to Hanagan.

1.6 NEED FOR RESEARCH

Different evaluation techniques usually yield different results. The resulting differences can be due to the different simplifying assumptions in each method and because of the general complex nature of the floor vibrations. It is under such considerations that several aspects of floor vibrations and the correlating modeling assumptions should be studied under greater detail. With greater accuracy of prediction, fewer problems are likely to arise in completed structures.

The major difficulty for prediction is determining peak acceleration of a floor system. To predict an accurate peak acceleration, less complex floor systems than those that were tested in the past were analyzed. A simpler system such as a footbridge or single-bay system has fewer variables to look at when compared to a complex, multi-bay system. Thus, there is a higher probability of accurately predicting the peak acceleration.

Chapter II looks at two simple systems. The first system is a cantilever staircase. A finite element model was made to predict the lowest natural frequency and peak acceleration of this system. The predictions were compared with actual test data of a heel drop. The second system is one of several Virginia Tech test floors. This one-bay floor system underwent various tests. Different excitations were applied to this system. Several retrofits were incorporated into the floor to change the vibration characteristics of the structure. Finite element models were also created to compare the results of the various tests.

Chapter III contains a discussion of the same laboratory floor subjected to a known dynamic forcing function. The finite element method, AISC Guide criteria, and the actual test data are compared. The test data provided information that allowed the measured system damping, mode shapes, and accelerations to be compared with the finite element method predictions.

Chapter IV discusses floor vibration data results from several buildings and the various configurations of the Virginia Tech lab floor. Comparisons were made to determine if a quick and accurate method of field analysis with only a handheld data collector and analyzer is possible.

Chapter V looks at the use of the finite element method for the prediction of peak acceleration for complex framing. The approach in this area of study starts with comparison of the AISC criteria with the results of the finite element model for a very simple system. The system complexity was then increased, and an attempt to pinpoint the source of discrepancies was made. Several techniques were utilized for finding the key differences between the AISC criteria predictions and those of the finite element model.

Chapter VI presents the conclusions of this study. Also contained in this chapter are recommendations for future research. Following this last chapter is an Appendix containing supporting data and drawings.

CHAPTER II
COMPARING FINITE ELEMENT MODELS TO TEST DATA

2.1 INTRODUCTION

From the review of previous research, it is evident that attempts to predict complex vibration characteristics have not been entirely successful. SAP2000-Nonlinear finite element model results were compared to test data obtained in simple, controlled environments. The first simple model is that of a cantilever staircase. The second model is the Virginia Tech lab floor with multiple geometric alterations or retrofits. These models are much more simple than those from previous research and allow a greater probability for the measurement data sets to match the theoretical values because of fewer system variables.

2.2 CANTILEVER STAIRCASE

This system is a cantilever staircase located in Doylestown, Pennsylvania. The member sizes and geometry were obtained from a set of plans courtesy of Marshall Erdman and Associates, Inc. Simplified details of the staircase are found in Appendix A. A heel drop was performed on the end of the staircase and the resulting accelerations were recorded using a handheld FFT analyzer. A simulated heel drop was applied in a finite element model and the results were compared with the measured staircase response. A visual comparison between the actual measured trace and that predicted from the finite element model can be seen in Figures 2.1 and 2.2, respectively. The magnitude of the simulated trace was scaled for ease of visual comparison with the actual trace. This is valid because the actual input force for the measured trace can only be assumed. Three percent modal damping was assumed for the finite element model. The simulated heel drop trace has less ambient noise present, which is characterized by a smoother wave due to fewer contributing frequencies in the theoretical model.

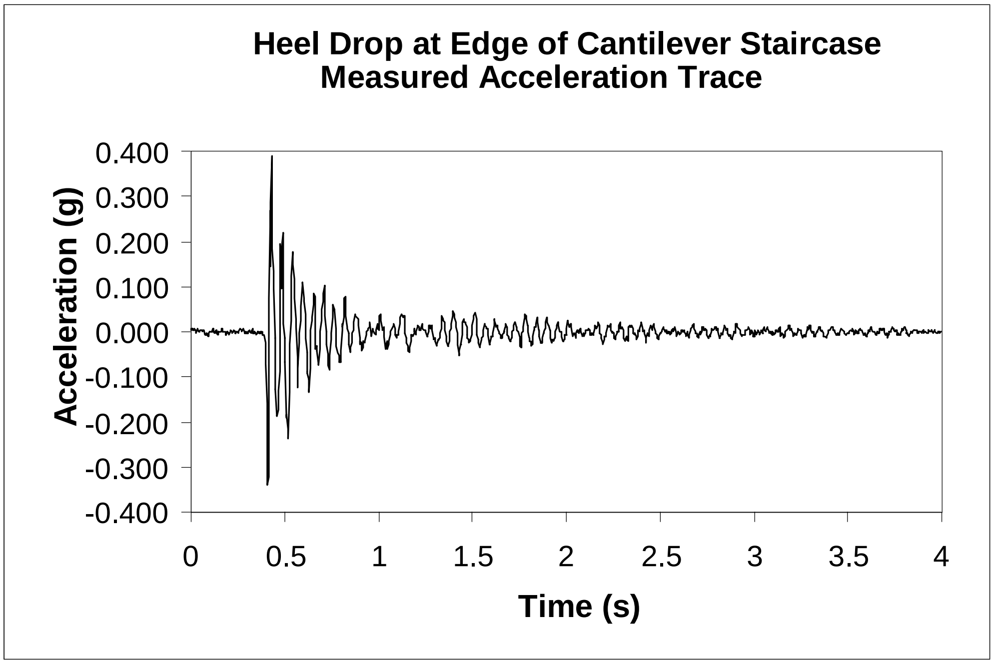

Figure 2.1 – Measured Heel Drop Acceleration Trace

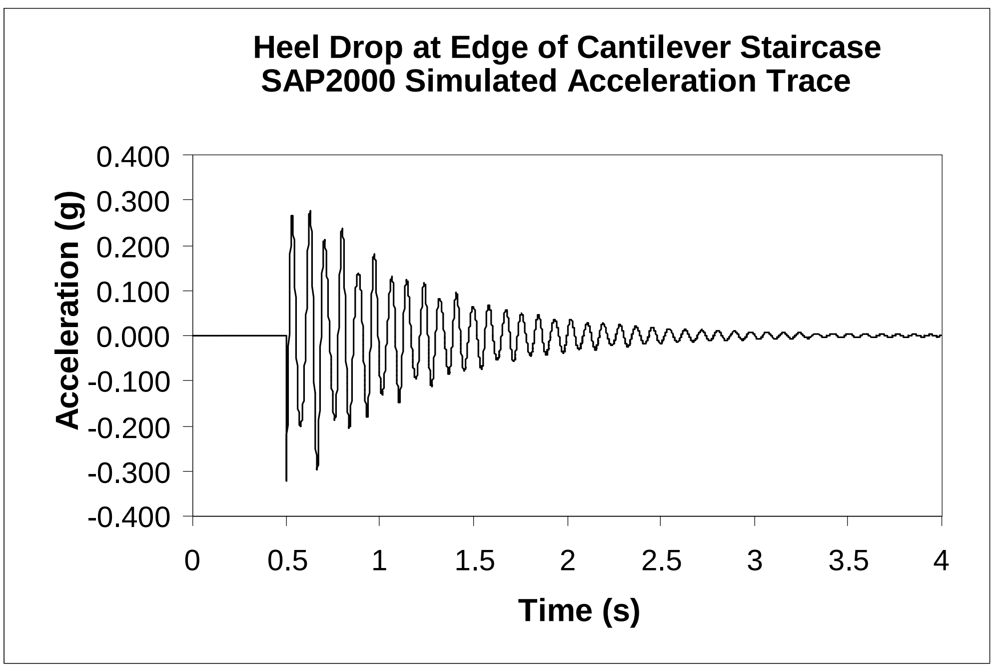

Figure 2.2 – Simulated Heel Drop Acceleration Trace (SAP 2000)

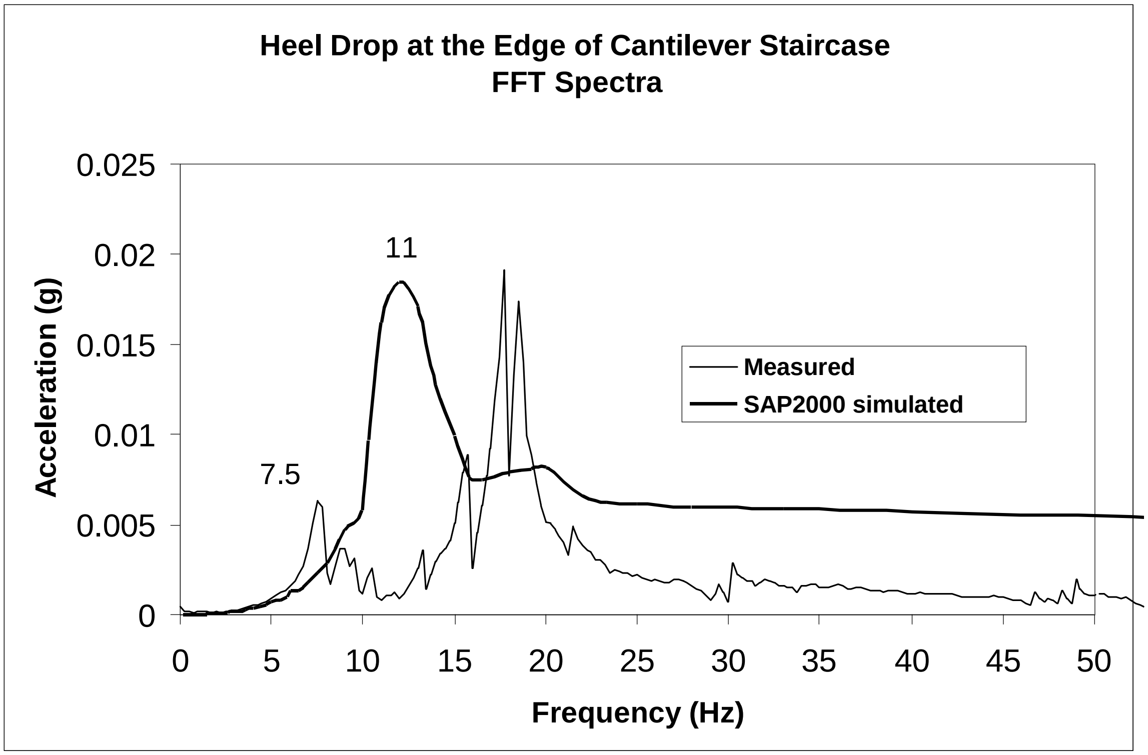

Figure 2.3 – FFT Spectra of Acceleration Traces

Figure 2.3 shows direct comparison between the finite element simulation and the measured heel drop. The curve for the finite element simulation was scaled to obtain a good graphic comparison. This is a legitimate procedure for two reasons: (1) the input force was not measured for the actual heel drop, and (2) the primary interest is in the relative participation of each frequency. Figure 2.3 shows a very crude resemblance between the simulated curve and the measured curve. Although both have two primary peaks, the fundamental frequencies are different. The measured fundamental natural frequency is 7.5 Hz, and the simulated fundamental natural frequency is 11.0 Hz. The comparison also reveals that the simulated model has less noise. This can be identified by the smoothness of the curve. Noise spikes are obviously present in the measured data. Possible sources for these spikes can be from environmental noise, loose connections, extraneous materials, or a number of other occurrences that are not taken into consideration by the finite element model.

2.3 VIRGINIA TECH LAB FLOOR

2.3.1 Test information

The Virginia Tech Lab floor is a suspended floor system supported on four columns with a concrete deck. The supporting members are 36LH450/300 joists, 36LH500/300 joists, and 36G10N11.0K joist girders as shown in Figure 2.4. The section properties of the joists and joist girders are shown in Figures 2.5 to 2.7. This laboratory floor had a dual purpose: (1) to function as a roof for an addition to the Virginia Tech Structures Lab and (2) to function as a "problem floor" that would be annoying to would-be occupants of an office building. Hand calculations (using Design Guide criteria) predicted the "problem floor" to have a natural frequency of 5.88 Hz and a peak acceleration of 2.37% g with 1% critical damping. (See Appendix B for these calculations.) Several retrofits were attempted in order to evaluate possible fixes for existing floors.

Nine configurations of the floor were tested. One configuration was the original, unmodified condition. Retrofit modifications were made for the other eight configurations. Table 2.1 lists the test configuration number and the corresponding test condition. Figure 2.8 illustrates all of the retrofit locations described in the table. Several types of excitation were performed on each configuration. Recordings were then made for each type of excitation: ambient, heel drop, walking perpendicular to joists, walking parallel to joists, and bouncing. A rating of human comfort level was chosen as well. The floors are ranked from 1 to 9 on acceptability (1 being the best). The frequency results are described in the following sections, while the human comfort ranking is discussed in Table 2.1.

The AISC Guideline procedures are only applicable for the unmodified floor and were used accordingly. SAP 2000 finite element models were made to compare with the data taken from the accelerometer. The only valid comparison that could be made with one reading location (in the center of the floor) was to examine the mode shapes and the corresponding frequencies. The frequencies that corresponded to a mode shape with vertical motion at the center of the floor were the only ones that are predicted to cause annoying vibration on the center of the floor.

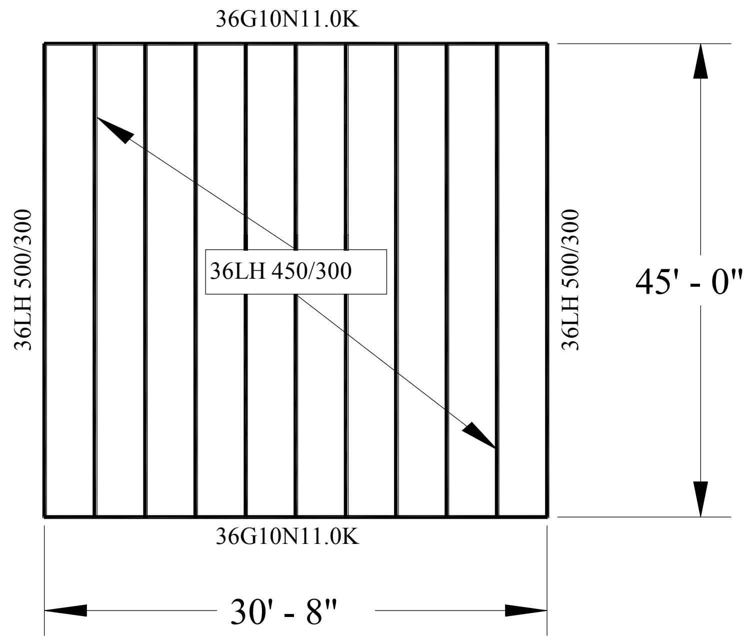

Figure 2.4 – Plan of Virginia Tech Lab Floor

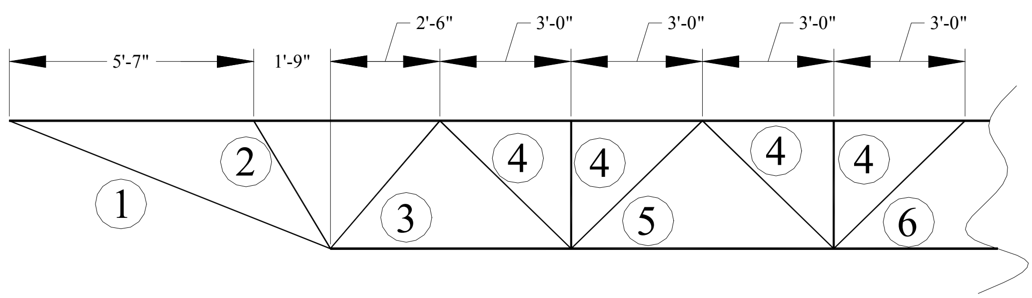

d = 36”

Overhang = 6”

Top Chord = 2*L*3X3X0.236

Bottom Chord = 2*L*2.5X2.5X0.22

Web 1 = 2*L*1.5X1.5X0.15

Web 2 = 1*L*1.5X1.5X0.129

Web 3 = 2*L*1.5X1.5X0.129

Web 4 = 1*L*1.25X1.25X0.118

Web 5 = 1*L*1.75X1.75X0.15

Web 6 = 1*L*1.5X1.5X0.15

C_r = 0.8627

I_{chords} = 1412 in^4

Figure 2.5 – 36LH450/300 Joist Details

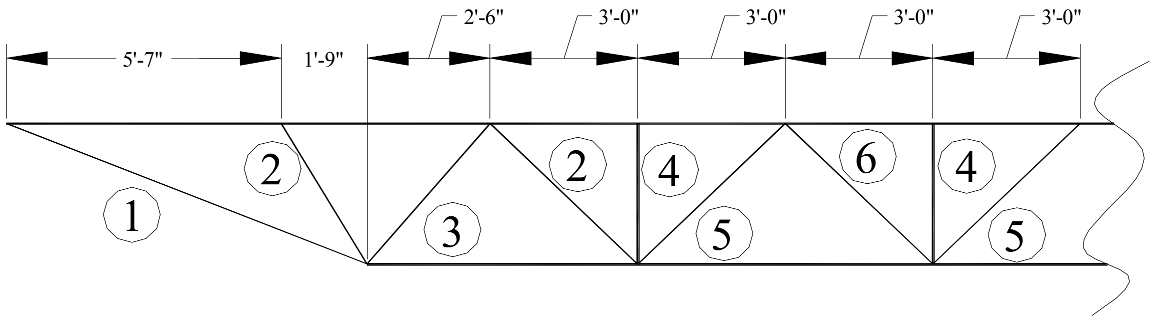

d = 36”	Web 3 = 2*L*1.5X1.5X0.15
Overhang = 6”	Web 4 = 1*L*1.25X1.25X0.13
Top Chord = 2*L*3X3X0.33	Web 5 = 1*L*1.75X1.75X0.15
Bottom Chord = 2*L*3X3X0.227	Web 6 = 1*L*1.25X1.25X0.117
Web 1 = 2*L*1.75X1.75X0.15	C_r = 0.8627
Web 2 = 1*L*1.5X1.5X0.127	I_{chords} = 1550 in^4

Figure 2.6 – 36LH500/300 Joist Details (End Joist)

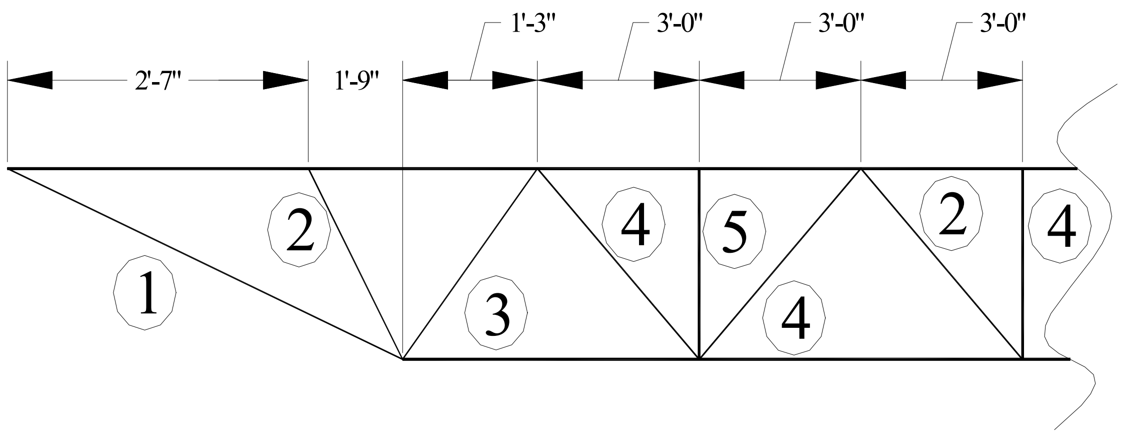

d = 36”	Web 2 = 2*L*1.5X1.5X0.15
Overhang = 6”	Web 3 = 2*L*2.5X2.5X0.25
Seat = 5”	Web 4 = 2*L*2X2X0.176
Top Chord = 2*L*4X4X0.375	Web 5 = 1*L*2X2X0.176
Bottom Chord = 2*L*4X4X0.375	C_r = 0.7550
Web 1 = 2*L*4X4X0.44	I_{chords} = 3270 in^4

Figure 2.7 – 36G10N11.0K Joist-Girder Details

Table 2.1 – Test Configuration Summary

Test Configuration Number **(TCN)**	**Test Conditions (See Figure 2.5 for Locations)**	**Comfort Ranking**
1	Unmodified	9
2	2 Posts at Location x-2 with bearing pads	2
3	2 Posts at location x-2 with expansion joint material	3
4	Diagonal posts at location x-1	6
5	Posts w/spreader beam at location B (inside of third point)	1
6	Posts w/spreader beam at location A (outside of third point)	7
7	Posts w/spreader beam at location C (diagonal third points)	5
8	Beam at bottom chords of joists along centerline ⊥ to joists	8
9	Damping posts at location x-2	4

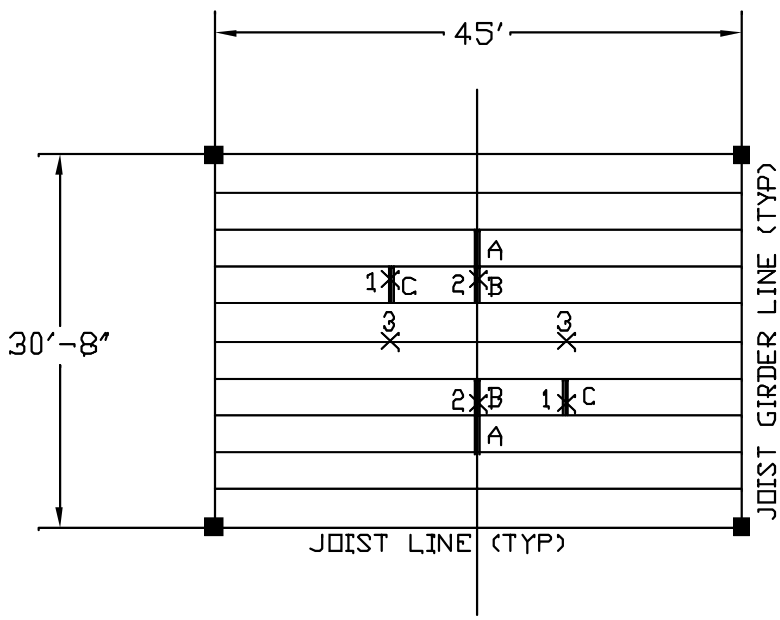

Figure 2.8 – Post and Beam Locations

2.3.2 Test Configuration 1

Test Configuration 1 of the Virginia Tech lab floor was the original floor. Table 2.2 shows a summary of the first three frequencies that contribute to annoying vibration in the center of the lab floor. These frequencies are taken from the peaks of the FRF plots located in Appendix C. All frequencies that were multiples of the excitation frequency were ignored unless it was also a natural frequency of the system. For example, if the walking excitation was 2.25 Hz, the frequencies of 2.25 Hz, 5.50 Hz, 7.75 Hz, etc. were ignored. However, if one of these multiples happened to match an expected natural frequency, it was recorded in the table. Thus, the modal frequencies that do not affect the center of the floor are not looked at for the comparison. This comparison is only to test the effectiveness of the values predicted by the finite element model. The readings with ambient and heel-drop excitation were analyzed first to find the frequencies. These gave expected natural frequencies to look for in the other excitations.

Table 2.2 – TCN 1 Data Summary

Excitation	f1 (Hz)	f2 (Hz)	f3 (Hz)
SAP 2000 Modal Analysis	5.86	9.02	19.56
Ambient	6.00	9.75	19.25
Heel Drop	5.75	9.50	19.00
Walking Parallel	6.00	9.50	19.25
Walking Perpendicular	6.25	9.50	19.00
Bouncing @ 3.75Hz	6.00	9.75	19.25

The AISC Guideline procedure for calculating the fundamental natural frequency of this floor yields a frequency of 5.88 Hz. This compares quite well with the 5.86 Hz value obtained from the SAP2000 finite element analysis. The AISC Guideline criterion does not provide any methods for obtaining higher natural frequencies.

It is obvious that the test data correlated rather well with the predicted values provided by the finite element analysis. It should be noted that an extra mode with a frequency of 15.36 Hz was predicted by SAP2000. This prediction is based on the activity at the center of the floor for the mode shape. However, this modal frequency did not appear in any of the measured test data. There is no known explanation for this extra modal frequency.

2.3.3 Test Configuration 2

Test Configuration 2 incorporates two posts supporting the floor to add stiffness. The posts are at the third points along the centerline that runs perpendicular to the joists as seen in Figure 2.9. Elastomeric bearing pads measuring 6in.x6in.x7/8in. were inserted between the floor and the post to ensure good contact and to possibly add damping. After the bearing pads were in place, a screw mechanism on top of the post was adjusted to apply a compressive force. Figures 2.10 to 2.12 show pictures of the posts. The posts were modeled in SAP2000 as rigid supports restraining motion in the vertical direction. Table 2.3 compares frequencies that contribute to annoying vibration in the center of the floor.

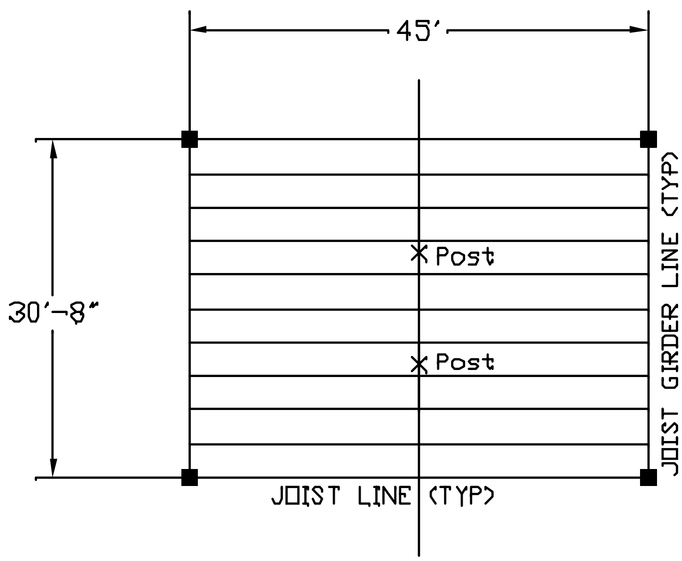

Figure 2.9 – TCN 2 Post locations

Figure 2.10 – View of Retrofit Posts at a Distance.

Figure 2.11 – Close-up of Intermediate Post Connection

Figure 2.12 – Typical Base of Retrofit Post

There is no method to accurately predict these frequencies by hand calculations because of the retrofit. However, it is evident that the SAP 2000 finite element model analysis predicted these three major contributing frequencies quite well. It is noted that the finite element model produced slightly higher frequencies. This is due to using a vertically rigid support for the retrofit posts. If a stiff spring element were used instead, it would have produced a softer model. This would yield slightly lower frequencies. The 15 Hz frequency component only appeared in the ambient trace, while the same trace did not contain the f4 frequency. The f4 frequency prediction also is about 15% higher than the test data when compared to the other modal frequency components. Overall, it is evident that there was approximately a 33% increase in the fundamental natural frequency of the system by this simple retrofit.

Table 2.3 – TCN 2 Data Summary

Excitation	f1 (Hz)	f2 (Hz)	f3 (Hz)	f4 (Hz)
SAP 2000 Modal Analysis	8.91	10.77	15.80-16.20	22.27
Ambient	8.50	10.00	15.00	---
Heel Drop	8.00	10.00	---	19.25
Walking Parallel	8-8.5	10.00	---	19.25-19.5
Walking Perpendicular	8.50	10.50	---	19.50
Bouncing @ 4.25Hz	8.50	9.75	---	19.25

2.3.4 Test Configuration 3

The third test configuration is identical to TCN 2 except the elastomeric bearing pad was replaced with expansion joint material. The expansion joint material used was typical expansion joint material for concrete slabs. A nine-inch square with a ¼" thickness was used. Table 2.4 compares frequencies that contribute to annoying vibration in the center of the floor.

Table 2.4 – TCN 3 Data Summary

Excitation	f1 (Hz)	f2 (Hz)	f3 (Hz)
SAP 2000 Modal Analysis	8.91	10.77	22.27
Ambient	8.25	10.00	19.25
Heel Drop	8.00	10.00	19.50
Walking Parallel	7.75, 8.25	10.00	19.50
Walking Perpendicular	8.25	10.25	19.25
Bouncing @ 4.00Hz	8.00	10.00	19.25

The only notable change from TCN 2 is that the ambient trace contained a 19.25 Hz peak instead of the 15 Hz peak. The SAP 2000 analysis predicted three frequencies between 15.80 Hz and 16.20 Hz. The actual test data did not show these frequencies.

2.3.5 Test Configuration 4

For this experimental configuration, the same post setup as used for TCN 2 was used but at different locations. The posts were located at diagonal points from the center of the floor as shown in Figure 2.13. Table 2.5 shows a summary of the three frequencies that compares frequencies that contribute to annoying vibration in the center of the floor.

When comparing this test configuration to that of the unmodified state, it is quite evident that the posts definitely aided in effective frequency increase although not as much as the retrofit of TCN 2. Increased frequency is less annoying at the same peak acceleration than a lower frequency. The finite element model was a little stiffer than what the test data shows for the f1 frequency. The f2 frequency was quite accurate, as was the f3 frequency.

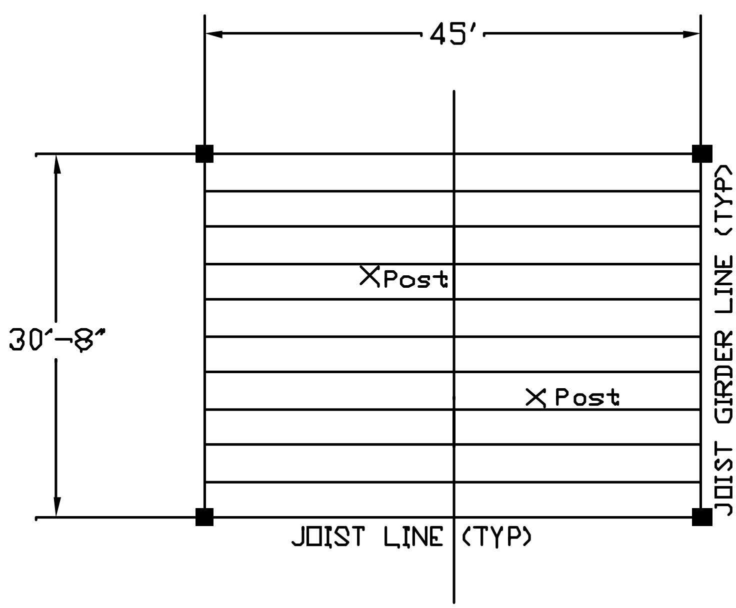

Figure 2.13 – TCN 4 Post Locations

Table 2.5 – TCN 4 Data Summary

Excitation	f1 (Hz)	f2 (Hz)	f3 (Hz)
SAP 2000 Modal Analysis	8.81	9.76	19.12 - 20.49
Ambient	8.00	10.00	19.25
Heel Drop	7.75	9.75	19.25
Walking Parallel	7.75	9.75	20.00
Walking Perpendicular	7.75	10.00	19.00, 20.00
Bouncing @ 4.25Hz	8.00	10.00	19.25

2.3.6 Test Configuration 5

This test configuration used a three-foot-long W6x20 beam centered on the top of two posts. This spreader beam spanned from the bottom of the top chord of one joist to the bottom of the top chord of the other joist. The posts were tightened with a screw mechanism to apply a compressive force. The beams for this fifth configuration are located as shown in Figure 2.14. Figure 2.15 shows a picture of how the spreader beam is supported by the post. Table 2.6 shows a comparison of the five frequencies that contribute to annoying vibration in the center of the floor.

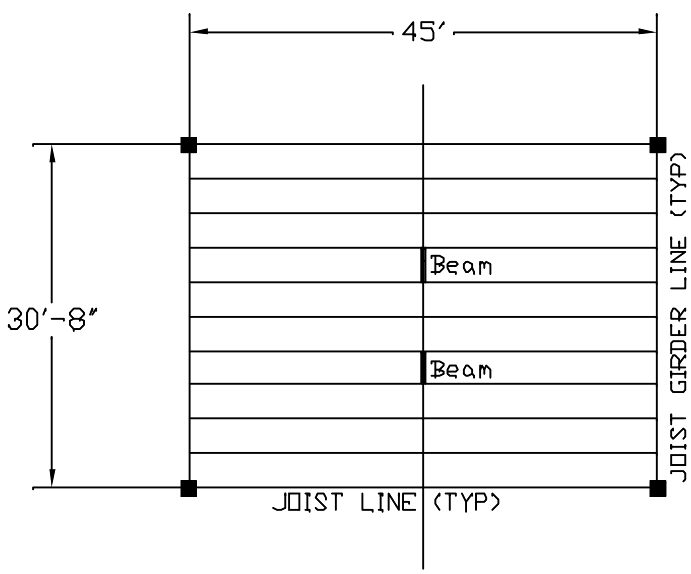

Figure 2.14 – TCN 5 Spreader-Beam Locations

Table 2.6 – TCN 5 Data Summary

Excitation	f1 (Hz)	f2 (Hz)	f3 (Hz)	f4 (Hz)	f5 (Hz)
SAP 2000 Modal Analysis	8.82	12.44	15.37	22.51	24.04
Ambient	8.25-8.75	10.25	12.75	19.50	20.25
Heel Drop	8.25	10.25	--	19.50	20.50
Walking Parallel	8.00	10.50	--	19.50	20.50
Walking Perpendicular	8.25	10.50	12.75	19.50	20.50
Bouncing @ 4.25Hz	8.25	10.50	--	19.50	--

Figure 2.15 – Typical Picture of Spreader Beam Supported by Post

Once again the SAP 2000 model predicts higher frequencies than recorded in the actual tests. This finite element model is even stiffer than the previous one when comparing the test data. The posts were modeled as rigid supports, which caused higher frequencies to be predicted in the analysis. However, both the finite element model and the test data agree that the frequencies were increased significantly compared to the unmodified arrangement (TCN 1). Because the frequencies were also a lot higher, they were more out of the range that usually annoys occupants. Out of all of the configurations, this produced the most comfortable floor by human perception.

2.3.7 Test Configuration 6

This testing configuration used a W6x20 spreader beam like TCN 5 except in this test, the beams were placed further out from the center of the bay as illustrated in Figure 2.16. Table 2.7 shows a summary of the first four frequencies that can contribute to annoying vibration in the center of the floor.

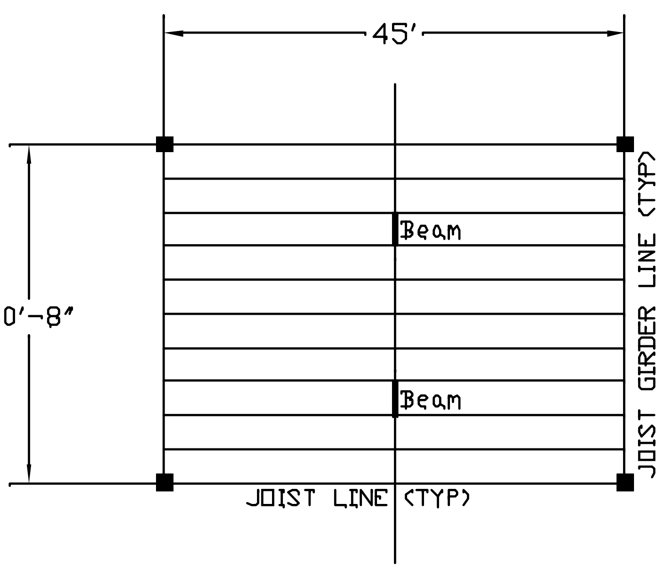

Figure 2.16 – TCN 6 Spreader-Beam Locations

Table 2.7 – TCN 6 Data Summary

Excitation	f1 (Hz)	f2 (Hz)	f3 (Hz)	f4 (Hz)
SAP 2000 Modal Analysis	8.28	10.21	17.66-18.26	23.65
Ambient	6.75	--	18.75-19.25	20.25
Heel Drop	6.75	10.25	19.00	20.25
Walking Parallel	7.00	--	19.00	20.75
Walking Perpendicular	6.75	--	18.50	20.25
Bouncing @ 6.75Hz	6.75	--	19.00	20.25

It is obvious that the measured frequencies did not change much from those of the original test setup found in TCN 1. This configuration is not recommended for effective stiffening of the floor. The beams are too far out from the center to effectively increase the frequency. However, the frequency is a little higher than the original as could be expected from basic intuitive reasoning.

The f1, f3, and f4 columns show that these three frequencies predicted by SAP 2000 appear in the recorded data. The f1 frequency is predicted to be about 23% higher than the actual floor frequency. The f4 frequency is predicted to be about 17% higher than the actual floor frequency. The f2 frequency peak only showed up in the heel drop excitation. The f3 frequency peak was predicted to be lower than what the test data showed. The only data not shown in the table was a notable frequency peak in the ambient trace of 7.75 Hz. This didn't show up anywhere else in the recorded data, nor was it predicted to occur. The accuracy of the assumption of rigid supports seems to decrease as the supports are placed further away from the antinodes of higher mode shapes.

2.3.8 Test Configuration 7

This test configuration was similar to TCN 5 and TNC 6 with the exception that the spreader beams were located diagonally from each other as shown in Figure 2.17. Table 2.8 shows a summary of the four primary frequencies that contributed to annoying vibration in the center of the lab floor.

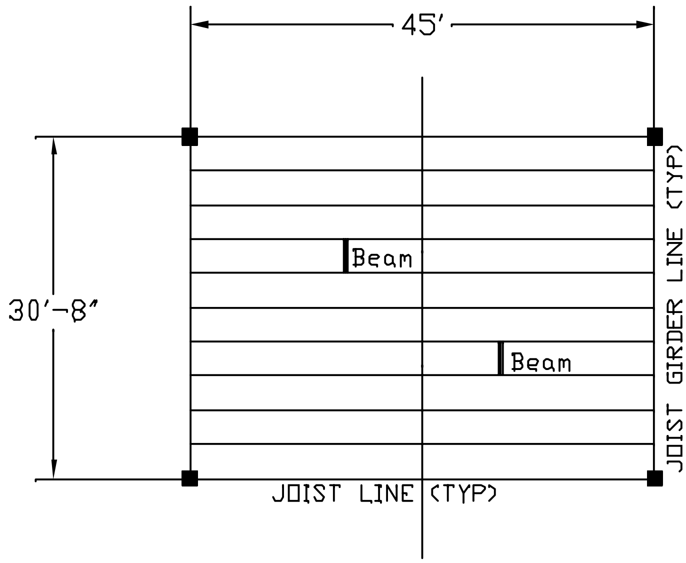

Figure 2.17 – TCN 7 Spreader-Beam Locations

Table 2.8 – TCN 7 Data Summary

Excitation	f1 (Hz)	f2 (Hz)	f3 (Hz)	f4 (Hz)
SAP 2000 Modal Analysis	8.77	11.29	19.06	20.74
Ambient	7.75	10.00	18.75	19.50
Heel Drop	7.75	10.00	19.25	19.75
Walking Parallel	8.00	10.75	19.25	19.75
Walking Perpendicular	8.00	10.00	18.50	19.75
Bouncing @ variable freq.	7.75	9.75-10.25	19.00	20.00

The table shows that the four peaks in the data analysis correlated quite well with the predicted values obtained from the finite element analysis. Once again, the finite element model was slightly stiffer than the actual test situation. This is from the assumption of the posts being perfectly rigid in the vertical direction. The finite element model did predict a natural frequency of 15.36 Hz to be present, but this frequency never appeared in the test data. This particular test configuration did effectively stiffen the floor to some degree, but paled in comparison with TCN 5 from a human perspective.

2.3.9 Test Configuration 8

This test configuration used a unique setup to attempt vibration reduction. A built-up steel beam was attached perpendicular to the bottom chord of all of the joists along the centerline of the floor. Figure 2.18 shows the location of the built-up member. The beam had the properties as described in Table 2.9. This configuration is suitable for a situation where posts or columns are not appropriate or permitted on the floor below.

Table 2.9 – Beam geometry

Depth	14 in.
Flange Width	6 in.
Web Thickness	3/16 in.
Flange Thickness	1/4 in.
Area	5.53 in.^{2}
Moment of Inertia	180.26 in.^{4}

Table 2.10 – TCN 8 Data Summary

Excitation	f1 (Hz)	f2 (Hz)	f3 (Hz)	f4 (Hz)
SAP 2000 Modal Analysis	6.03	10.17	16.71	19.56
Ambient	6.00	10.50	13.75	18.75
Heel Drop	6.00	10.75	18.75	21.75
Walking Parallel	6.00	10.25	18.50	21.75
Walking Perpendicular	6.00	10.50	18.50	21.25
Bouncing @ 2 Hz	6.00	10.75	18.75	21.75

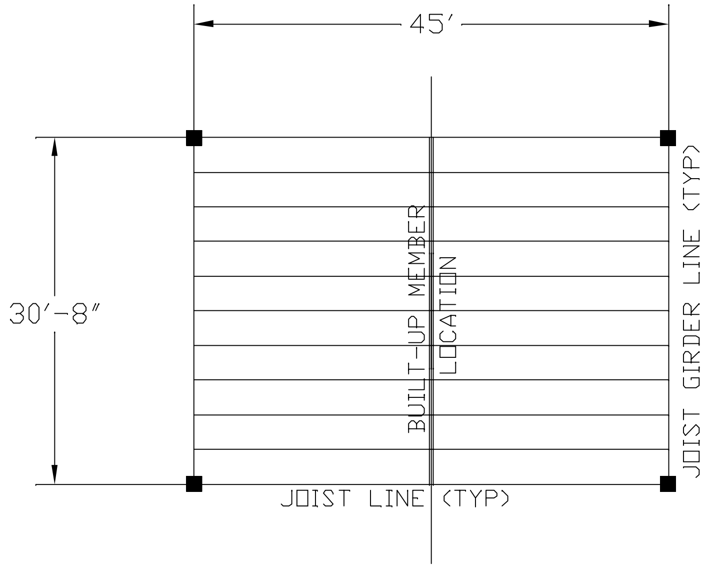

Figure 2.18 – TCN 8 Built-up Beam Location

The finite element model predictions compare rather well with the test data. The first mode frequency (represented by column f1) was predicted very accurately. The other contributing frequencies were higher than what was predicted by the finite element model. This was the only case where the model was less stiff than the actual floor. This method of fixing vibration problems was actually the least effective out of all the modified test configurations. From human perception, there was not any notable difference from the unmodified state when standing on top of the floor during excitation.

2.3.10 Test Configuration 9

This test configuration is similar to TCN 2. Although the post locations are the same, the difference between TCN 9 and TCN 2 is that damping elements were inserted between the posts and the floor. These damping elements were made with a set of 5 in.-long double-angles and a 3.5 in.-long tee-beam. Two pieces of elastomeric bearing pad were inserted vertically between the steel members. Figure 2.19 illustrates how the damper was assembled. A 5/8 in. diameter bolt was inserted through slotted holes in the assembly and tightened. The loose holes in the tee beam and damping elements ensured that shear force would only be transmitted through the bearing pads rather than the bolt. This is what causes the damping element to be effective. After the damping elements were in place, a screw mechanism was adjusted to apply a compressive force within the post. The SAP 2000 finite element model treated the posts as rigid supports restraining motion in the vertical plane. Table 2.11 shows a summary of the first three frequencies that contribute to annoying vibration in the center of the lab floor.

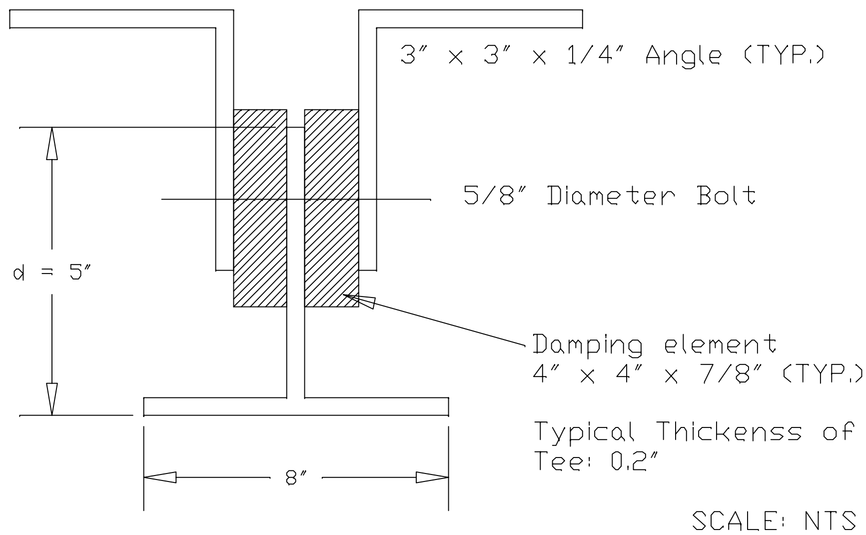

Figure 2.19 – Damping Element Cross Section

Table 2.11 – TCN 9 Data Summary

Excitation	f1 (Hz)	f2 (Hz)	f3 (Hz)
SAP 2000 Modal Analysis	8.91	10.77	22.27
Ambient	7.25	10.50	19.00
Heel Drop	7.25	10.25	19.25
Walking Parallel	7.25	10.75	19.50
Walking Perpendicular	7.25	10.25	19.25
Bouncing @ 3.75 Hz	7.25	10.25	19.25

The three peak contributing frequencies that appear in the test data are predicted by the finite element analysis. The frequency of f2 was accurately predicted. This model was stiffer than the actual test floor because of the assumption of rigid supports. For this reason, the frequencies of f1 and f3 were predicted to be significantly higher than measured. There were three predicted modal frequencies from 15.80-16.20 Hz that did not appear in any of the readings. The reason for this is not known.

This retrofit did moderately well in reducing the effects of annoying vibration. However, the damping posts acted as a softer spring element than the bearing pad or expansion joint material (TCN 2 and TCN 3, respectively). The test data verifies this with the lower frequencies obtained from the floor system.

2.4 COMMENTS AND CONCLUSIONS

The heel drop and ambient excitations provided the best FFT spectra for obtaining the natural frequencies. One difficulty present with the bouncing and both walking excitations was eliminating the peaks in the FFT spectrum caused by the input excitation. This was necessary to obtain an accurate comparison with the mode shapes provided by SAP 2000. It should be noted that the frequency of the paces in the walking excitation did show significant peaks in the FFT spectrum. The occupants of the floor system can feel these frequencies, and in some cases this can be an unpleasant experience. Although the finite element model can accurately predict natural frequencies that appear in the system, it should be noted that the data showed other significant peak frequencies caused by the type of excitation.

Walking excitation applied steps at frequencies of 1.75-2.50 Hz to the system along either centerline of the floor. There was a small spike in the FFT spectrum at the walking frequency. For every multiple of the walking frequency, there were sequentially greater spikes as these multiples approached the natural frequency of the floor system. Although the finite element modal analysis predicts the natural frequencies, it should be noted that all the disturbing frequencies are not always the exact natural frequencies of the system, but rather they are frequencies within a given range of that natural frequency.

Different locations on the floor will experience different annoying frequencies based on the relative displacement at each particular location on the mode shape. For example, the first natural frequency of TCN 1 is between 5.75 Hz and 6.00 Hz. The readings were taken on the anti-node of the system, which was in the center of the floor. This shows that the most annoying frequency in the center of the floor will be within this range. However, the second mode frequency predicted by the finite element model showed a node at the center of the floor. This would not be perceptible to occupants in the center of the floor nor would it appear in a single reading if the reading was taken in the center of the floor. Thus, this frequency could be more disturbing than the first natural frequency to people on the other portions of the floor where the anti-nodes for this second mode occur.

The SAP2000 model did predict accurate contributing frequencies in most models. It should be noted that to get all of the important frequencies of the floor, readings should be taken at different locations within the floor system. This comparison was sufficient for determining how well the finite element program compared with an actual floor system. For increased accuracy, a refinement could be made by modeling the support posts as stiff springs rather than rigid supports in the vertical direction. The four corner columns are accurately represented by rigid supports in the vertical direction due to their heavier size compared to the support posts.

The best retrofit was the retrofit in TCN 5 with the spreader beam located just inside of the third points of the bay. The frequencies were increased significantly from those of the original floor. This frequency increase allowed vibrations of similar amplitude to be less annoying because frequencies get less annoying the more they are above 8 Hz. Although good frequency increases were present with other retrofits, this case had a far better human comfort level. This retrofit with the spreader beam provided a larger contact area. The spreader beam supported the floor on the bottom of the top chord of the joists. This caused the load transfer to go from a larger area of the slab to the joists and then to the post. This could help reduce rotation of other modes, which would reduce their participation in vibration as well. The second best modification was TCN 2 where the posts were used without the spreader beams.

Although the results of TCN 2 and TCN 3 were very similar, the elastomeric bearing pad of TCN 2 did exhibit more durability of sustained compression than the expansion joint material. Therefore the expansion joint material is not really recommended due to its low elasticity. Over a sustained period of time and pressure, the expansion joint material would become less effective in maintaining constant contact between the steel plate on top of the post and the underside of the roof. Due to poor durability, TCN 3 was the only test configuration that utilized the expansion joint material.

CHAPTER III
MATCHING EXCITATIONS OF TEST FLOOR WITH DESIGN GUIDE

3.1 INTRODUCTION

The Virginia Tech lab floor in the unmodified condition was subjected to various tests to compare actual test data with the assumptions and predictions made by current modeling standards. In the first part of this series of tests, damping was measured and compared with the amount of damping typically assumed for such a system. Secondly, mode shapes were measured in the field and compared with those predicted by SAP2000. Thirdly, a sinusoidal excitation with the magnitude specified in the Design Guide criteria was applied to the lab floor setup. The peak acceleration was measured and compared with the predicted value from the Design Guide.

3.2 EXPERIMENTAL SETUP

The equipment used to test the Virginia Tech lab floor in its unmodified condition included the handheld FFT analyzer, accelerometer, HP analyzer, force plate, and a shaker device. The basic testing setup is shown in Figure 3.1 below in the case where the accelerometer data is read from the HP analyzer. This basic setup was used for all tests with minor adjustments for each one.

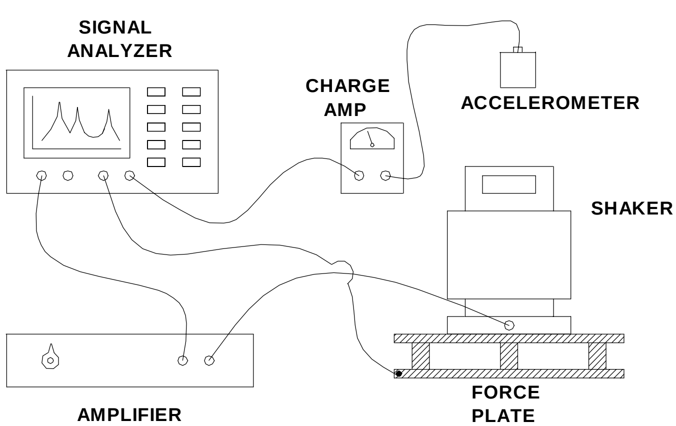

Figure 3.1 – Basic Testing Measurement Chain

The shaker device consists of a heavy mass that is driven by an electromagnetic force. The shaker accepts a signal generated from the HP analyzer after passing through an amplifier to produce any desired forcing function. The force plate is placed under the shaker to measure the force transferred by the shaker to the floor system. The HP signal analyzer can also be used to record data from the force plate output. This basic setup was used for the damping, mode shape, and acceleration experiments.

As previously stated, Figure 3.1 only illustrates the basic testing setup. Slight modifications to this basic setup were made for each test. For the experimental modal analysis the setup was modified by having the accelerometer and charge amplifier connected to a laptop computer with data recording software rather than the HP signal analyzer. In all other tests, the handheld FFT analyzer unit and accelerometer (without charge amplifier) were used to record data instead of the HP signal analyzer. The readings taken by the handheld FFT analyzer were acquired in a similar manner as in the previous tests discussed in Chapter II.

3.3 DAMPING COMPARISON

Design Guide 11 suggests that damping in a floor system is in the range of 1% to 3%. To determine the actual damping of the lab floor system, a series of readings was taken to generate a spectrum response curve. The lab floor was driven at varying sinusoidal frequencies with a constant amplitude. Peak accelerations were measured for each frequency. The spectrum response curve is the peak acceleration plotted with respect to the forcing frequency. Table 3.1 shows a list of driving frequencies and the corresponding value of the measured peak acceleration. Figure 3.2 gives the actual plot of the spectrum response curve.

Table 3.1 – Spectrum Response Data

Frequency (Hz)	Peak Acceleration (%g)		Frequency (Hz)	Peak Acceleration (%g)
2	0.134		6	4.16
2.5	0.268		6.25	2.3
3	0.268		6.5	1.5
3.5	0.317		6.75	0.979
4	0.548		7	0.758
4.5	0.608		7.25	0.576
4.75	0.754		7.5	0.356
5	0.859		8	0.271
5.25	1.28		8.5	0.616
5.5	2.15		9	0.143
5.75	7.75			

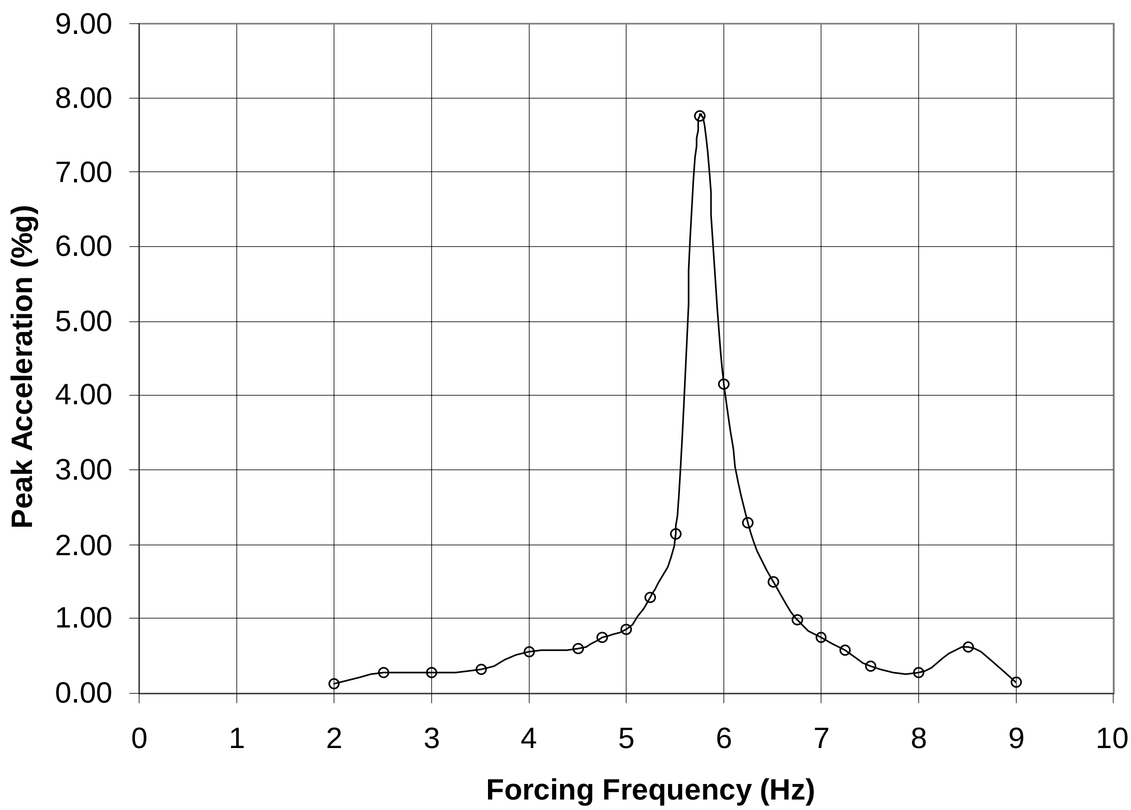

Figure 3.2– Spectrum Response Curve

The half-power bandwidth method and the spectrum response curve were used to calculate damping. The maximum peak acceleration was 7.75% g. This value was then multiplied by a factor of 0.707 which gives an acceleration value of 5.48% g. The two corresponding frequencies (f_1 and f_2) are read from the graph as 5.625 Hz and 5.925 Hz, respectively. Equation 3.1 is then used to calculate the damping, $\boldsymbol{\xi}$**:**

$$\xi = \frac{f_2 - f_1}{f_2 + f_1} \tag{3.1}$$

Using the values for f_1 and f_2, damping is 2.60% of critical. This is within the range of 1% to 3%, but it is rather high for a floor system consisting only of a concrete slab and supporting members. The only damping present was from testing equipment and a graduate research student. To increase damping accuracy without acquiring new sets of data, a new point was added from data already taken.

Adding a new data point on the spectrum response curve at the frequency of 5.88 Hz provided a more accurate curve. This 5.88 Hz data point was calculated by scaling the peak amplitudes from both curves in Figure 3.14 to match the force used in the original spectrum response curve. The two acceleration values obtained were averaged and added to the modified plot. The average calculated value of the peak acceleration for 5.88 Hz was 9.36% g. Using the half-power bandwidth calculation, a new damping of 2.04% was obtained. This is more reasonable than the 2.60% damping calculated from the original plot.

Increasing the resolution of the spectrum response curve cannot really help provide much more accuracy than that provided by addition of this calculated point. This is because the curve is already well defined by using the 5.88 Hz point. The advantage of the 5.88 Hz frequency reading is that the peak fundamental natural frequency is located at 5.88 Hz. No known solution past this modification will help increase the accuracy of this spectrum response curve. Figure 3.3 shows this modified spectrum response curve.

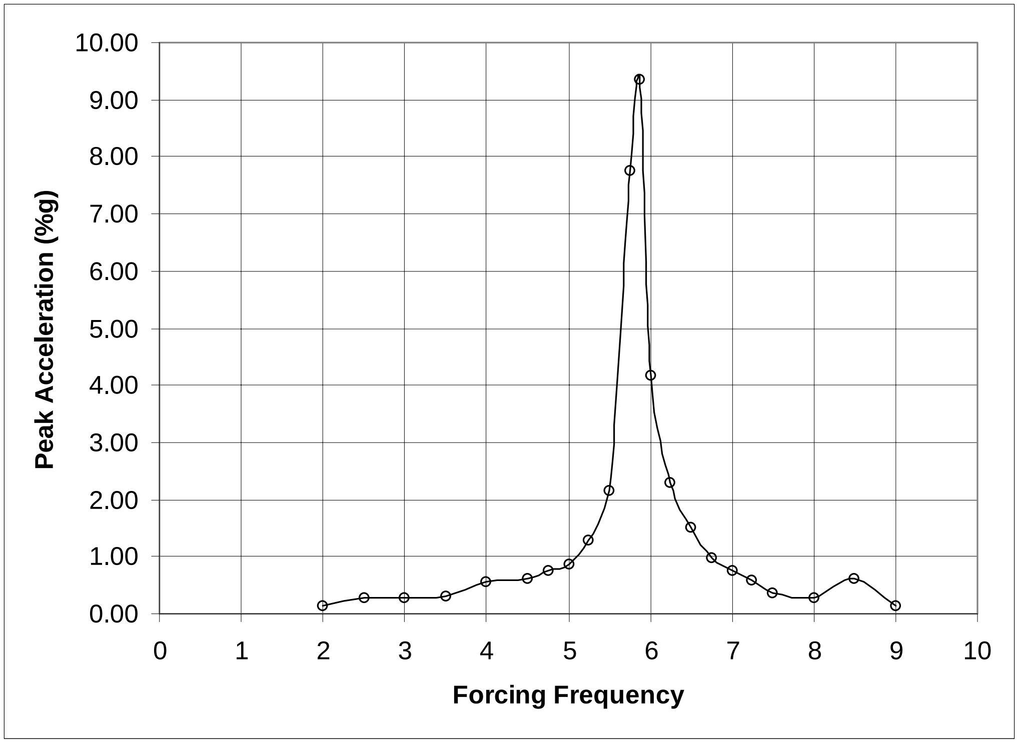

Figure 3.3 – Modified Spectrum Response Curve

3.4 MODE SHAPES

3.4.1 Introduction and Experimental Procedure

The comparison between the predicted mode shapes and the measured mode shapes is summarized in this section. The mode shape contains information on how the system undergoes displacement. The modal analysis also provides the frequency at which this happens. The mode shapes are useful for determining the locations of the floor system that are prone to excitation with the least amount of effort. It is also important to know the mode shape to properly determine a retrofit for a problem system. This is especially true when damping posts are used.

The mode shapes and the corresponding frequencies were predicted using SAP 2000 for the first three modes of the unmodified lab floor system. These mode shapes were also measured on the actual laboratory floor. To measure the mode shapes, a 7x7 grid (with a total of 49 points) was set up on the lab floor. The shaker device was placed at a grid-point location that was assumed to have a limited participation in most of the lower modes. The shaker input was a burst-chirp function as shown in Figure 3.4.

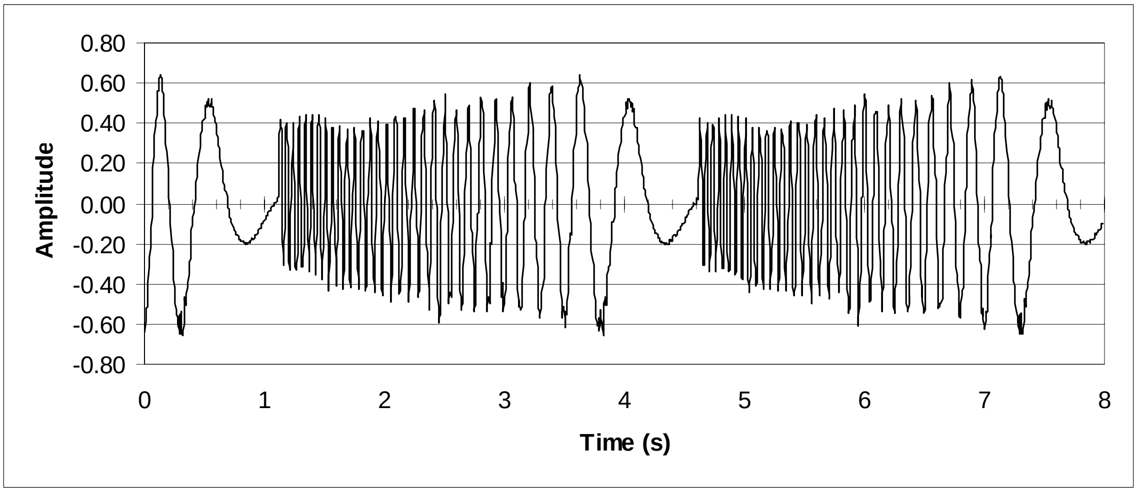

Figure 3.4 – Burst-Chirp Function

This burst-chirp function is a sinusoidal type of wave with a varying frequency that starts at 50Hz and decays to 0Hz. About two repetitions take place in the time space of eight seconds. Figure 3.4 shows a plot of the whole eight-second interval for the burst-chirp excitation. Seven data sets were taken consecutively for each of the 49 grid points. For each of the points, the Frequency Response Functions were calculated from averaging the spectra of the seven consecutive time windows. This averaging process reduces unwanted noise. The Hanning Window function (Equation 3.2) is plotted in Figure 3.5. This function is multiplied by the time signal to obtain an increased frequency resolution when generating the frequency response spectra.

$$w(t) = \frac{1}{2}\left[1 + \cos\left(\frac{2\pi t}{T}\right)\right] \qquad |t| \le \frac{T}{2} \qquad \textbf{(3.2)}$$

where t is time, T is the time length of the interval, and w is the multiplier value of the window function.

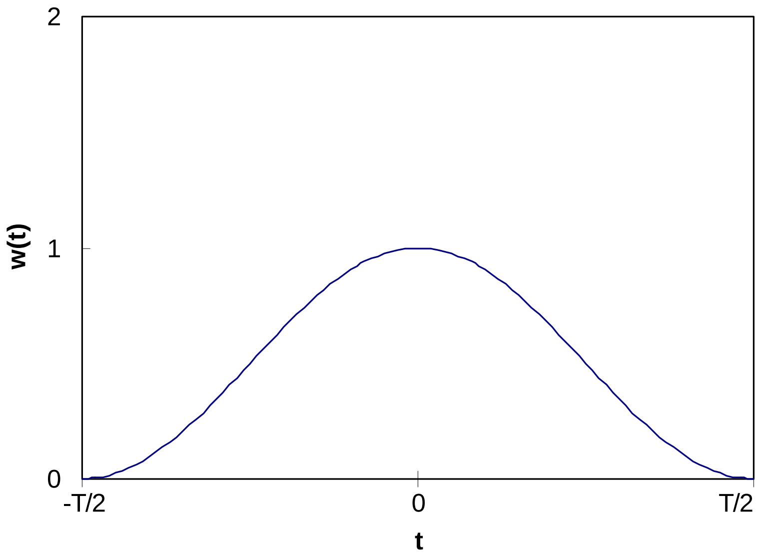

Figure 3.5 – Hanning Window Function

The resulting increased frequency resolution prevents a phenomenon called leakage. Leakage is the spreading of the true spectrum components to other frequencies. Leakage can occur if the excitation is not exactly periodic during the time frame in which the data were recorded. Preventing this leakage phenomenon produces more accurate mode shape plots and frequency response spectra.

3.4.2 SAP2000 Predicted Mode Shapes

Any finite element model can be improved with a finer mesh. An optimum mesh was chosen to provide accuracy and time efficiency for running the model. The figures in this section only show the shell elements and do not show the nodes, or frame elements. The shape of the truss displacement is not important in this study, where only the shape of the floor surface is observed.

Figure 3.6 shows the shape of the finite element mesh without any displacements. Also shown are the global X, Y, and Z axes. As the figure illustrates, there are quite a number of shell elements in this mesh.

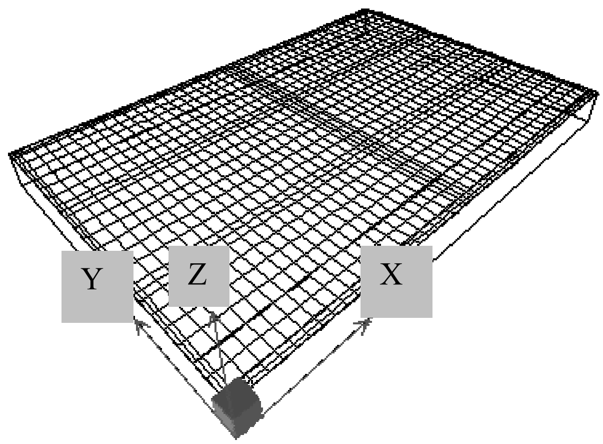

Figure 3.6 – Finite Element Mesh Grid for Laboratory Floor

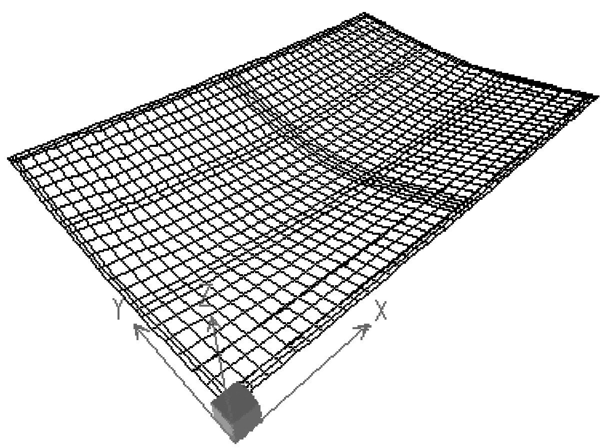

Figure 3.7 – First Mode of Laboratory Floor

The first mode shape (Figure 3.7) corresponds to a predicted frequency of 5.88 Hz. The mode shape is similar to the deflected shape caused by uniform gravity loading for a system of this type. The highest displacement is in the center where the only anti-node in this mode shape is located. All four edges have a low amount of activity although they are active.

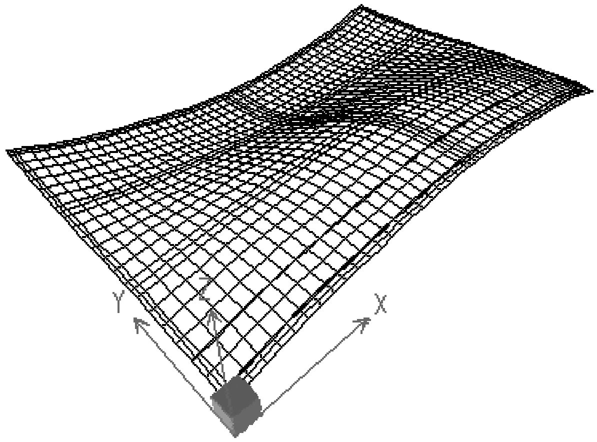

Figure 3.8 – Second Mode of Laboratory Floor

The second mode shape shown in Figure 3.8 corresponds to a predicted frequency of 7.84 Hz. This mode shape has four node points and one nodal line. The four nodes are at the corners of the bay. The nodal line runs parallel to the joist line (long direction/x-axis) in the center of the bay. Thus, if a damping post is placed in the center of the bay, it will be of little or no effect in reducing the effects of this mode. However, the antinodes occur at the location where the edge of the bay intersects the centerline of the bay parallel to the y-axis (and parallel to the girders). (The damping post locations used in TCN 2, TCN 3, TCN 5, and TCN 9, theoretically should have been very effective in reducing the effects of this second mode; see Chapter II for details.)

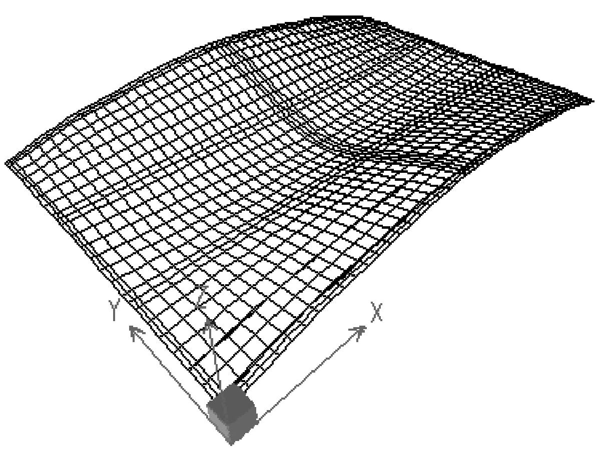

Figure 3.9 – Third Mode of Laboratory Floor

The third mode shape (Figure 3.9) corresponded to a predicted frequency of 8.98 Hz. The girder lines (parallel to y-axis) on each edge had practically no displacement in this mode. The other nodal lines were at the third points of the bay and were perpendicular to the girder lines (parallel to x-axis). There are three main anti-nodes along the centerline of the bay parallel to the girder lines (parallel to y-axis). The anti-nodes that occur on this centerline are located in the center of the bay and at the edge of the bay. It is apparent from examining this third mode shape that little effect of vibration reduction can be expected from any of the Test Configurations of Chapter II due to the locations of the nodal lines. A single post placed in the center of the bay should be effective in reducing the effects of this mode shape.

3.4.3 Measured Mode Shapes

The measured mode shapes and frequencies presented in this section were calculated from the data obtained as described in Section 3.4.1. Figure 3.10 shows the grid of data points where readings were taken. These data points are located at the 49 grid intersections in the figure. Due to the time it takes to record and analyze data for one point, a more refined grid was not found to be suitable for the purpose of this comparison.

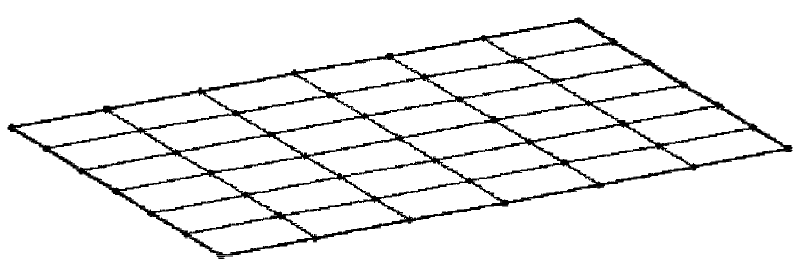

Figure 3.10 –Floor Grid Used for Testing

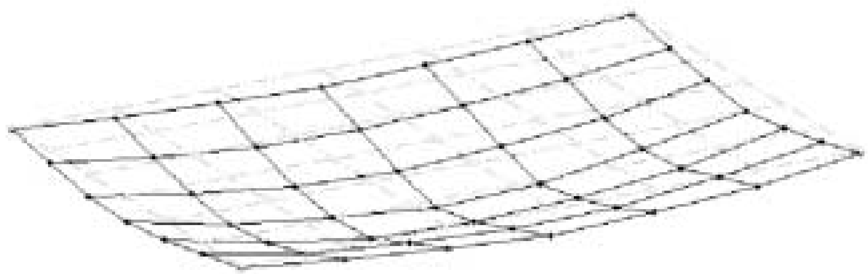

Figure 3.11 – First Mode

The first mode shape is shown in Figure 3.11. It had a measured frequency of 5.90 Hz (versus 5.88 Hz predicted). The mode shape is similar to the deflected shape caused by uniform gravity loading for a system of this type. The highest displacement is at the center where the only anti-node in this mode shape is located. The participation of the edges seems more visible in this measured test than what was predicted by the SAP 2000 finite element model.

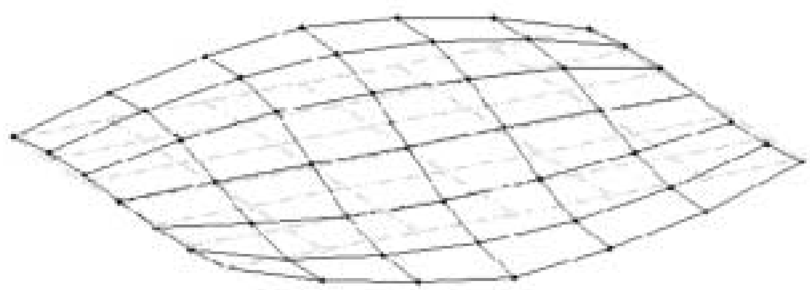

Figure 3.12 – Second Mode

The second mode shape shown in Figure 3.12 had a measured frequency of 7.82 Hz (versus 7.84 Hz predicted). This mode shape has four node points and one nodal line. The four nodes are at the corners of the bay. The nodal line runs parallel to the joist line (long direction) in the center of the bay. The antinodes occur at the center of the bay, and where the edge of the bay intersects the centerline of the bay along the short direction (parallel to the girders). The measured shape shows more activity along the girder edges than what was predicted by SAP 2000.

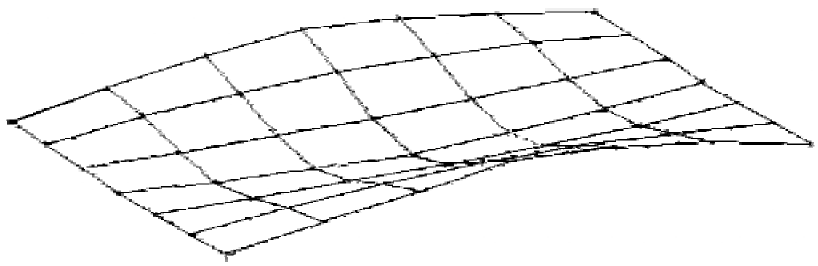

Figure 3.13 – Third Mode

This third mode shape (Figure 3.13) had a measured frequency of 9.62 Hz (versus 8.98 Hz predicted). The girder lines (parallel to short direction) on each edge had practically no displacement in this mode. The other nodal lines were at the third points of the bay and were parallel to the joist line (long direction). There are three main anti-nodes. One is in the center of the bay, and the other two are located at the intersections with the centerline of the bay that is parallel to the girder lines (short direction) and the edge of the bay.

3.4.4 Summary and Comparison

The predicted mode shapes and corresponding frequencies compared rather well with the measured data. Table 3.2 shows measured and predicted frequencies of the mode shapes.

Table 3.2 – Measured and Predicted Frequencies of Mode Shapes

Mode Number	Predicted Frequency (Hz)	Measured Frequency (Hz)
1	5.88	5.90
2	7.84	7.82
3	8.98	9.62

There is excellent agreement between the predicted and measured modal frequencies of the first two modes. Although all of the mode shapes have a good shape comparison, the third modal frequency doesn't correlate between the measured and predicted frequencies as well. In this case there is a 0.64 Hz difference between the values from finite element model and the SAP 2000 prediction. It appears that higher modes are generally harder to accurately predict. The more elaborate testing effort and data acquisition method in the Experimental Modal Analysis (EMA) made it possible to accurately predict the second mode shape. The corresponding frequency for this second mode shape cannot be measured by placing the accelerometer at the center of the floor, as the tests in Chapter 2 were performed.

3.5 ACCELERATION DUE TO SINUSOIDAL EXCITATION

3.5.1 Introduction

The purpose of this section is to compare predicted peak accelerations using Design Guide criteria and SAP 2000 finite element models with peak accelerations obtained from data recorded in the field tests. In previous research in this area, finite element models compared well with the design guide criteria and test data for the fundamental natural frequency of a system. However, there was always a problem when correlating the peak accelerations. Using the Design Guide criteria, the peak accelerations would rarely be predicted to be similar to those obtained from a finite element model analysis. This section compares both of these two methods of prediction with an actual field test for the unmodified floor.

The shaker assembly was placed in the center of the lab floor to excite the system at constant known magnitude and frequency. This magnitude and frequency are then used in the predicted calculations. The predictions are compared with the actual test data to see which method of prediction is more accurate. Predictions based on the Design Guide criteria were only able to be used on the unmodified floor system due to the geometric conditions.

3.5.2 Design Guide Prediction

Calculations for the design guide criteria can be found in Appendix B. The value of a_p/g for a damping ratio of 3% is 0.99% g. When using a damping ratio of 2.04%, the expected value is 1.46%g. The calculations are based on a forcing function with a frequency of 5.88 Hz and a magnitude of 8.30 lbs. This calculated value of 1.46% g is the value of peak acceleration that will be compared with the other data.

3.5.3 SAP 2000 Prediction

The SAP 2000 finite element model was used in the dynamic load analysis. A sinusoidal forcing function having an amplitude of 8.30 lbs and a frequency of 5.88 Hz was placed on the center of the floor in the model. When using 2.04% of critical damping, the finite element analysis yielded a result of 1.21% g. This is about 17% less than the predicted value from the Design Guide criterion.

3.5.4 Measured Data

Two data sets were recorded to measure the peak acceleration in a way that would be comparable to the theoretical predictions. The ideal walking excitation was a sine wave at 5.88 Hz with an amplitude of 8.30 lbs. Because of instrumentation restrictions, an amplitude of 8.30 lbs could not be accurately applied. Amplitudes of 10.29 lbs and 20.59 lbs were applied to the system. These amplitudes represent voltage signals of 1.0mV and 0.5mV respectively from the force plate. Since the relationship between the amplitude of the force and that of the predicted peak acceleration is linear, a simple ratio is used to calculate a_p/g for an amplitude of 8.30 lbs. The acceleration traces of the system are found in Figure 3.14.

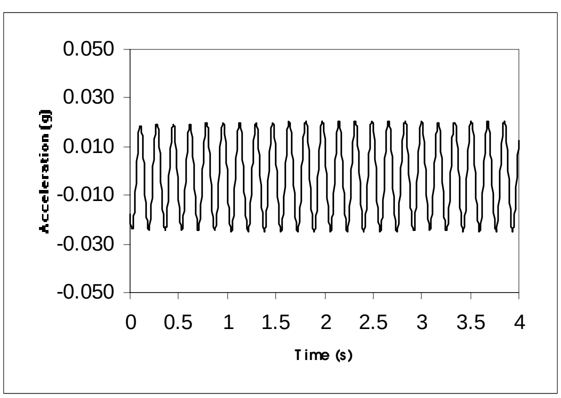

a) Input of 10.29lb @ 5.88Hz

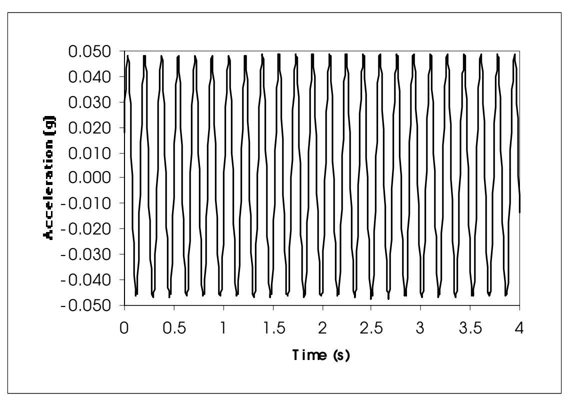

b) Input of 20.59lb @ 5.88Hz

Figure 3.14 – Acceleration Traces from Sinusoidal Excitation

The most direct way of measuring the peak acceleration is taken from obtaining the minimum and maximum values in the trace. To compensate for any error due to a signal offset, the maximum value of the trace is subtracted from the minimum value of the trace. After obtaining the value of the differences, the resulting answer is divided by two. This is an effective way to get the average peak acceleration for a trace that is assumed to be a perfect sine wave. The peak value is then taken and multiplied by a ratio to obtain the peak acceleration for the 8.30 lb force.

The minimum and maximum values from Figure 3.14(a) are -0.0251g and 0.0204g. These values provide an average peak acceleration of 2.28% g for the 10.29 lb excitation force. Applying the ratio to convert this value to a comparable acceleration for the 8.30 lb force results in a peak acceleration of 1.83% g. The minimum and maximum values for the 20.59 lb amplitude forcing function in Figure 3.14(b) are -0.0472g and 0.0490g. The comparable peak acceleration for the 8.30 lb force is 1.93% g. Averaging these values results in a measured peak acceleration of 1.87% g.

3.5.6 Summary and Comparison

The peak accelerations predicted by using the AISC Design Guide procedures and SAP2000 had about a 19% difference. However, there was a larger difference between both of the predicted values and the measured results. The measured data resulted in a peak acceleration of 1.87% g that is higher than the FEM value by a factor of about 1.55. It is higher than the hand calculations by a factor of about 1.28.

3.6 CONCLUSIONS AND COMMENTS

Overall, measured data presented in this chapter compared rather well with tested data. Modal frequencies and shapes were predicted to a pleasing degree of accuracy. The damping determined from experimental data seemed rather high at a value of 2.04%. Although this was in the assumed range of 1% to 3%, it was still on the high side because of the lack of anything in the whole system to provide damping. If the measured damping of the system was lower, the peak accelerations predicted would have been higher. This would make the data correlate better. For both the Design Guide-based calculations to match the measured peak acceleration of 1.87% g, the required damping in the actual system would have had to be 1.61% of critical. For the finite element model to match, the damping in the actual system would have to be 1.32% of critical damping. This would have been a good damping assumption based on the emptiness of the floor system. The only damping provided came from one graduate research student, some testing equipment, and the structural system itself. The damping felt very low from a human perception due to how the excitation would continue to ring throughout the system for a seemingly prolonged time. The problem between the three methods comparing well may lie within the damping measurement. Both of the values of 1.61% and 1.32% of critical damping are more reasonable than the 2.04% of critical damping that was measured. The predicted values are the closest two values.

CHAPTER IV

EVALUATION OF FLOOR SYSTEMS BY FIELD ANALYSIS

4.1 INTRODUCTION

This chapter discusses the possibility of accurately evaluating a floor system without the need of complex finite element models. Creating finite element models is a time-consuming and expensive way to evaluate a floor system to determine whether it meets the acceleration criterion discussed in the Design Guide. Performing hand calculations can be time-consuming as well, but the floor system geometry may not allow for hand calculations. In such situations, it would be desirable to have a method for performing a quick field evaluation of a system using a portable accelerometer and hand-held data analyzer. Such an evaluation would provide information on the necessity of a retrofit for the system.

Floor vibration data from several buildings in the United States of America was compiled. These data contain information about the location, floor excitation, fundamental natural frequencies, root-mean-square acceleration, peak acceleration of the trace, peak acceleration from traces filtered below both 10 Hz and 18 Hz, and remarks on human comfort level of the vibration. Human comfort levels were rated by a member of the measurement team on a scale of perceptibility from 0 to 5, where 5 is the best performance. The data were analyzed in attempt to find some correlation between human comfort level and one of the other pieces of data for each excitation.

4.2 DATA ANALYSIS

The data taken from the different buildings were sorted in various ways in an attempt to find some correlation between the rating of the system and other variables present in the system. Six different plots were made. The plots are: peak acceleration versus the rating, RMS acceleration versus the rating, peak acceleration from traces filtered below 10 Hz versus the rating, peak acceleration filtered below 18 Hz versus the rating, fundamental natural frequency versus the rating, and fundamental natural frequency times the peak acceleration versus the rating.

Figure 4.1 shows the relationship between the peak accelerations of all the floor systems and their corresponding rating. From the given data, it is evident that there is too much scatter to make any correlation between peak acceleration and rating.

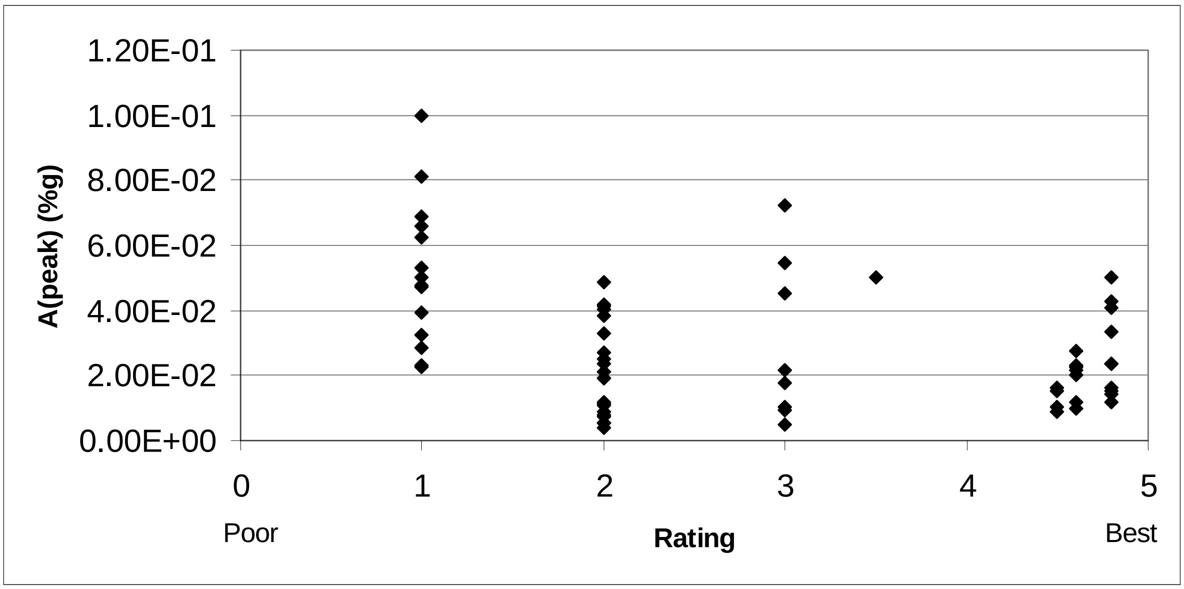

Figure 4.1 – Peak Acceleration Versus Rating

Figure 4.2 shows the relationship between the RMS accelerations of all the floor systems and their corresponding rating. The data are similar to those in Figure 4.1. Thus, no relation between RMS acceleration and the rating can be established.

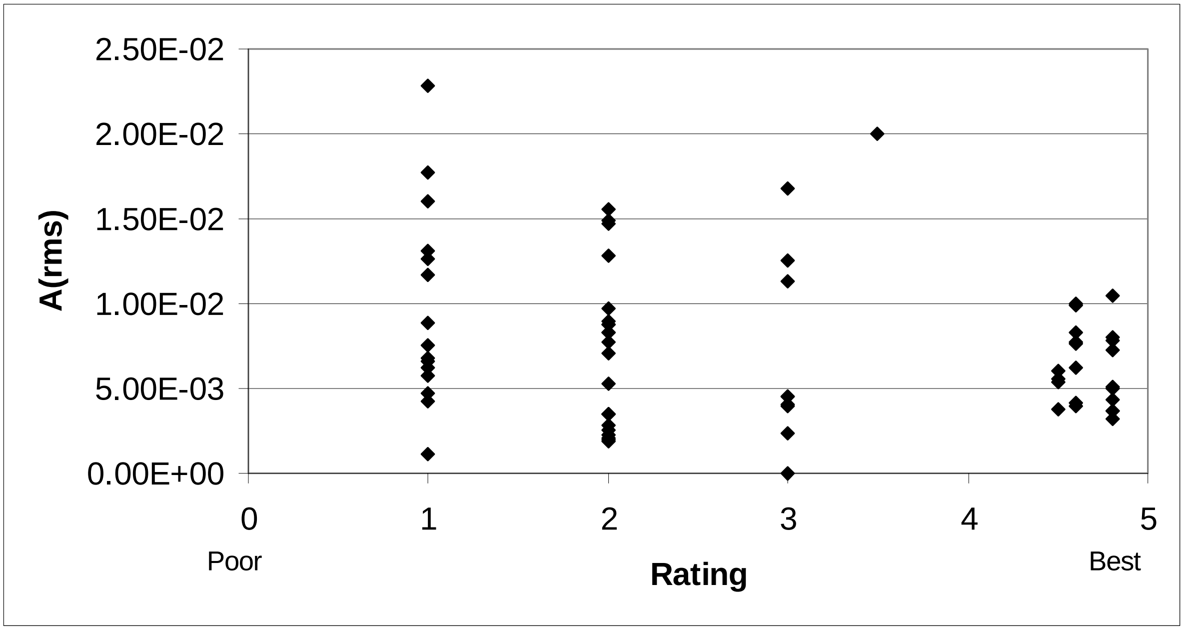

Figure 4.2 – RMS Acceleration Versus Rating

The filtering process performed on the traces to obtain peak accelerations is an approximate method that uses Equation 4.1. This was used to obtain both peak accelerations for the traces filtered below 10 Hz and 18 Hz.

$$a_{peak} = 1.5\sqrt{\sum_{i=0}^{n} a_{i*r}^{1.5}} \quad \textbf{(4.1)}$$

where a_{peak} is peak acceleration, r is the frequency resolution (0.25 Hz in this case), n is equal to the desired frequency to filter below times the resolution, and a is the acceleration value of the FFT. The results for filtering below 10 Hz and 18 Hz, respectively, versus the rating are show in Figures 4.1 and 4.2. Unfortunately, the plots in Figures 4.3 and 4.4 do not show any good relationships between these filtered peak accelerations and the floor ratings.

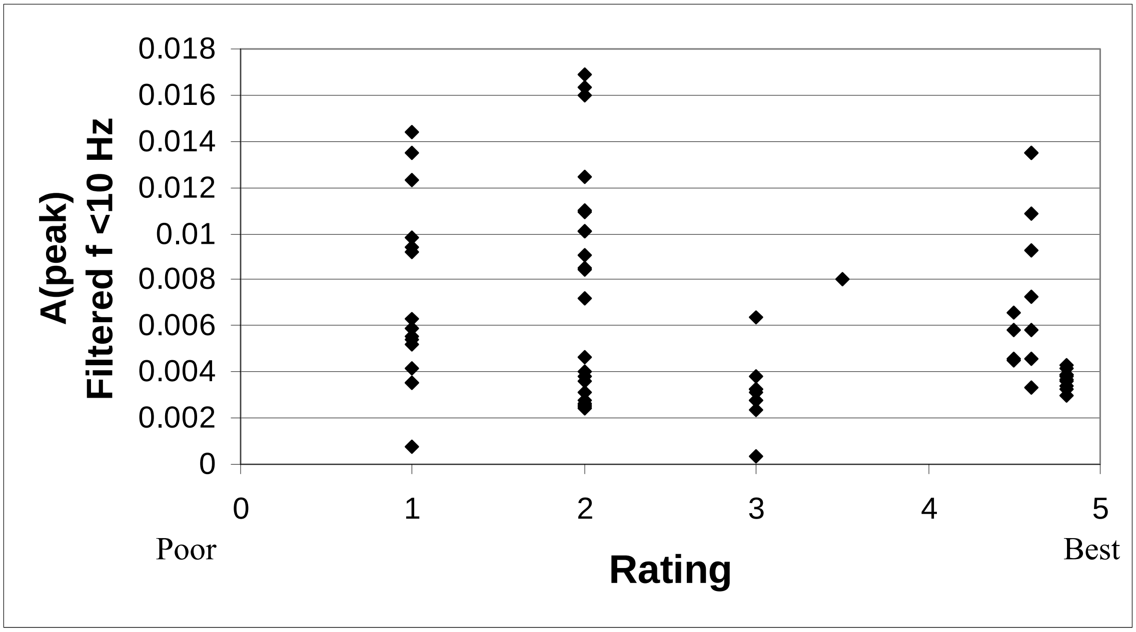

Figure 4.3 – Peak Acceleration From Trace Filtered Below 10 Hz Versus Rating

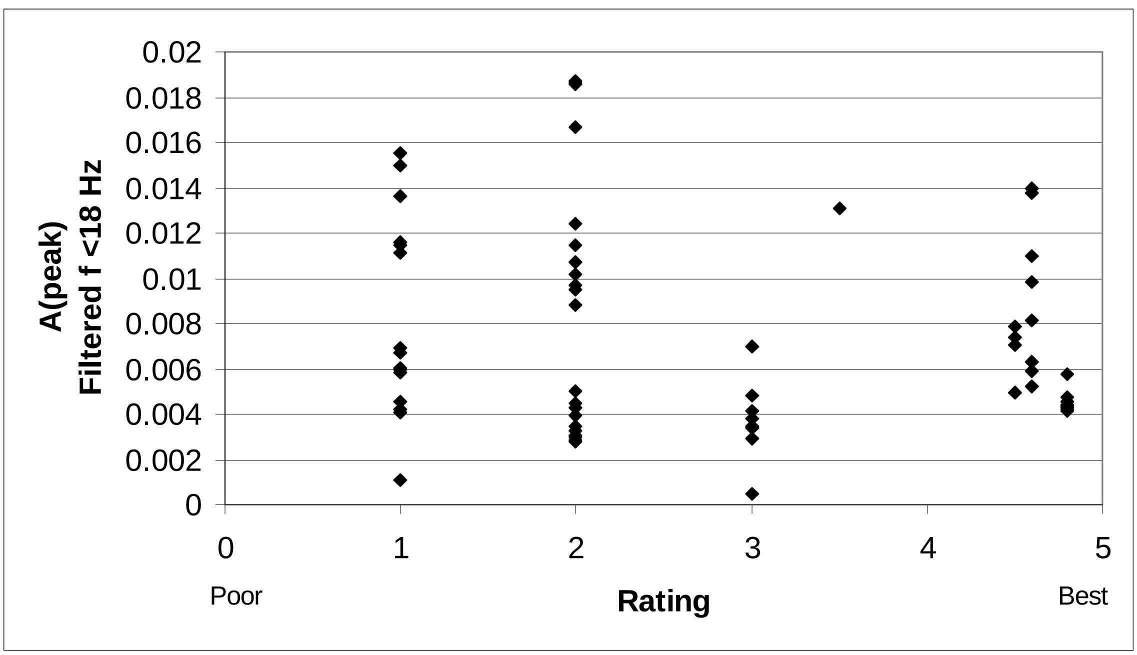

Figure 4.4 – Peak Acceleration From Trace Filtered Below 18 Hz Versus Rating

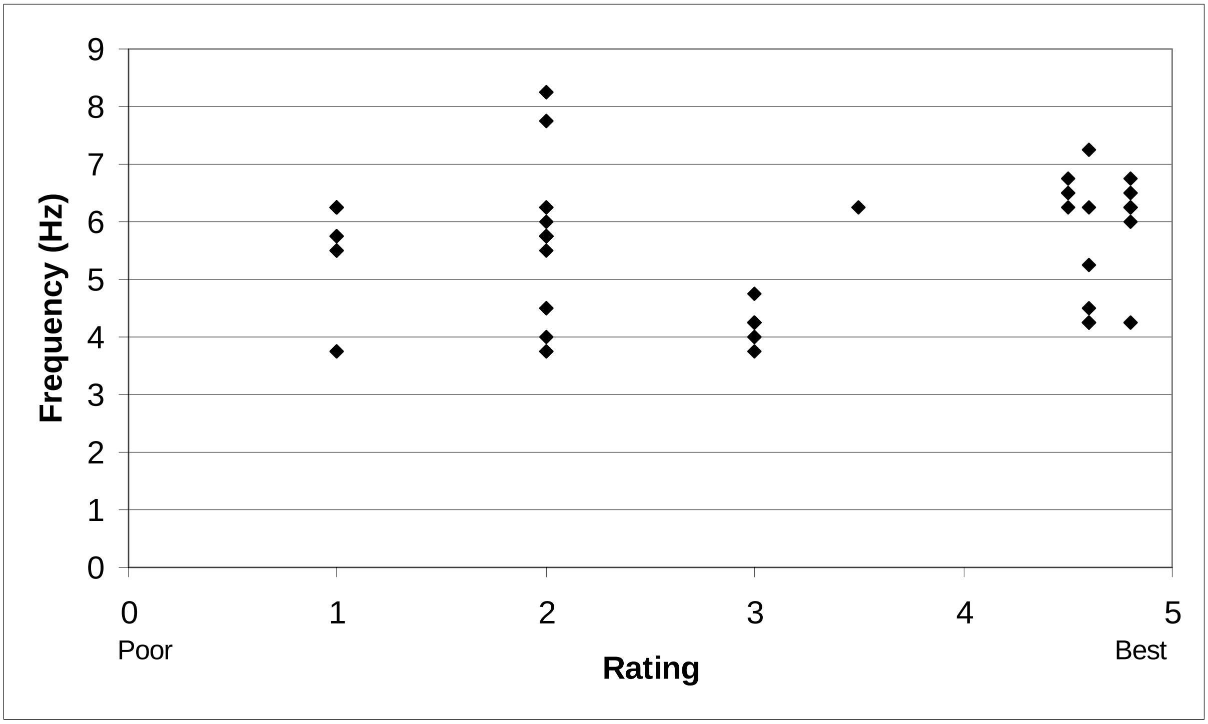

Figure 4.5 – Fundamental Natural Frequency Versus Rating

Figure 4.5 shows a relationship between the fundamental natural frequency of a system and the ratings of the floor system. Like all of the previous plots, there is no significant relationship between the two variables.

When using the Reiher-Meister scale, the acceptability of a system depends on the fundamental natural frequency times the peak acceleration of a heel-drop. The peak acceleration of the system taken from walking excitation was multiplied by the fundamental natural frequency and then the value was plotted with respect to the floor system rating. The plot is shown in Figure 4.6. Theoretically, this plot should have showed some type of relationship. However, there was nothing that could be derived from this data.

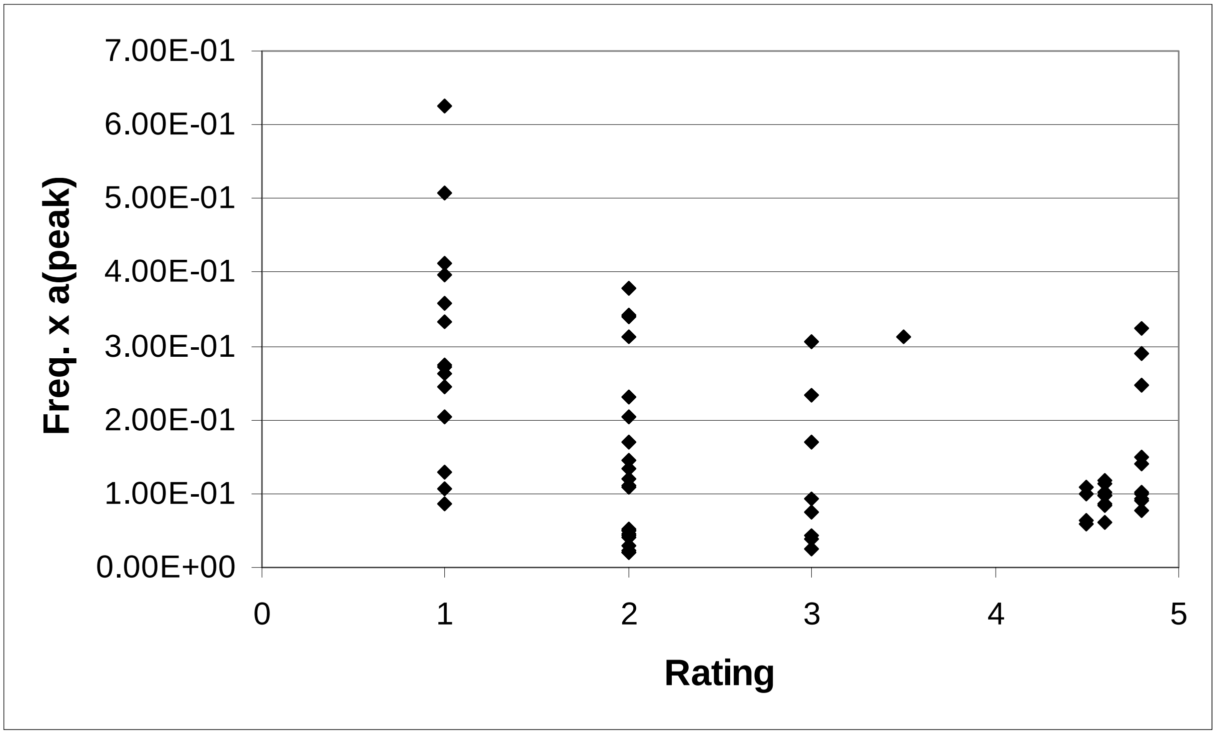

Figure 4.6 – Frequency Times Peak Acceleration Versus Rating

4.3 CONCLUSIONS, SUMMARY, AND RECOMMENDATIONS

From these analyses, there is no apparent way to determine the acceptability of a floor system with only an accelerometer and a handheld data analyzer. There are too many variables to consider in such an analysis.

One main problem with a simple analysis (as noted in Chapter II) is that different locations on the floor will experience different annoying frequencies based on the relative displacement at each particular location on the mode shape. Some regions of the floor are more susceptible to frequencies that come from higher mode shapes. Thus, it is difficult to say that only one frequency will be the most annoying on a particular floor system. For this reason, it is necessary to take readings at several different locations in the floor system to discover the annoying frequencies at all locations that will have occupants. Readings should be taken where occupants are located on the floor—not just in the center of the bay.

Suggested analyses of a floor include rating the floor in many different areas. The areas of the floor should be rated by a person on a suitable scale. The problem area(s) should be located by this method and noted. Once all problem areas are discovered, the FFT spectra that occur in the problem areas can then be analyzed. The FFT spectrum should be used to find the main contributing frequencies at each problem location. These data can then be compared to the results of a finite element analysis to determine which mode shape contributes to the vibration. After the problem mode shape is determined, a retrofit can be placed in a location that would best eliminate or limit participation of the problem mode. The best location for a retrofit is at an anti-node.

The use of a finite element model is required for a detailed analysis instead of hand calculations if the first mode shape is not the contributing mode shape to the most annoying vibration. The finite element analysis is the only one of the two methods used in this study that will predict multiple mode shapes and the corresponding frequencies.

CHAPTER V

PREDICTION OF ACCELERATION FOR COMPLEX FRAMING USING THE DESIGN GUIDE EXCITATION

5.1 INTRODUCTION

This chapter contains a discussion of the attempts to create a method to predict the acceleration of a floor system with complex framing. The study in this chapter is purely analytical. Finite element models in SAP 2000 were analyzed and the resulting data were compared with the predicted values obtained by using the design guide criteria. First a verification of the dynamic load analysis in SAP 2000 was performed by a comparison of results with hand calculations. Afterwards, a mesh refinement procedure was performed to get a mesh that would give accurate results in a convenient space of time. Once a desired mesh was found, a simple footbridge model was analyzed and the results were compared with predicted values obtained from the Design Guide procedure. The finite element models were increased in complexity until the results diverged from values predicted from using the Design Guide. The reason for this procedure was to locate the source of difference between the two methods.

5.2 SAP 2000 VERIFICATION

The first procedure incorporated in this analytical study was a verification process to ensure the accuracy of the program and the modeling techniques used. The first step in the verification was checking the natural frequency of a simple spring-mass system. For a spring-mass system as shown in Figure 5.1, the natural frequency is equal to the inverse of the period. Equation 5.1 illustrates this relationship. The period for the same system is equal to 2π times the square root of the ratio of the mass to spring stiffness. This is in symbolic form in Equation 5.2.

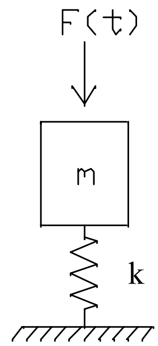

Figure 5.1 – Typical Spring-Mass System

$$f_n = \frac{1}{\tau} \tag{5.1}$$

where f_n is the natural frequency measured in Hz and τ is the period measured in seconds defined by the following equation:

$$\tau = 2\pi\sqrt{\frac{m}{k}} \tag{5.2}$$

where m is the mass of the system and k is the spring stiffness.

For the first comparison, a spring stiffness of 100 pounds per inch and a mass of 100 mass-pounds which is equal to 0.25880 lb*s^2 per inch was used in hand calculations. This yields a period of 0.320 seconds, which is equivalent to a frequency of 3.12 Hz. A finite element model was then made to simulate this spring mass system. Figure 5.2 shows the finite element model that was used. It was very simple as it only used two joints connected by an intermediate spring. One joint was fixed and the other joint was free in the vertical direction (Z-axis). A mass was assigned equal to the mass used in the hand calculations. The SAP2000 finite element analysis provided a period of 0.320 seconds. This is exactly the same number as produced by the hand calculations. A global acceleration equal to the acceleration due to gravity was placed on the system to check the deflection of the spring. The deflection was one inch, which further verifies the spring constant as 100 lb/in.

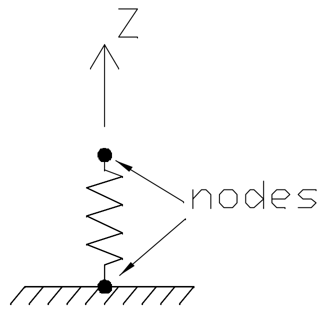

Figure 5.2 – SAP2000 Finite Element Model (FEM) of Spring-Mass System

The next step in the verification of this system was to apply a forcing function F(t) which was equal to 100 lb suddenly and constantly applied to the system starting at time t = 1 sec. Figure 5.3 shows a plot of the forcing function F(t). This force was applied without applying the previous gravity load to the system. The theoretical peak displacement by hand calculations is equal to a total of –2 in. in the Z-axis direction. The resulting trace produces a sinusoidal wave that oscillates between 0 in. and –2 in. on the Z-axis at the natural frequency of the system (3.13 Hz). The finite element analysis produced exactly these results.

The theoretical peak acceleration produced from this type of forcing function is equal to the force divided by the mass. This value is 386.4 in./s². This exact value was also produced by the SAP2000 finite element analysis.

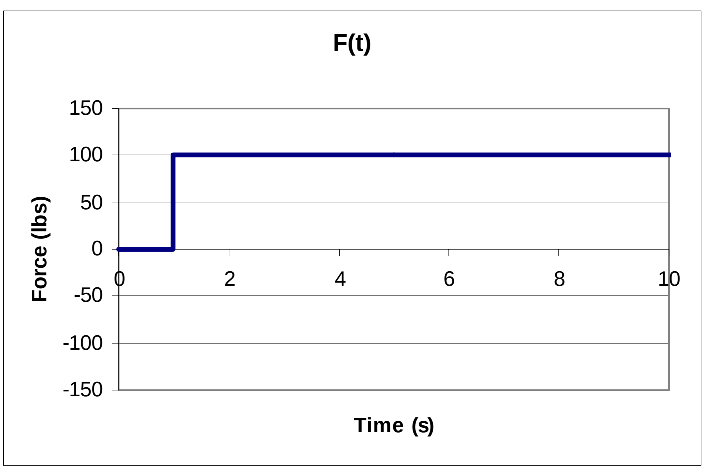

Figure 5.3 – Forcing Function F(t)

The next step in the verification process was to add damping to the spring-mass system, producing a spring-mass-damper system. A damping ratio of 3% of critical damping (or $\zeta = 0.03$) was chosen for the system. This low amount of damping is a typical value found in many structural systems. Figure 5.4 shows a schematic of a spring-mass-damper system.

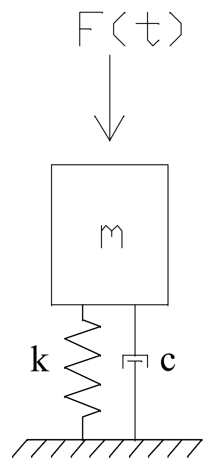

Figure 5.4 – Spring-Mass-Damper System

The Spring-Mass-Damper System was subjected to the previous forcing function F(t) (Figure 5.3). The plot of the displacement trace is shown in Figure 5.5.

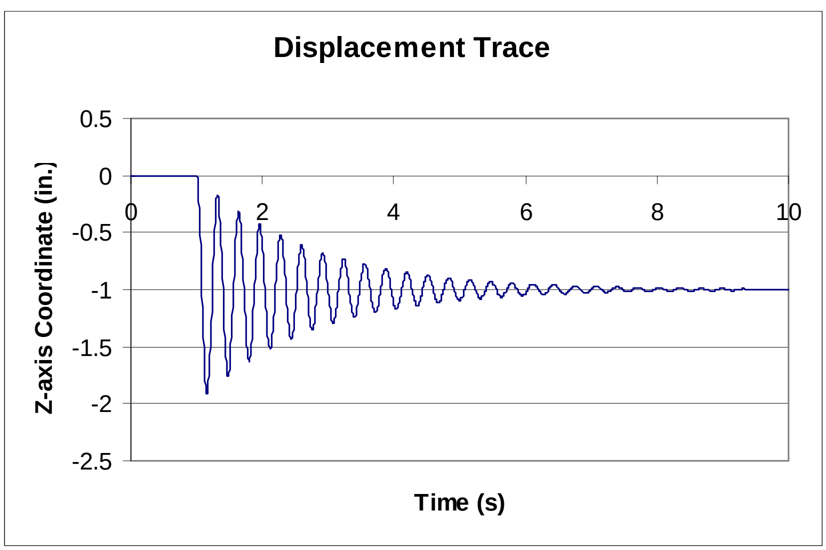

Figure 5.5 – Displacement Trace of Spring-Mass-Damper System

The assigned damping was verified by calculating the log decrement (denoted by δ). The log decrement value was calculated using values obtained from the displacement trace in Equation 5.3. The log decrement value is then converted to the damping ratio ζ using Equation 5.4 and compared with the original value input into the system (3% in this case) to check the trace accuracy output by SAP2000.

$$\delta = \frac{1}{n}\ln\frac{X_0}{X_n} \tag{5.3}$$

where X_0 is the value of an arbitrary peak in the response trace, X_n is the value of the peak to the right of X_0 after n cycles, and n is the number of full cycles between the two chosen peaks.

$$\delta = \frac{2\pi\zeta}{\sqrt{1-\zeta^2}} \tag{5.4}$$

where ζ is the damping ratio.

For this particular trace, X_0 was -0.910 in., X_n was -0.293 in., and n was 6. This gave a log decrement value of δ = 0.189. Using this value for δ in Equation 5.4, and solving for ζ, gives a damping ratio of ζ = 0.030, as anticipated.

The next verification procedure was to apply the forcing function $\mathrm{F(t)} = 1\mathrm{lb}\cdot\sin(\omega\,\mathrm{t})$ with ω = 19.657 rad/sec to the spring-mass-damper system. The value ω is equal to 2π divided by the period τ. Theoretically, the value of the maximum amplitude of displacement Δ_z for this case can be obtained by using the relation shown in Equation 5.5. Solving for Δ_z after substituting in the appropriate values for spring stiffness k and damping ratio ζ yields a maximum displacement of 0.1667 in. The SAP2000 analysis yielded 0.166 in., an error of 0.28%.

$$\frac{\Delta_z}{1\mathrm{lb}/k} = \frac{1}{2\zeta} \tag{5.5}$$

The excellent comparisons in the previous areas of verification allowed for more complicated verification models. The next procedure in the verification process used a uniformly loaded, simply supported beam. The classical formula for fundamental natural frequency of this beam due to bending only is given by

$$f_n = \frac{\pi}{2}\sqrt{\frac{gE_s I_t}{wL^4}} \tag{5.6}$$

where f_n is the fundamental natural frequency of the beam, g is acceleration due to gravity, E_s is the modulus of elasticity, I_t is the moment of inertia about the axis of bending, w is load including the self-weight of the beam, and L is the length of the beam.

Table 5.1 shows a summary of two trials of a verification of the SAP2000 ability to predict the natural frequency of a steel W14x30 beam. The beam was simply supported and consisted of eight frame members and a total of nine nodes. The error was about 0.2% in predicting the fundamental natural frequency for trials when compared to the hand calculations. This excellent comparison allowed further verification.

Table 5.1 – Summary of Beam Fundamental Natural Frequency

Length (ft)	Fundamental Natural Frequency (Hz)	SAP2000 Value (Hz)	Error %
8	194.6	194.2	-0.200
45	6.15	6.14	-0.195

Using the 45 ft W14x30 steel beam again for the next step, a forcing function was placed on the beam at the center. The forcing function had the form of $\mathrm{P(t)} = \mathrm{F} \cdot \sin(\omega\,\mathrm{t})$. The frequency ω was chosen to be the natural frequency such that $\omega = \omega_n$. The value of F was chosen to be the Design Guide loading force for the fundamental natural frequency f_n. Thus the forcing function $\mathrm{P(t)} = 7.59\mathrm{lb} \cdot \sin(2\pi \cdot 6.137\,\mathrm{t})$ was used in the finite element model. The 7.59 lb amplitude is equal to 65 lb*exp(-0.35(6.137)). Using the hand calculation method provided by the Design Guide procedure, a peak acceleration a_o = 18.74% g is obtained. The finite element analysis yielded 18.66% g resulting in a 0.42% error. Once again this is a very excellent comparison.

The next step in verification was to add a uniform mass to the beam to see if the finite element analysis will provide the same results as predicted by the hand calculations. The mass was added to the beam by modifying the mass of the steel. For this step, there was a 0.18% error in the fundamental natural frequency and a 0.13% error in the peak accelerations. Another method of adding mass that was verified was to add lumped masses at each node. This method produced only 0.09% error in the peak accelerations. Either way, there were extremely accurate comparisons in the verification process as a whole, which leads to the conclusion that the SAP2000 finite element program is not flawed in its basic operation of dynamic analysis.

5.3 MESH REFINEMENT

The mesh refinement is a process that helps the finite element user determine the best mesh to use in his testing. A mesh that is not optimized will either take too much time to run if too many elements are used, or it will have poor accuracy if not enough elements are used. Therefore a process is required to find the optimum number of elements to use in the mesh.

The optimum number of elements for the mesh was determined by modeling a beam with a concrete slab on the top and increasing the number of shell elements used for the slab. The beam centroid formed a centerline to the slab looking in a plan-view of the model. The best shell element to use is one with an aspect ratio of 1 (i.e., a square element). A square element was used for the slab, starting with one row of shell elements on each side of the beam. Then the shell elements were divided into four equal parts, which made two rows of shell elements on each side of the beam. The process continued until there were 16 shell elements on each side of the beam. Figure 5.6 shows a drawing of the typical beam and slab finite element model with one shell element on each side of the beam. Figure 5.7 shows a drawing of a model with two shell elements on each side of the beam.

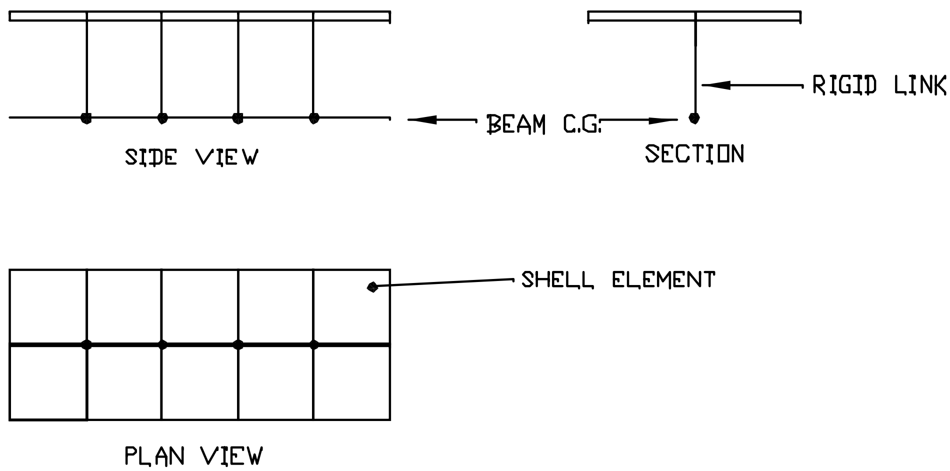

Figure 5.6 – One Shell Element on Each Side of Beam

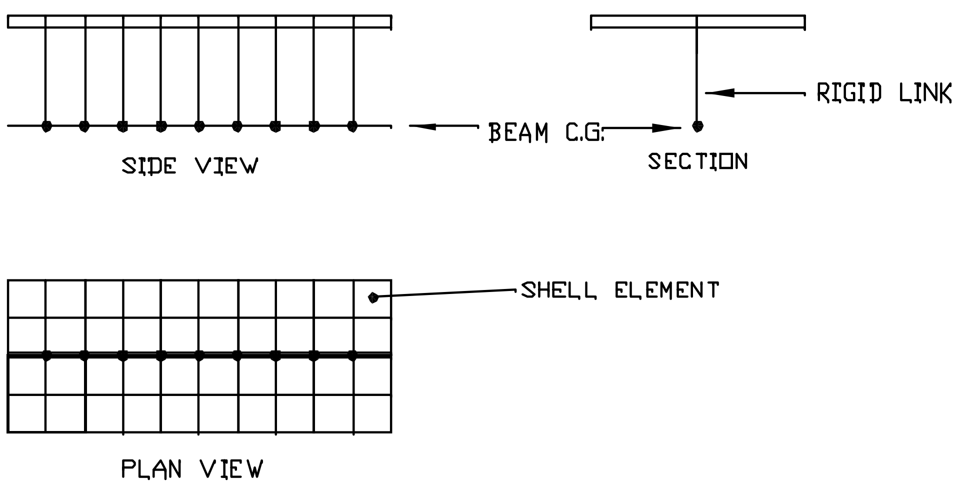

Figure 5.7 –Two Shell Elements on Each Side of Beam

Each of the finite element models from one shell element on each side to sixteen shell elements on each side was analyzed. A fundamental natural frequency, self-weight deflection, and a point load deflection were calculated for each of the five meshes. Table 5.2 summarizes the data that were acquired from this analysis. After the data in Table 5.2

were generated, they were plotted to determine the optimum mesh. The three plots are shown in Figures 5.8, 5.9, and 5.10. They give the same conclusion that mesh number three, four elements per side, was best for use in this study. For a total slab width of 96 in., this would make each shell element 12 in. square. Thus for almost all models 12 in. squares were used where applicable. The 12 in. square is also a convenient size for modeling.

Table 5.2 – Data for mesh refinement

mesh number	shells per side	fn (Hz)	self wt. defl (in.)	pt. load defl. (in.)
1	1	6.83	0.2534	0.0203
2	2	6.96	0.2494	0.0197
3	4	7.00	0.2484	0.0195
4	8	7.01	0.2481	0.0195
5	16	7.01	0.2480	0.0195

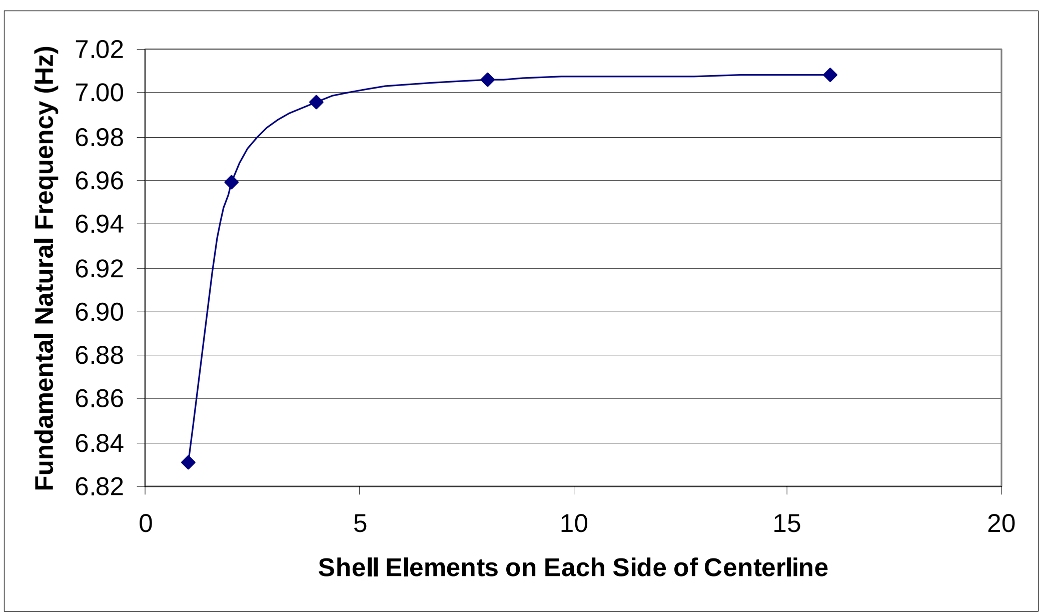

Figure 5.8 – Fundamental Natural Frequency Versus Number of Shell Elements per Side

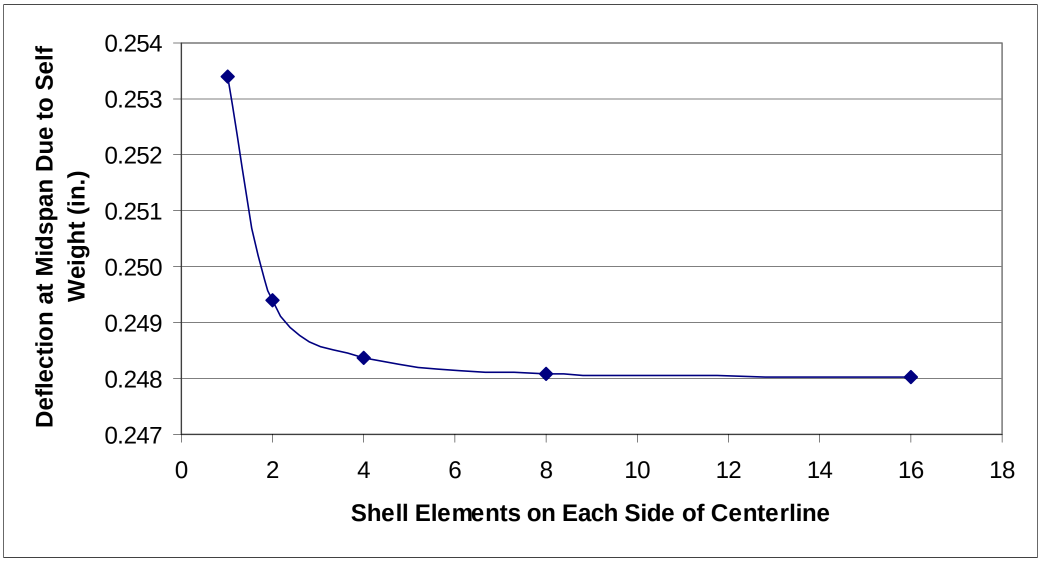

Figure 5.9 – Deflection Due to Self-Weight Versus Number of Shell Elements per Side

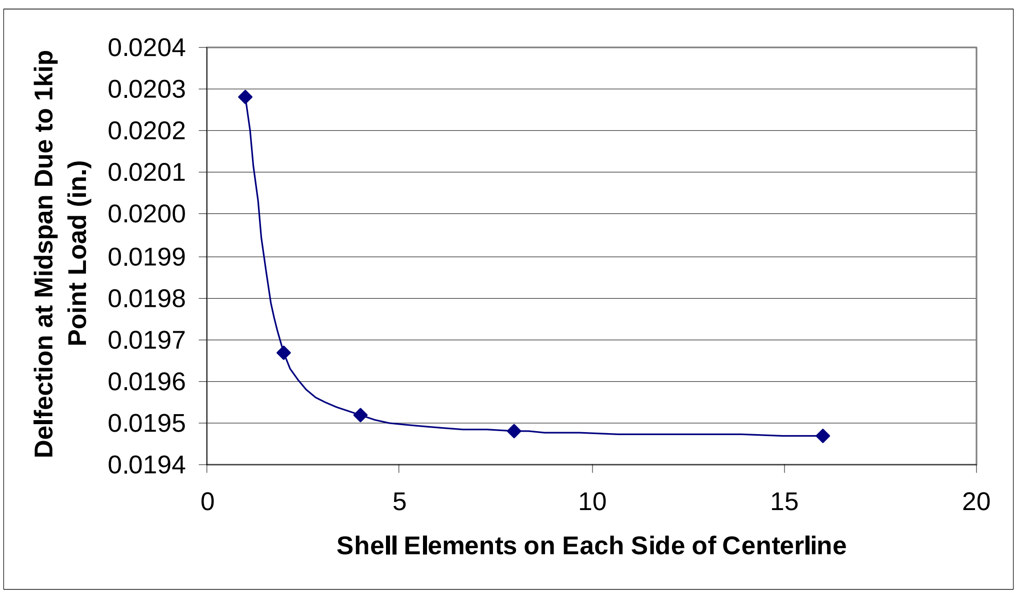

Figure 5.10 – Deflection Due to Point Load Versus Number of Shell Elements per Side

5.4 EFFECTIVE SLAB WIDTH OF FOOTBRIDGE

After determining an optimum number of shell elements to use for modeling the slab, models with a concrete slab were analyzed and the results compared to the hand calculations using the Design Guide procedure. The simplest model with a concrete slab is that of a footbridge. Thus, hand calculations for a footbridge were performed and compared with finite element data. There was a suspicion that the problem that caused the finite element model to differ from hand calculations could lie within the area of the effective slab width for vibration.

To attempt to make this comparison, the effective width b_e of the slab was determined. This effective width is equal to the minimum of either the center-to-center spacing of the members or 0.4 times the length of the supporting members. All shell elements were square elements with a size of 12 in. x 12 in., which conveniently divided the length of the beam into even sections. The value of the slab width s was substantially larger than the b_e value. If the finite element analysis produced different numbers, then that would indicate that the effective slab width that participated in vibration in the finite element program would be different from what was assumed by the hand calculations.

Two sets of models were used. The first set of models used a beam length of 32 ft and the second set used a 50 ft beam. The 32 ft beam was a W18x35 shape and the 50-ft beam was a W33x118. The two data sets are summarized in the Tables 5.3 and 5.4. The fundamental natural frequency and deflection due to self-weight were computed by the finite element program and by use of the Design Guide procedures. A plot of the SAP2000 values versus the theoretical hand calculated values for f_n was analyzed for both test cases. The only variable in each set of models was the beam spacing. The slab width used in SAP2000 was the spacing, and the effective slab width b_e was used for the Design Guide procedure. The beams were of sufficient length so that shear deformations could be neglected.

Table 5.3 – 32 ft Beam Data

Model No.	s (in.)	b_e (in)	FE f_n (Hz)	Predicted f_n (Hz)	% difference
sw32-1	96	96	7.00	7.13	-1.84
sw32-2	144	144	5.89	6.03	-2.34
sw32-3	168	153.6	5.50	5.62	-2.14
sw32-4	192	153.6	5.18	5.27	-1.63
sw32-5	216	153.6	4.92	4.97	-1.09
sw32-6	240	153.6	4.69	4.73	-0.89
sw32-7	360	153.6	3.42	3.36	1.79
sw32-8	288	153.6	4.32	4.32	-0.12

Table 5.4 – 50 ft Beam Data

Model No.	s (in.)	b_e (in)	FE f_n (Hz)	Predicted f_n (Hz)	% difference
sw50-1	120	120	6.86	6.94	-1.17
sw50-2	168	168	6.08	6.19	-1.73
sw50-3	216	216	5.51	5.64	-2.25
sw50-4	240	240	5.28	5.42	-2.58
sw50-5	288	240	4.89	4.98	-1.89
sw50-6	360	240	4.43	4.48	-1.18
sw50-7	408	240	4.18	4.22	-0.92
sw50-8	480	240	3.88	3.91	-0.84

Figure 5.11 shows a typical cross-section of the footbridge finite element model (FEM) created in SAP2000. The data gathered from these experiments showed that there was little difference between the predicted fundamental natural frequencies and the finite element natural frequencies. Figures 5.12 and 5.13 contain data plots of fundamental natural frequencies for finite element analyses versus the predicted values for each system of beams. The solid line is the one-to-one slope on which every point should theoretically lie.

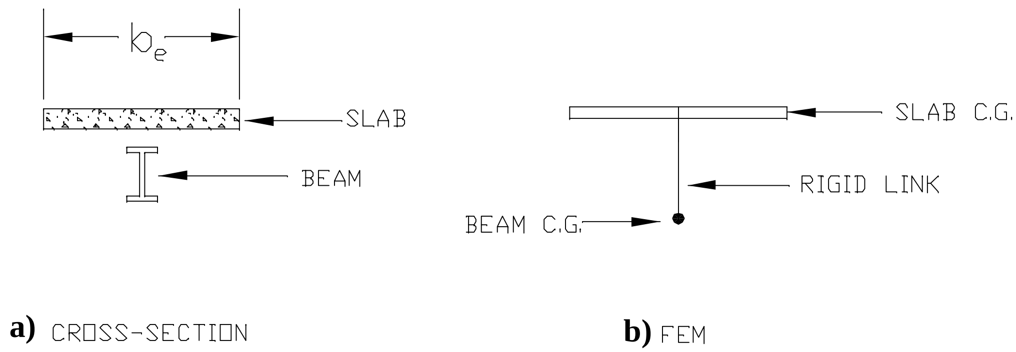

Figure 5.11 – Typical Cross-Section of Footbridge and FEM

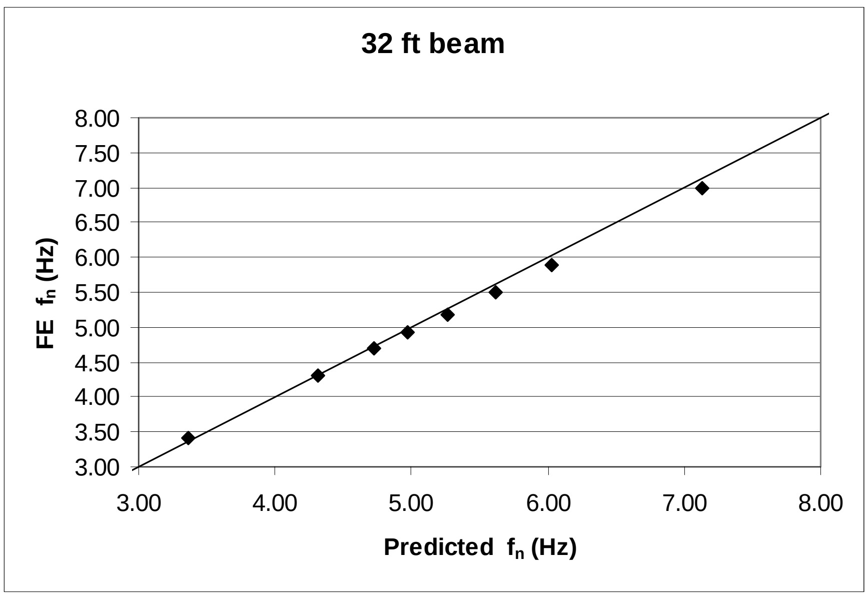

Figure 5.12 – Difference Plots for 32 ft Beam System

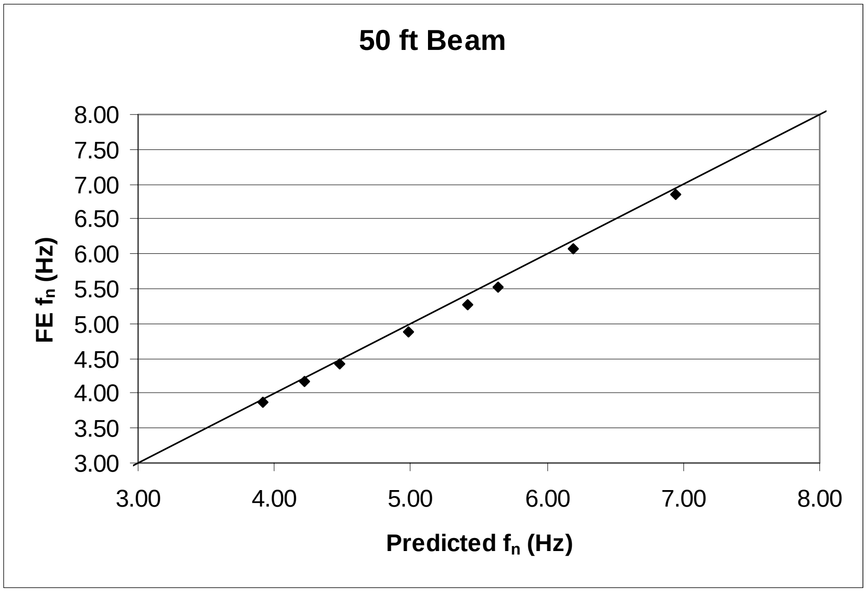

Figure 5.13 – Difference Plots for 50 ft Beam System

It is obvious that the problem does not lie within this area of the study. These plots show very little error between the two methods of analysis. Because of this, larger systems with more complex framing (several beams) can start to be compared to each other. The peak acceleration values matched just as well. They are included in the results in the following section on multiple beam systems.

5.5 MULTIPLE BEAM SYSTEMS

After determining that the Design Guide effective slab width for a one-beam system was correct, larger systems that included multiple beams were studied. The systems started off as a one-beam footbridge and were enlarged to a wide bay-like footbridge with many beams. All beams were simply supported.

The sinusoidal forcing function prescribed by the Design Guide was applied at the center of the finite element floor. The peak acceleration obtained by the analysis was compared to the value obtained from hand calculations. The assumption of the hand calculation method is that after the system reaches a certain width, it changes from a footbridge to a bay. For the assumption of a footbridge, the whole mass is used in the calculation. If the system is too wide to be considered a footbridge, the mass beyond the effective panel width B_j is not assumed to participate in the vibration due to damping over an extended area in the system. These sources of damping are due to frictional damping and energy dispersion. Equation 5.7 is used to calculate B_j.

$$B_j = C_j (D_s / D_j)^{1/4} L_j \qquad \textbf{(5.7)}$$

where D_s = transformed slab moment of inertia per unit width, D_j = effective moment of inertia of tee-beam per unit width, and C_j = 2 for most joists or beams and 1 for joists or beams parallel to an interior edge. If the edge joist or beam is more than 50% stiffer than the interior beams or joists, C_j is taken as 2, even though it is an edge member. L_j is the length of the joist or beam. The value of B_j has a maximum of 2/3 of the floor-width in direction of the beams.

When this value of B_j is calculated, it is used in determining the effective mass of the whole panel that participates in vibration. Since this value is limited to a maximum of 2/3 the beam-length in this case, when the length perpendicular to the beams exceeds a certain value, B_j no longer increases though the whole mass of the system does. This increases the peak acceleration obtained from hand calculations compared to that obtained from a finite element model. The finite element model cannot take into account frictional damping and energy dispersion. Thus, over a long enough period of time the whole width of the system actively participates in the vibration as it assumes the first modal shape. This is only natural as the frequency at which the bay is being driven is the frequency of the first mode shape.

An animated video created by the finite element program illustrates the displacement of the floor during the excitation. The largest motion occours at the source of the input and the other displacements ripple out in waves similar to those found in a pond after a rock is tossed. Unlike the rock-in-the-pond analogy, the forcing function is not removed. For this reason, after enough time is elapsed, the displacement trace of the whole bay is almost exactly like the first mode shape. The first mode shape has the same basic shape for each bay that was investigated. This mode shape is illustrated in Figure 5.14.

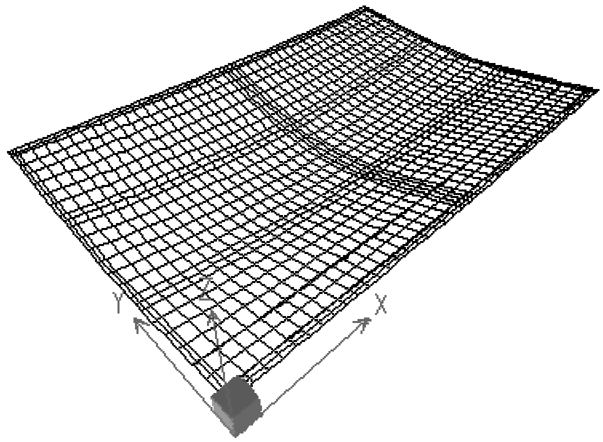

Figure 5.14 – Typical Mode Shape for the Fundamental Natural Frequency

In Figure 5.14, the beams are parallel to the Y-axis (short direction) and the supports are along the edges in the direction parallel to the X-axis (long direction). The only modal participation at the supported ends was from rotation and not displacement.

Plots of acceleration versus number of beams were created. These systems had evenly spaced beams. The plots show that the acceleration calculated by the AISC Design Guide criterion levels off after the system becomes greater than the effective panel width, B_j. On the other hand, the finite element models are asymptotic to zero. This shows that there is no limit to the width of the participating mass in the bay when using finite element analysis. These plots are shown in Figures 5.15 and 5.16. The plot in Figure 5.15 is for data from a system with 50 ft beams spaced at 14 ft on-center. The system had a fundamental natural frequency of 6 Hz. The plot in Figure 5.16 is from a system with 25 ft beams spaced at 10 ft on-center. The fundamental natural of this system was 10 Hz. Damping for these two systems was 3% of critical damping.

Both of the following figures show the relation between values from the Design Guide calculations and two types of finite element models. The first type of finite element model was created using SAP2000, and it only allowed one-way bending in the system. The second type of finite element model was also created using SAP2000 and all degrees of freedom were considered in the analysis.

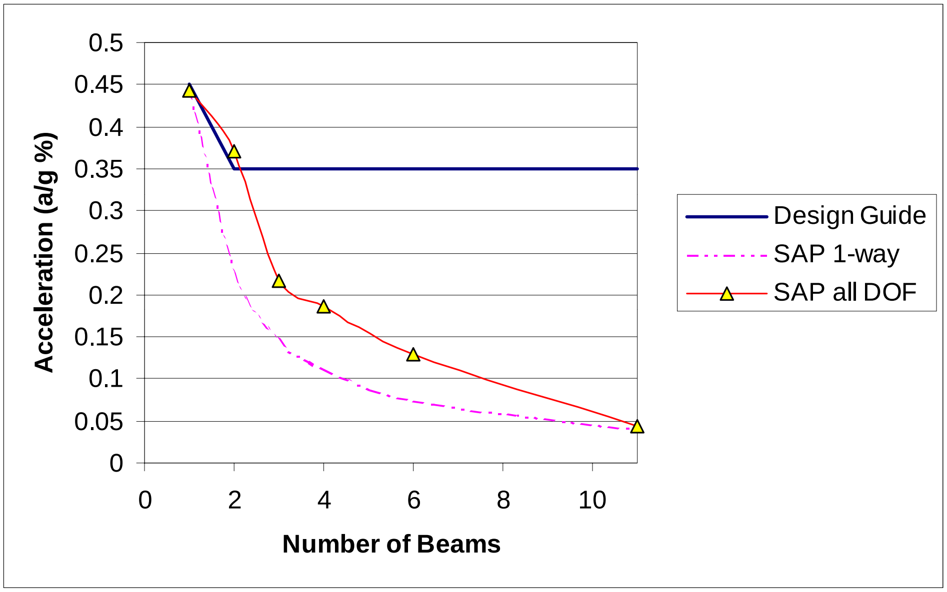

Figure 5.15 - Acceleration for System Versus Number of 50 ft Beams

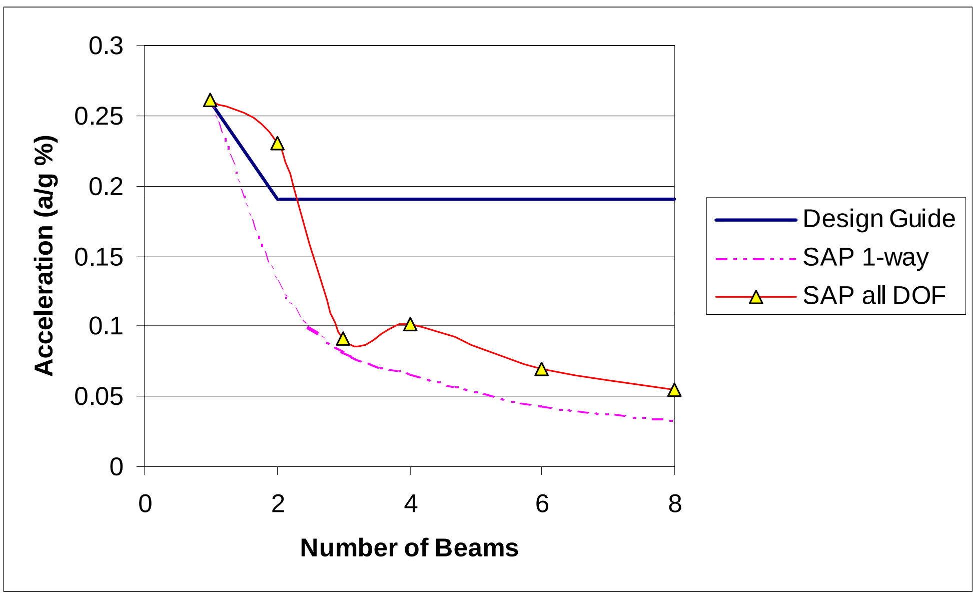

Figure 5.16 – Acceleration for System Versus Number of 25 ft Beams

Every finite element analysis matched very well with the hand calculations for a footbridge model (for one beam) when bending in only one direction was considered. However, the finite element analysis results were very different from the hand calculation results when the FE model was not restrained in a simple bending mode. It is also seen in the plots that the peak acceleration values match for the system with one beam, where the system is considered a footbridge. However, for larger systems the B_j value approaches the limiting value of 2/3 of the length of the floor for the hand calculations. SAP2000 cannot be used if the effects due to energy dispersion and frictional damping (which increases with panel area) are to be considered. Thus, the accumulation of these effects causes acceleration values from SAP2000 to become asymptotic to zero as the number of beams increases.

5.6 MULTIPLE BAY SYSTEM

The discrepancy is obviously between the assumptions of the effective panel width calculation and not being able to account for these assumptions in SAP2000. This problem can carry over to systems having multiple bays. So it was important to solve the problem on the simplified systems first. The attempt to modify finite element models to match the results of the AISC Design Guide criterion was also made. Many different techniques were attempted in order to reach this goal.

The reason for trying to match the AISC criterion by the finite element models was to shed light on the source of the discrepancy. Placing columns for rotational restraints, omitting portions of mass within the bay, plotting static deflection, breaking down the acceleration components by the modal participation, and applying alternate forcing functions were some of the techniques used to obtain matching accelerations. **All of these were performed before the source of the difference in the FE models and hand calculations was realized.** That source of the difference is that SAP2000 did not include frictional damping and energy dispersion like the hand calculations account for. For this reason, the methods are described with their basic results and why they did not work. Excessive detail is not provided because they are all tangential to the direction of finding a solution.

Placing columns as rotational restraints changes the frequency of the system depending on the column stiffness. This approach does not help because it changes the frequencies as compared to the hand calculations, which do not consider the stiffness of the columns. This method is not recommended because it does not use the same modeling assumptions as the hand calculations.

Portions of mass were omitted in the bay beyond the effective panel width. This drastically increased the natural frequency of the system. This increase in natural frequency of the system makes the results even worse because previously it was possible to match peak accelerations.

Static deflection plots were made to see what was happening in the SAP2000 model. A static point load was placed in the middle of the bay, and the resulting deflected shape was plotted. The distances to the inflection points were measured to see if there was some relation between this and the effective panel width. This was done with the expectation that a new effective panel width equation could be determined from FE models. However, this was done before realizing that SAP2000 did not include frictional damping that increases with panel area. Thus, none of these plots were of any use since the source of error most likely lies within the FE models instead of the hand calculations.

To obtain the modal contributions, the acceleration trace was analyzed to obtain the peak acceleration. The components of the acceleration trace were then broken down according to each mode and analyzed to determine the relative contribution of each mode shape. The thought behind this was that participation of higher modes in SAP2000 could have been causing some discrepancy between the hand calculations and the FE models. Table 5.5 shows an example of a system that had a peak acceleration of 0.2274% g. The table shows that almost all of the contribution is from the first mode and the error was not because of this.

Table 5.5 - Modal Contributions

Mode	Freq. (Hz)	Acceleration (% g)
1	3.10	-0.1952
2	11.72	0.0000
3	12.24	-0.0205
4	17.06	0.0000
5	23.81	-0.0111

Mode	Freq. (Hz)	Acceleration (% g)
6	23.37	0.0000
7	26.95	-0.0005
8	27.70	0.0000
9	33.11	0.0000
10	35.21	0.0000

Forcing functions at different frequencies were used in order to attempt a match of the FE model results with the hand calculations. However, the forcing functions that produce the maximum peak acceleration are those which have the same frequency as that of the first natural frequency of the floor. All other frequencies produce a smaller peak acceleration value. This was not desired in this case, since the peak accelerations from the FE models were already too small.

None of these methods prevailed in bridging the gap between peak accelerations obtained from finite element models and those derived from hand calculations.

5.7 CONCLUSIONS AND SUMMARY OF RESULTS

All of the FE results matched the Design Guide procedure results well until the system width exceeded the effective panel width calculated from the design guide calculations. The error definitely lies within this area. The problem is that SAP2000 cannot directly account for frictional damping in systems, nor can it account for energy dispersion. The only damping it can consider is viscous modal damping. The effective panel width equation accounts for effects of energy dispersion and frictional damping, which increases with increased panel size. Further research is required in this area to find an appropriate way to account for these effects by using FE models.

CHAPTER VI
CONCLUSIONS AND RECOMMENDATIONS

6.1 INTRODUCTION

This chapter presents the final conclusions derived from the four main areas of this study.

The first area of research dealt compared finite element models with real structural systems. These structural systems were simple systems. This provided an opportunity to explore modeling techniques of a cantilever staircase and to see how well a heel-drop trace could be simulated in the model. The other structural system was the Virginia Tech Laboratory Floor. This simple system modeling allowed experimentation with retrofits to reduce vibration.

The second area of research also used the Virginia Tech Laboratory Floor. The floor was used for various experiments. All of these experiments were focused on comparing finite element models with test data. The first experiment was done to measure damping. The second experiment was done to compare mode shapes. The third experiment was done to compare peak accelerations with a known sinusoidal forcing function.

The third area of research was done to find an inexpensive method of field-testing for a floor system. This method of testing would determine the acceptability of the floor system with a quick evaluation and without use of a finite element model.

The fourth area of research was an analytical pursuit of the source of difference between the accelerations determined by the procedure in the AISC Design Guide and the accelerations produced by a finite element model.

Also found in this chapter are areas of future research.

6.2 GENERAL CONCLUSIONS

6.2.1 Research Area One – The Staircase and Retrofits

The staircase experiment did not yield very good results. The actual staircase had a natural frequency of 7.5 Hz and the finite element model yielded a frequency of 11.0 Hz.

The experiment with the retrofits on the Virginia Tech Lab floor showed that different locations on the floor can experience different annoying frequencies. Those frequencies that are most annoying are based on how close an occupant is to an anti-node for a certain mode. The experiment also shows how a second-mode frequency could be more disturbing than the fundamental natural frequency to people on portions of the floor where the anti-nodes for this second mode occur. Another factor in determining the most annoying frequency for a particular system is the excitation frequency.

Another discovery from this area of research was that a retrofit should be placed at the anti-node of the most annoying frequency of the floor instead of necessarily at the center. Placement of a retrofit at the center is satisfactory when the most annoying frequency is the fundamental natural frequency. This is because the anti-node for that mode shape is usually located there. However, if complaints from occupants arise from areas that are affected more by higher modes, then placing the retrofit at the center of the bay will not be the most effective method of vibration reduction.

The best type of retrofit used posts and a spreader-beam assembly. The second best retrofit used only the post at a point location, and supported the floor on the underside of the deck. However, the retrofit with the spreader-beam provided a larger contact area. The spreader-beam supported the floor on the bottom of the top chord of the joists. This caused the load transfer to go from a larger area of the slab to the joists and then to the post. This could possibly help reduce rotation of other modes, which would reduce their participation in vibration depending on how much rotational restraint is provided by the spreader-beam assembly.

6.2.2 Research Area Two – Virginia Tech Lab Floor Experiments

Damping measurement on the Virginia Tech Lab Floor did not match the assumed value. The value of damping obtained (2.04% of critical) was about twice as much as what was expected for an empty floor. This caused the values of peak acceleration to not match the finite element model. If the damping were in the range of 1.32% to 1.61% of critical damping, then the peak acceleration values would have matched. The Experimental Modal Analysis (EMA) provided a mode shape plot with an excellent match to the finite element data. This research shows that the mode shapes that really exist in a floor can be predicted well with a finite element model.

6.3.3 Research Area Three – Field Evaluation

The results from this area of research could not be used to establish a practical method for determining the acceptability of a floor by only using a hand-held analyzer, an accelerometer, and a series of walking tests. Also, measurements at more than one location on a bay are needed, depending on where the occupants are located.

Several data points on each bay should be read to determine the frequencies that contribute to annoying vibrations. The FFT spectrum will provide the frequencies that contribute the most to vibration in each area of the floor. This data can then be compared to the results of a finite element analysis to determine which mode shape contributes most to the vibration. After the problem mode shape is determined, a retrofit can be placed in a location that would best eliminate or limit participation of the problem mode. The best location for a retrofit is at an anti-node.

The use of a finite element model is required for a detailed analysis instead of hand calculations if the first mode shape is not the mode shape that contributes to the most annoying vibration. The finite element analysis is the only method used in this study that will predict multiple mode shapes and their corresponding frequencies.

6.3.4 Research Area Four – Missing Link Between AISC and FE Methods

All of the results matched well until the system width exceeded the effective panel width calculated from the Design Guide criteria. The error definitely lies within this area. The problem is that SAP2000 cannot directly account for frictional damping in systems, nor can it account for energy dispersion. The only damping it can consider is viscous modal damping. The effective panel width equation accounts for effects of energy dispersion and frictional damping, which increases with increased panel size. Further research is required in this area to find an appropriate way to account for these effects by using FE models. Due to this error, larger floor systems modeled will have matching frequencies, but the peak accelerations will not match. Although the location of the problem was established, a solution could not be determined from this research.

6.3 AREAS OF FUTURE RESEARCH

6.3.1 Modeling considerations

There are many areas possible for future research in the field of floor vibrations. The first part of this study (in Chapter II) left an opening in the area of the finite element modeling. Instead of assuming rigid supports for the retrofit posts, they could have been modeled as springs with appropriate stiffnesses. This closer investigation would provide more accurate results in predicting the effectiveness of retrofits in floor systems.

A finite element model for predicting the heel-drop spectrum and natural frequency of a cantilever staircase was not accomplished. Further research in this area could be explored. This would be especially useful if the natural frequency of the staircase was such that it excited the natural frequency of the floor system to which it is attached. The reason for this is that annoying vibration on a floor system could come from the staircase, which is not considered in hand calculations.

6.3.2 Other areas of research

Further research in the area of floor vibrations is needed where the AISC Design Guide does not provide methods to analyze certain floors by simple hand calculations. Such floors cannot use these hand calculations due to inherent complexities. A lot of research is needed in the computer modeling aspect of floor vibrations.

List of References

Allen, D. E., and Murray, T. M. (1993). "Design Criterion for Vibrations Due to Walking." *AISC Engineering Journal*, 4th qtr., 117-129.

Band, B. S. Jr. (1996). "Vibration Characteristics of Joist and Joist-Girder Members." M.S. Thesis, Virginia Polytechnic Institute and State University, Blacksburg, Virginia.

Beavers, T. A. (1998). "Fundamental Natural Frequency of Steel Joist Supported Floors" M.S. Thesis, Virginia Polytechnic Institute and State University, Blacksburg, Virginia.

Gibbings, D. R., Easterling, W. S., and Murray, T. M. (1993). "Analysis of Composite Joists." Report No. CE/VPI 93/12. Virginia Polytechnic Institute and State University, Blacksburg, Virginia.

Hanagan, L. M. (1994). "Active Control of Floor Vibrations." Ph. D. Dissertation, Virginia Polytechnic Institute and State University, Blacksburg, Virginia.

Lenzen, Kenneth H. (1966). "Vibration of Steel Joist Concrete Slab Floors." *Engineering Journal*, American Institute of Steel Construction, 2(3), pp. 133-136.

Murray, T. M. (1975). "Design to Prevent Floor Vibrations." *Engineering Journal*, AISC, 12(3), 82-87.

Murray, T. M. (1981). "Acceptability Criteria for Occupant-Induced Floor Vibrations." *Engineering Journal*, AISC, 18(2), 62-69.

Murray, T.M. (1991) "Building Floor Vibrations" *Engineering Journal*, AISC, 28(3), pp. 102-109.

Murray, T. M., Allen, D.E and Ungar, E. E. (1997). *AISC Steel Design Guide Series 11: Floor Vibrations Due to Human Activity.* American Institute of Steel Construction, Chicago.

Reiher, H. and Meister, F. J. (1931). "The Effect of Vibration on People" (in German). *Forchung auf dem Gebetite des Ingenieurwesens*, 2(2), p. 381. (Translation: Report no. F-TS-616-Re H.Q. Air Material Command, Wright Field, Ohio, 1949).

Rottmann, C. E. (1996). "Use of Tuned-Mass Dampers to Control Annoying Floor Vibrations." M.S. Thesis, Virginia Polytechnic Institute and State University, Blacksburg, Virginia.

Shamblin, C. L. (1989). "Floor System Response to Heel-Drop Impact." M.S.Thesis, Virginia Polytechnic Institute and State University, Blacksburg, Virginia.

Sladki, M. J. (1999). "Prediction of Floor Vibration Response Using the Finite Element Method." M.S. Thesis, Virginia Polytechnic Institute and State University, Blacksburg, Virginia.

Treadgold, T. (1828). *Elementary Principles of Carpentry,* 2nd Ed., Publisher unknown.

APPENDIX A

CANITLEVER STAIRCASE PLANS

The plans of the cantilever staircase include only structural members that are essential to strength. The railing components are not shown here, as they are not essential to the modeling process (with the exception of addition of weight and mass). The supports are on the left side of the staircase and were modeled as fixed supports.

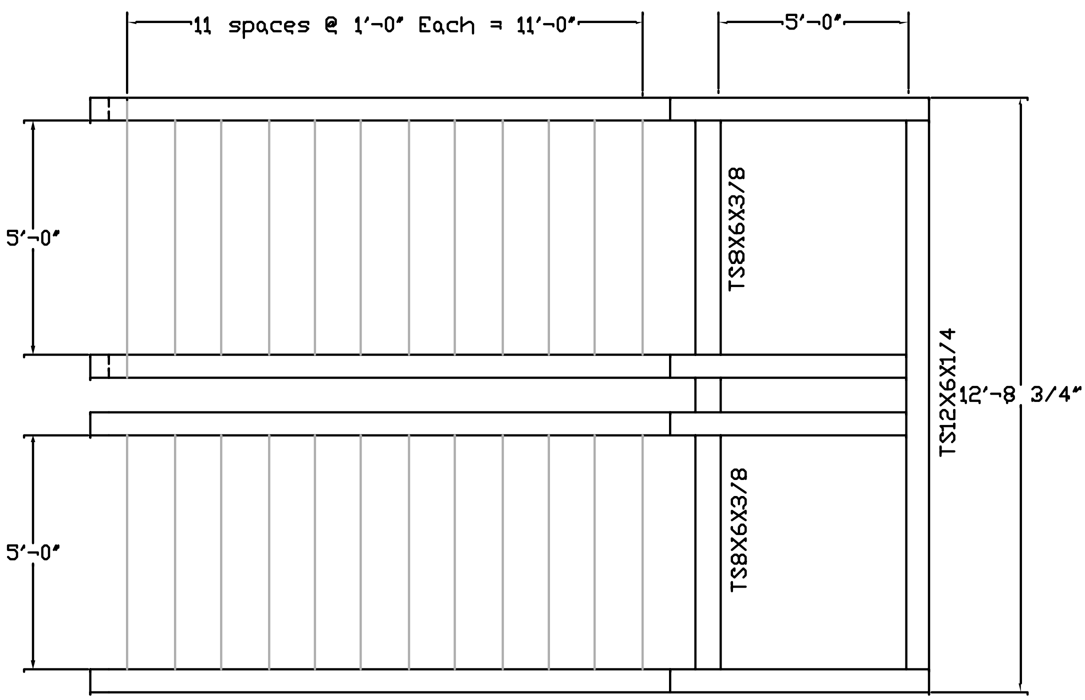

Figure A.1 – Plan View of Staircase

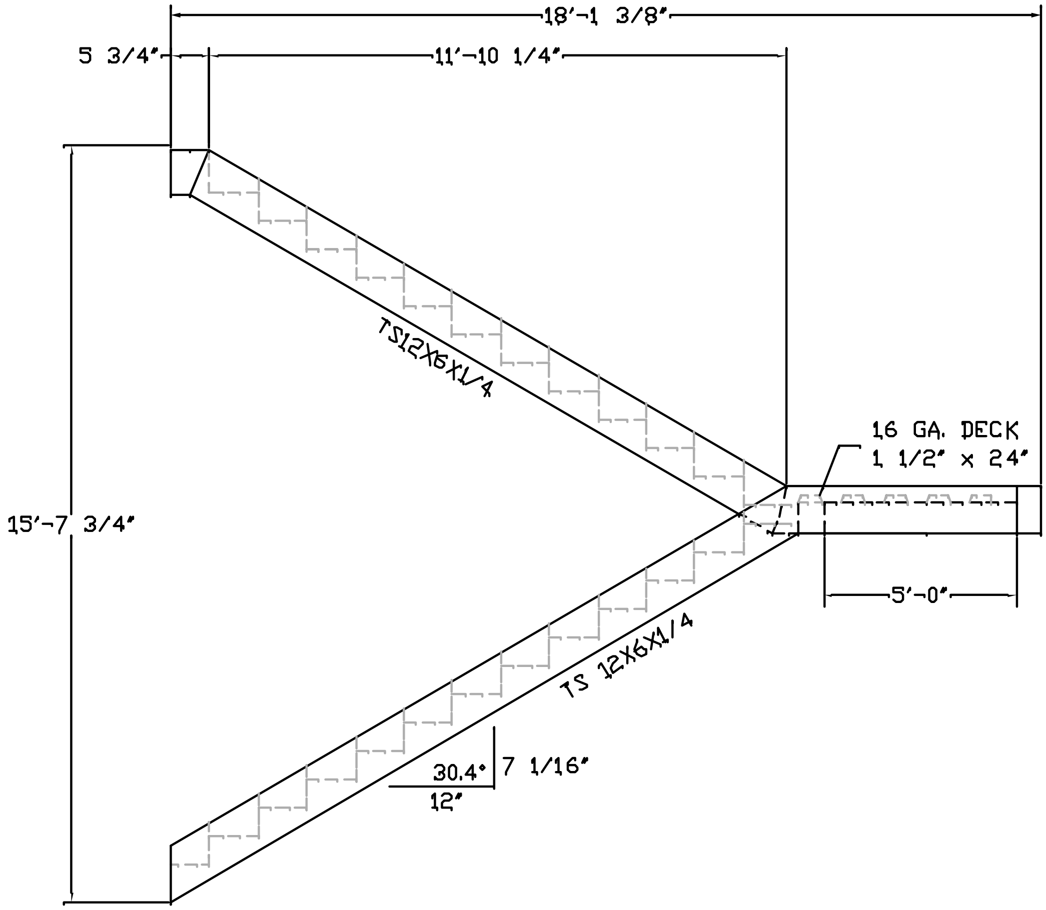

Figure A.2 – Elevation View of Staircase

APPENDIX B

DESIGN GUIDE CALCULATIONS FOR LAB FLOOR

VIBRATION ANALYSIS:

Activity: Walking
Occupancy Category: Office or Residence
Evaluation Criterion: Walking, AISC Design Guide, Chapter 4
Reference: Murray, T.M., Allen, D.E. and Ungar, E.E, "Floor Vibrations Due To Human Activity", Design Guide, June 1997

Constant Force,	P_o = 65 lb
Modal Damping Ratio,	ß = 0.03
Acceleration Limit,	a_o/g x 100% = 0.50 %
Joist bottom chords are not extended	
Girders are not continuous at columns	

	Section	w, plf	I_{tr},in^4	f, Hz.
Beam	joist	116.9	1960.4	8.49
Left Girder	jg	896.3	2988.1	8.15
Right Girder	jg	896.3	2988.1	8.15
Bay (Using smaller girder frequency)				5.88

Evaluation:

Combined mode a_p/g= 0.79 % > 0.50 %

The system DOES NOT SATISFY THE CRITERION.

LOADING DATA:

3.1c psf Deck	=	33.5 psf
Dead loads	=	0.0 psf
Collateral loads	=	0.0 psf
Live loads	=	0.001 psf

Actual beam and girder weights
Tributary width for girder = 44.00/2 = 22.00 ft.

CONCRETE/SLAB DATA:

Concrete	d_c= 3.00 in.	f_c'= 3.5 Ksi
	wt= 145 pcf	E_c= 3267 Ksi

Modular ratio, n= $E_s/(1.35\ E_c)$ = 6.58

Deck height: 0.625 in.
Effective concrete thickness in deck: 0.3125 in.

SUPPORTED MEMBER CALCULATIONS:

Built-up member: joist (16.4 plf)
A= 4.824 in.^{2} I_{chords}= 1412 in.^{4} y_c= 15.86 in.
Spacing: S = 36 in.
Span: L_j = 44.00 ft.
Uniform load: w_j = (33.5 + 0.0 + 0.0 + 0.001) x 36.00/12 + 16.4
= 116.9 plf
Moment of inertia:

Effective concrete width	= min(0.4 L_j, S)	=	36.000 in.
Effective concrete depth		=	2.375 in.
Transformed concrete width		=	5.475 in.
Transformed concrete area		=	13.003 in.^{2}
Distance to neutral axis	(Above joist c.g.)	=	13.935 in.
Tr. moment of inertia using actual chords	I_{comp}	=	2517.0 in.^{4}

$6 \le L_j/D = 14.67 \le 24$ (OK)
$C_r = 0.90[1\text{-}\exp(-0.28(L/D))]^{2.8} = 0.8627$

$$\gamma = \frac{1}{C_r} - 1 = \frac{1}{0.8627} - 1 = 0.1592$$

$$I_{eff} = \frac{1}{\dfrac{\gamma}{I_{chords}} + \dfrac{1}{I_{comp}}} = \frac{1}{\dfrac{0.1592}{1412} + \dfrac{1}{2517.0}} = 1960.4 \text{ in.}^4$$

$$\delta_j = \frac{5 w_j \times L_j^{\ 4}}{384 E_j I_{eff}} = \frac{5 \times 116.9 \times 44.00^4 \times 1728}{384 \times E_s \times 1960.4} = 0.173\text{in}$$

Frequency = 0.18 x $[g / \delta_j]^{0.5}$ = 0.18 x $[386 / 0.173]^{0.5}$ = 8.49 Hz.

C_j = 1.0
Floor Width = 30.00 ft.

D_s = $(12\ d_e^3)/(12\ n) = (12 \times 2.6875^3)/(12 \times 6.58)$
= 2.95 in^4/ft.

D_j = I_{eff}/S = 1960.4/3.00
= 653.47 in^4/ft.

B_j = min[$C_j\ (Ds/Db)^{0.25}\ L_j$= 11.40 ft.; 2/3 x 30.00 ft.= 20.00 ft.]
= 11.40 ft.

Continuity Factor=1.0 since max. adj. L_j=0.0 ft $\leq$ 0.7 L_j=30.80 ft.
$W_j = wB_jL_j$ (*w* is weight supported per unit area)
W_j = 1.0 x (0.117/3.00) x 11.40 x 44.00 = 19.6 Kips

GIRDER CALCULATIONS:

Built-up member: jg (38.9 plf)
A= 11.44 in.2 I_x= 3270 in.4 y_c= 18.00 in.

Tributary width		=	22.00 ft.
Span:	L_g	=	30.00 ft.
Equivalent uniform load:	w_g	=	22.00 x (116.9/3.00) + 38.9
		=	896.3 plf

Moment of inertia:
Min[0.2 L_g, L_g/2] = 72.000 " (10.950" transformed)

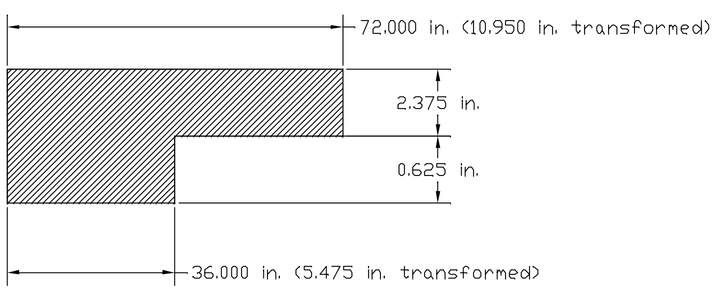

Effective concrete width		=	72.000 in. and 36.000 in.
Transformed concrete width		=	10.950 in. and 5.475 in.
Transformed concrete area		=	26.006 $in.^2$ and 3.422 $in.^2$
Joist Seat Depth		=	5.00 in.
Distance to neutral axis		=	13.907 in. (Above girder c.g.)
Transformed moment of inertia	I_{comp}	=	8224 $in.^4$

$6 \leq L_j/D = 10.00 \leq 24$ (OK)
$C_r = 0.90[1\text{-}\exp(-0.28(L/D))]^{2.8} = 0.7550$

$$\gamma = \frac{1}{C_r} - 1 = \frac{1}{0.7550} - 1 = 0.3245$$

$$I_{eff} = \frac{1}{\dfrac{\gamma}{I_{chords}} + \dfrac{1}{I_{comp}}} = \frac{1}{\dfrac{0.3245}{3270} + \dfrac{1}{8224}} = 4528 \text{ in.}^4$$

$I_{mod} = C_r I_{Chords}$

$I_g = I_{mod} + (I_{eff} - I_{mod}) = (0.755)(3270) + (1/4)[4528 – 0.755(3270)] = 2988.13 \text{ in.}^4$

$$\delta_g = \frac{5w_g \times L_g^{\ 4}}{384E_s I_g} = \frac{5 \times 896.3 \times 30.00^4 \times 1728}{384 \times E_s \times 2988.13} = 0.189\text{in.}$$

Frequency = $0.18 \text{ x } [g / \delta_b]^{0.5} = 0.18 \text{ x } [386 / 0.189]^{0.5} = 8.15$ Hz.

$C_g = 1.6$
Floor Length = 44.00 ft.
D_b = $I_{tr}/S = 1960.4/3.00$
= 653.47 in^4/ft.
D_g = I_{tr}/Avg. Lb = 2988.1/22.00
= 135.82 in^4/ft.
B_g = min[Cg $(Db/Dg)^{0.25}$ Lg= 71.09 ft.; 2/3 x 44.00 ft.= 29.33 ft.]
= 29.33 ft.
Continuity Factor = 1.0 since Not Continuous
W_g = wB_gL_g (*w* is weight supported per unit area)
W_g = 1.0 x (0.896/22.00) x 29.33 x 30.00
= 35.9 Kips

COMBINED MODE CALCULATIONS:

Using girder with smaller frequency:

δ_b = 0.173 in. δ_g = 0.189 in.

System frequency, f_n= 0.18 [386/(δ_b+ δ_g)]=5.88 Hz

W_b= 34.3 Kips W_g = 35.9 kips

$$w_c = \frac{\delta_b}{\delta_b + \delta_g} w_b + \frac{\delta_b}{\delta_b + \delta_g} w_g$$

W_c = [(0.173/0.362) x 19.6] + [(0.189/0.362) x 35.9] = 28110 lbs

ß = modal damping ratio = 0.03

$(a_p/g) = [P_o\ e^{(-0.35\ fn)}]/(ß\ Wc)$
$= [65\ e^{(-0.35 \times 5.88)}]/(0.03 \times 28110)$
= 0.99 % > 0.50 % - DOES NOT SATISFY CRITERION
Since f_n= 5.88 Hz ≤ 9 Hz - Stiffness criterion does not need to be checked.

APPENDIX C
FRF SPECTRA PLOTS

These FRF Spectra Plots are taken from the data readings on the Virginia Tech laboratory floor during the retrofit tests.

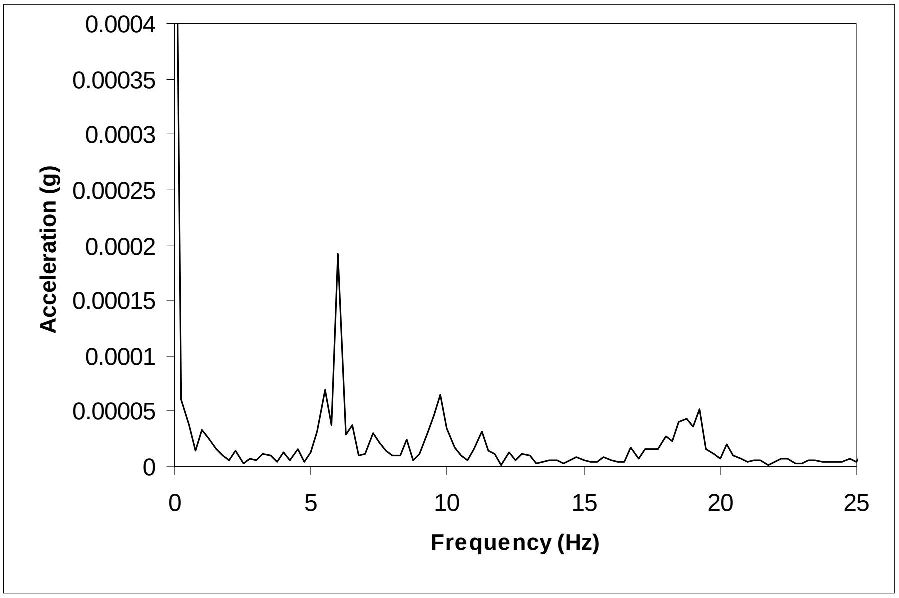

Figure C.1 – FRF Spectrum from Ambient Excitation for TCN 1

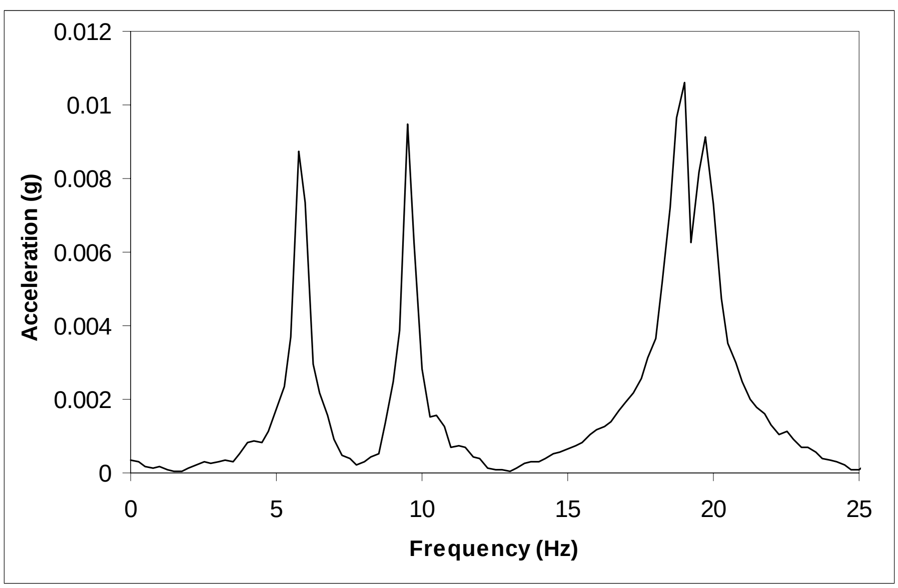

Figure C.2 – FRF Spectrum for Heel Drop Excitation for TCN 1

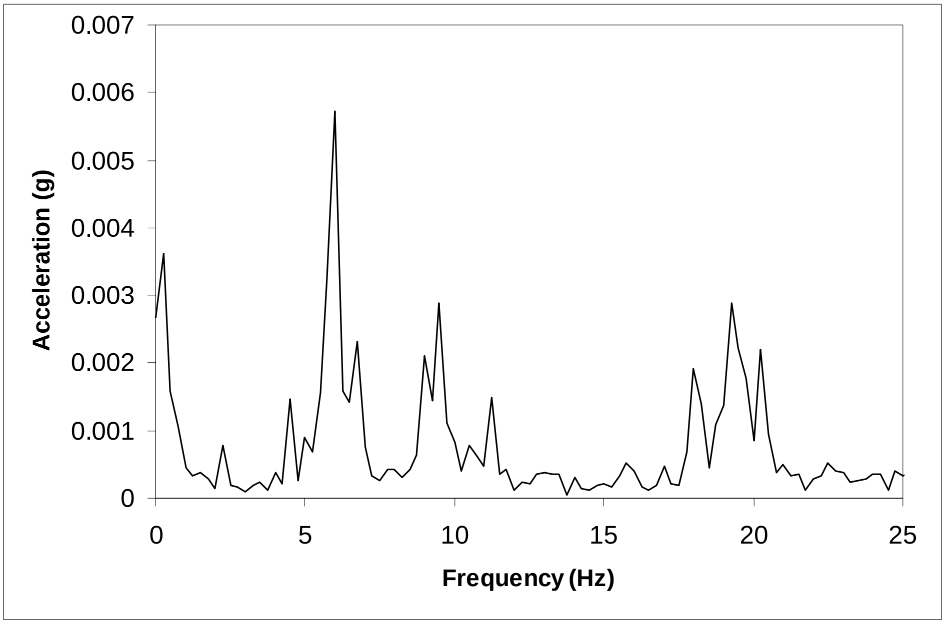

Figure C.3 – FRF Spectrum for Walking Parallel Excitation for TCN 1

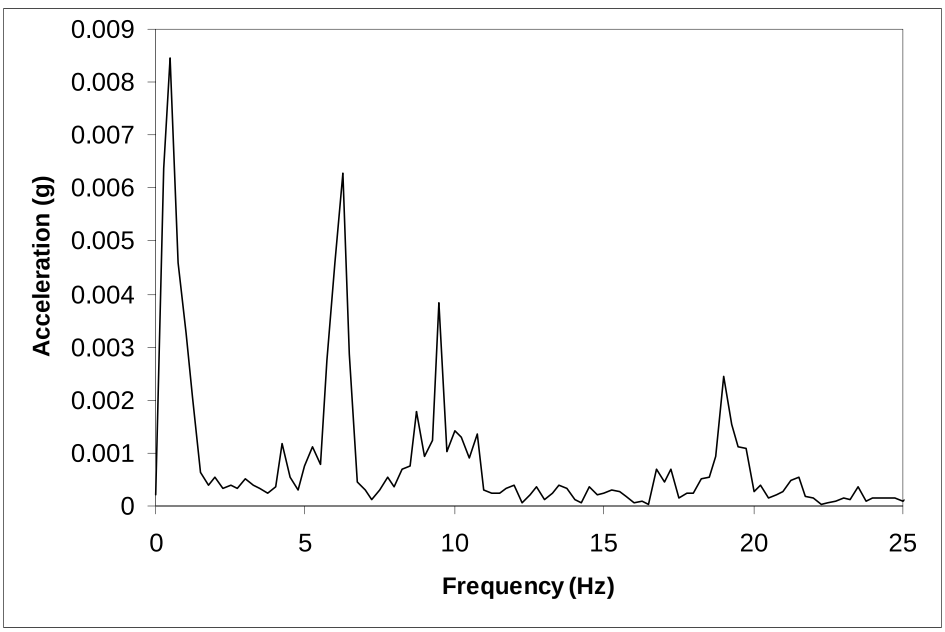

Figure C.4 – FRF Spectrum for Walking Perpendicular Excitation for TCN 1

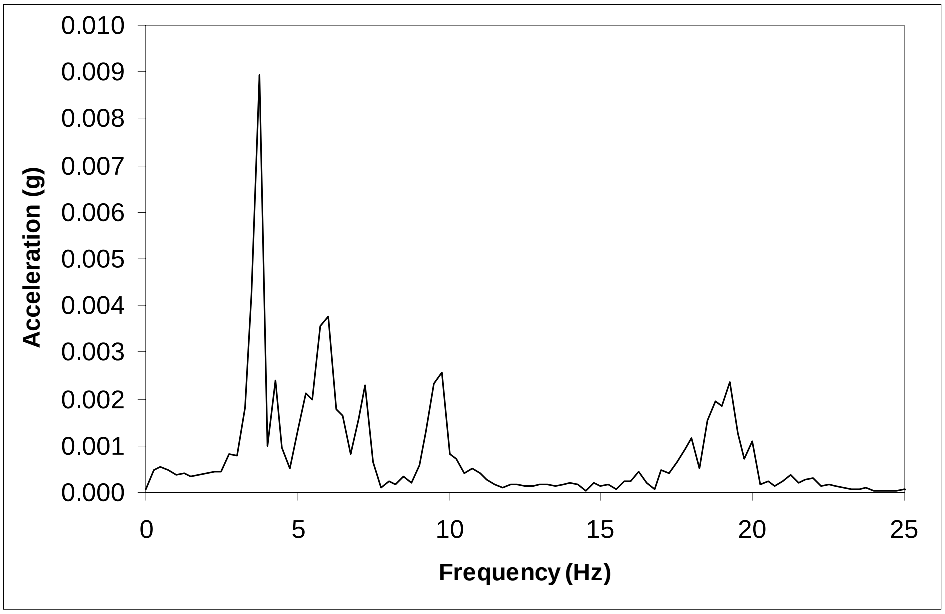

Figure C.5 – FRF Spectrum for Bouncing Excitation for TCN 1

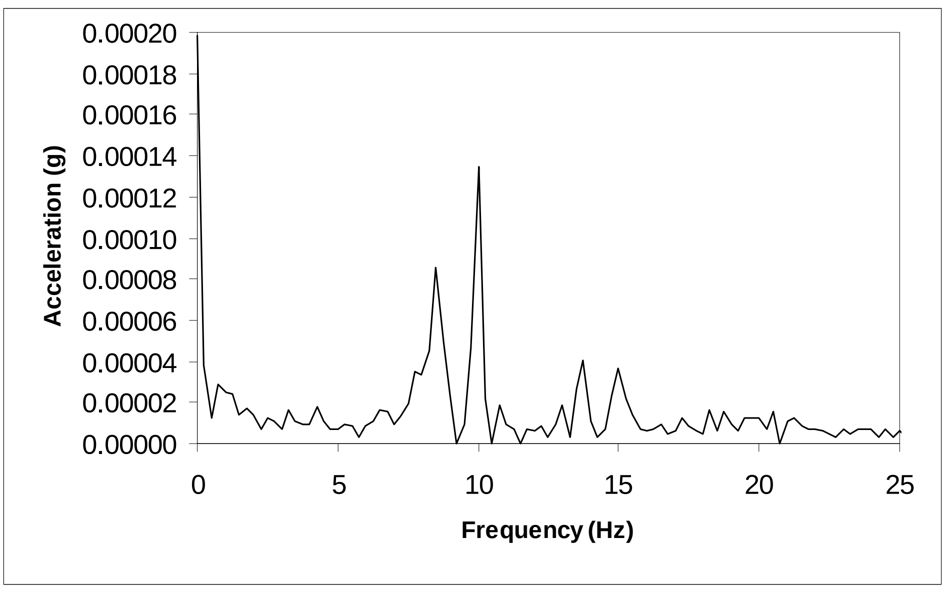

Figure C.6 – FRF Spectrum for Ambient Excitation for TCN 2

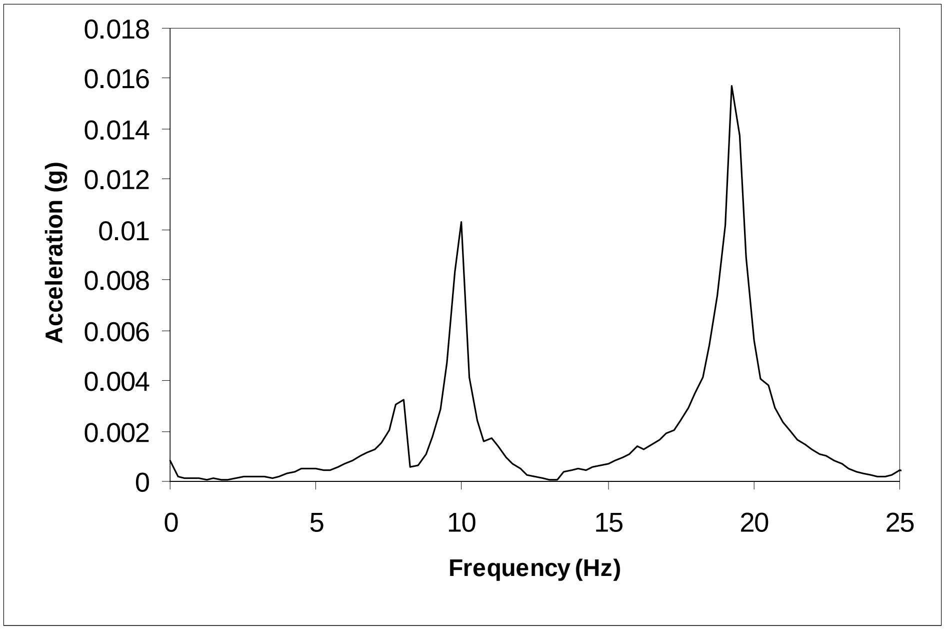

Figure C.7 – FRF Spectrum for Heel Drop Excitation for TCN 2

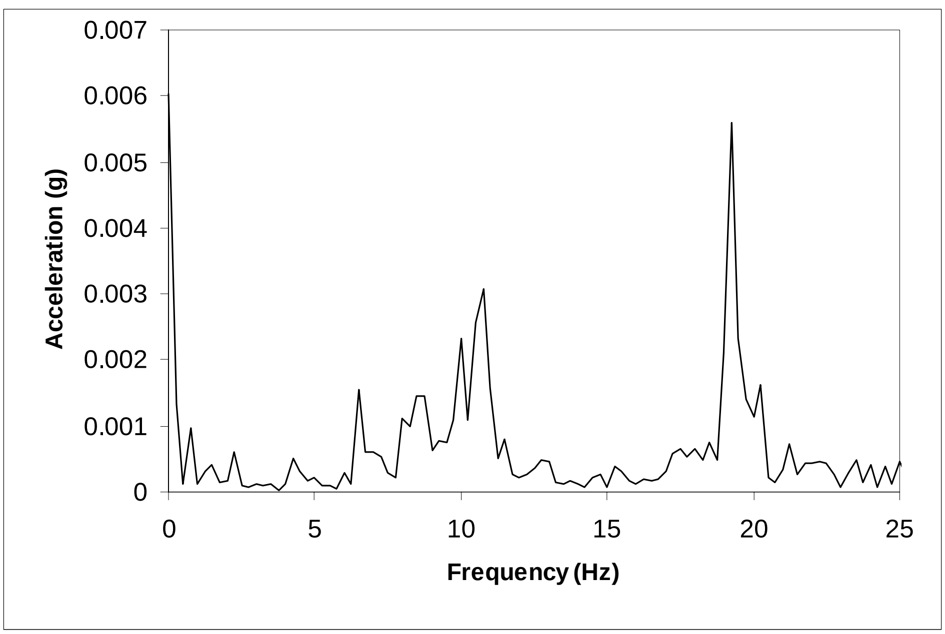

Figure C.8 – FRF Spectrum for Walking Parallel Excitation for TCN 2

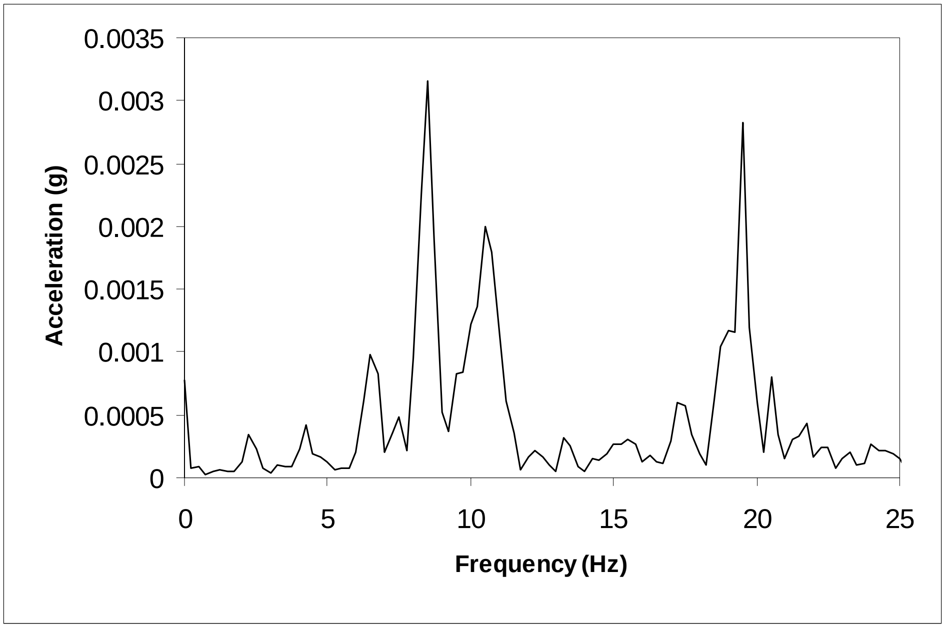

Figure C.9 – FRF Spectrum for Walking Perpendicular Excitation for TCN 2

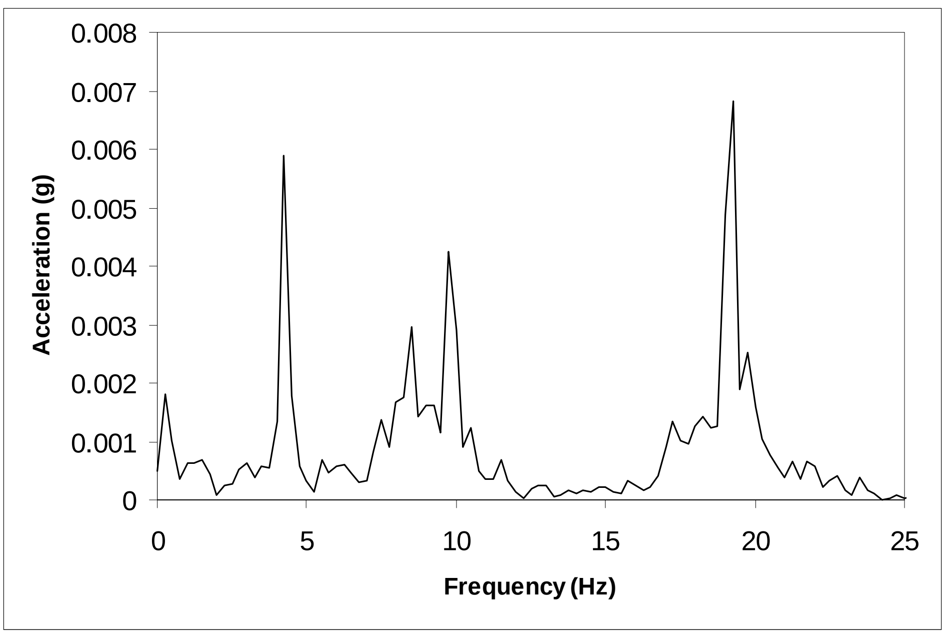

Figure C.10 – FRF Spectrum for Bouncing Excitation for TCN 2

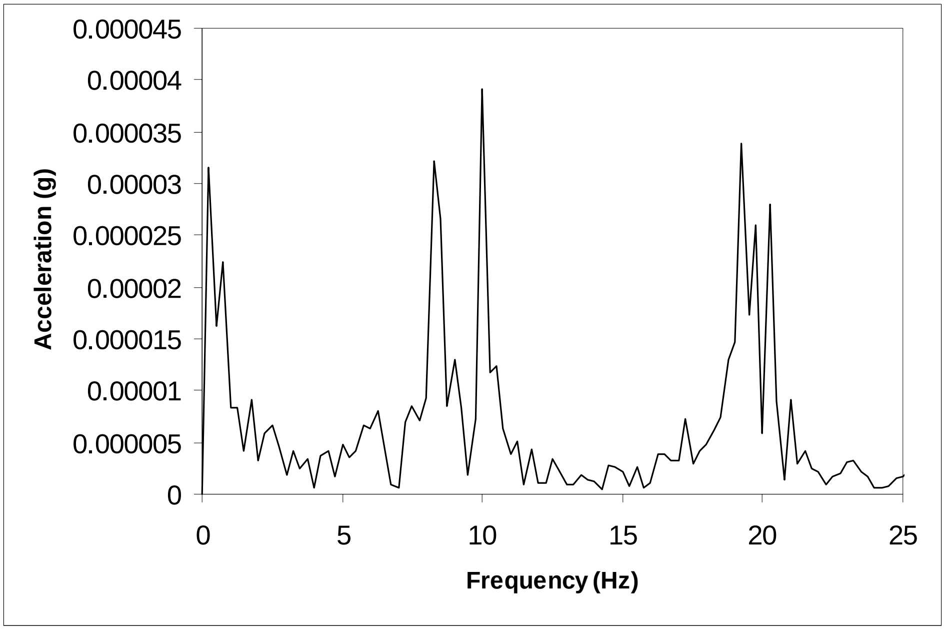

Figure C.11 – FRF Spectrum for Ambient Excitation for TCN 3

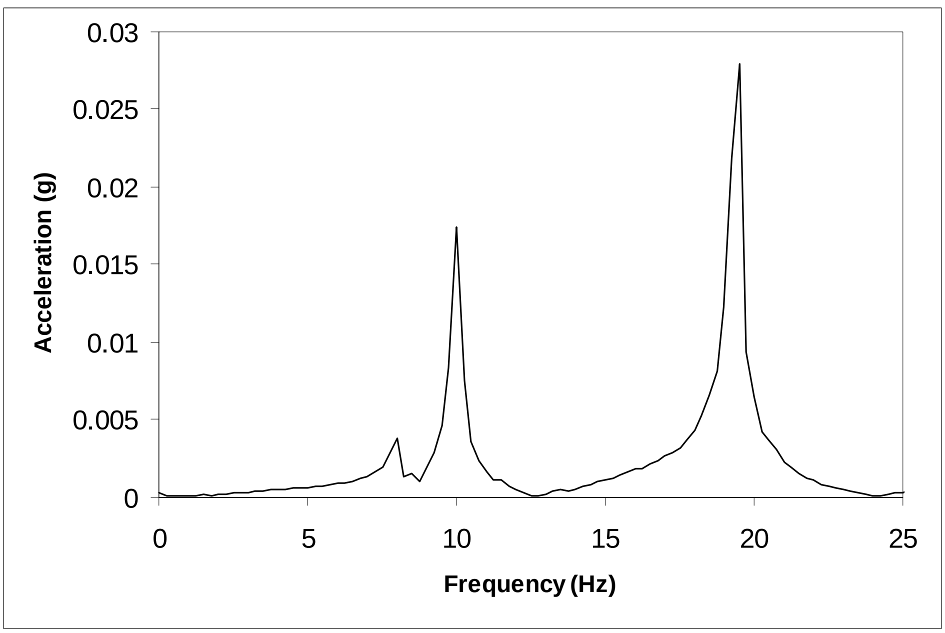

Figure C.12 – FRF Spectrum for Heel Drop Excitation for TCN 3

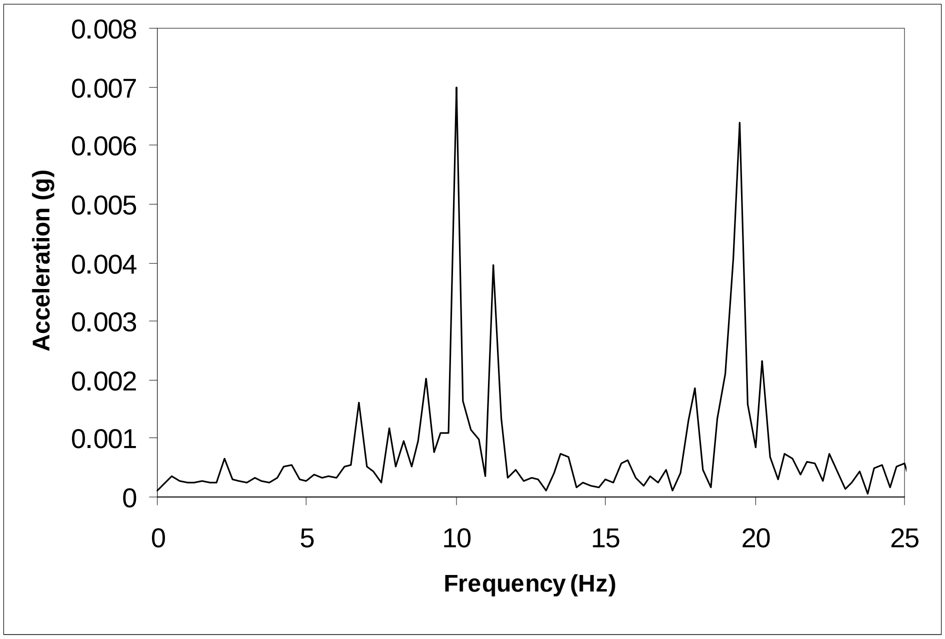

Figure C.13 – FRF Spectrum for Walking Parallel Excitation for TCN 3

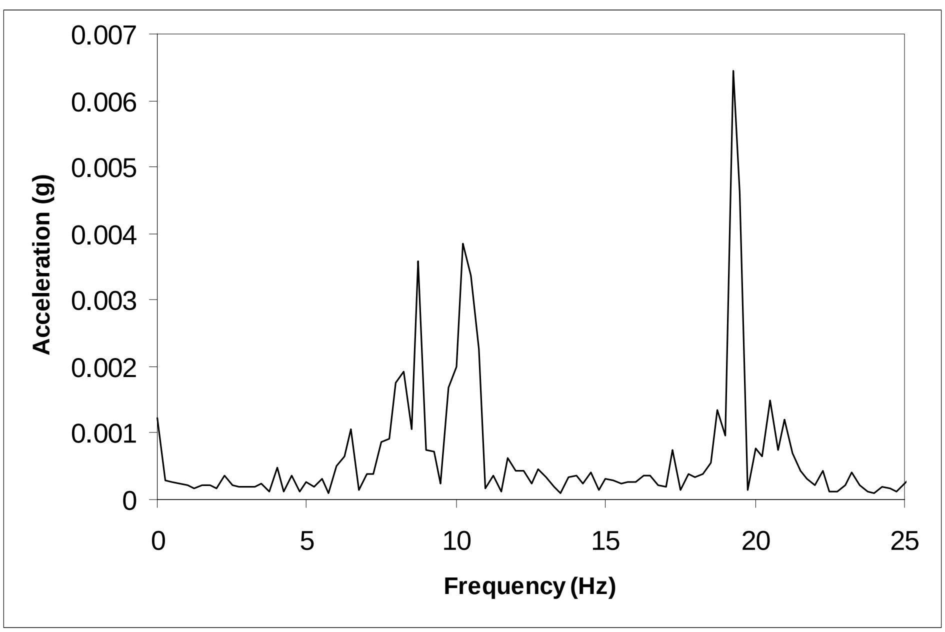

Figure C.14 – FRF Spectrum for Walking Perpendicular Excitation for TCN 3

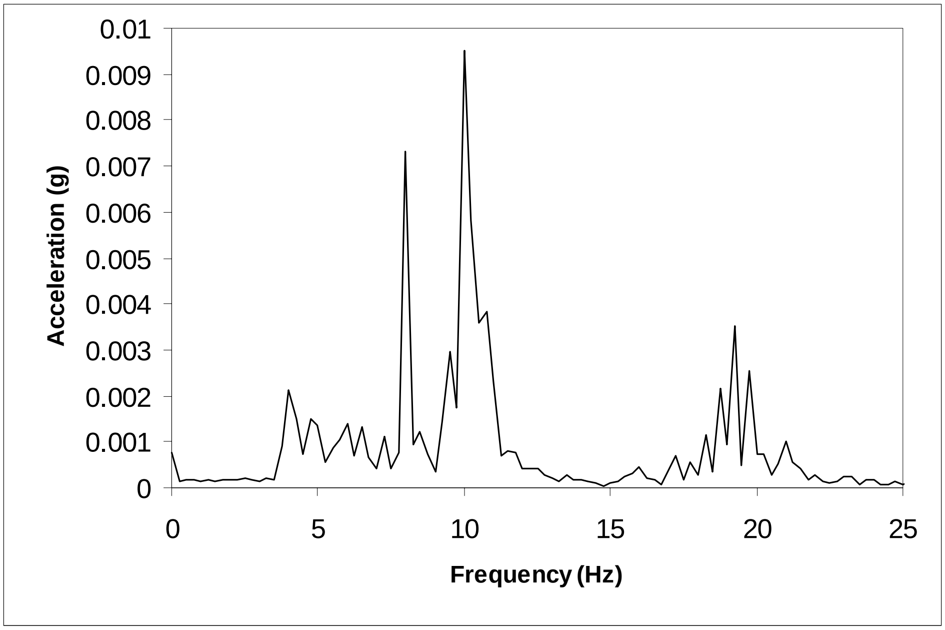

Figure C.15 – FRF Spectrum for Bouncing Excitation for TCN 3

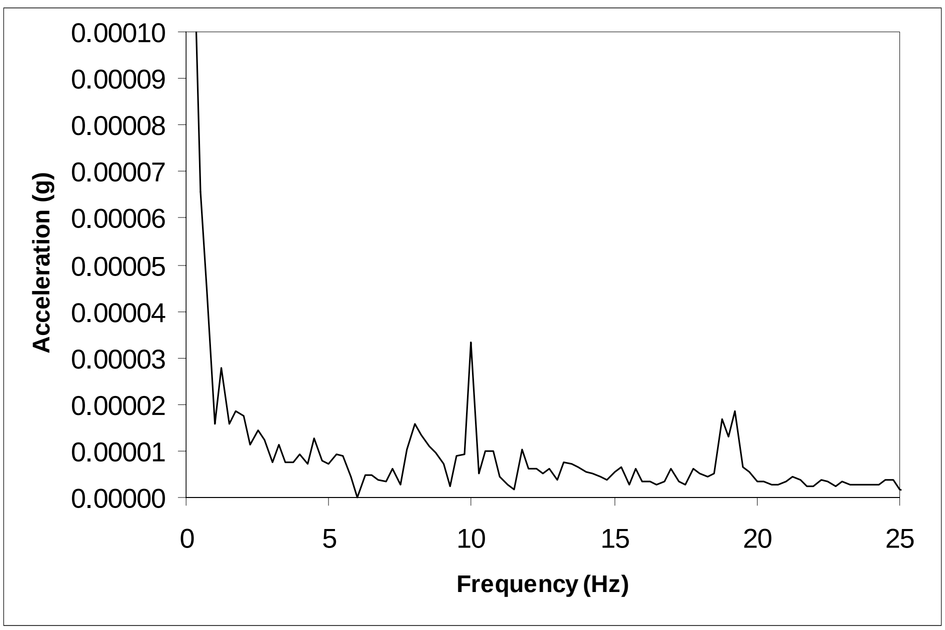

Figure C.16 – FRF Spectrum for Ambient Excitation for TCN 4

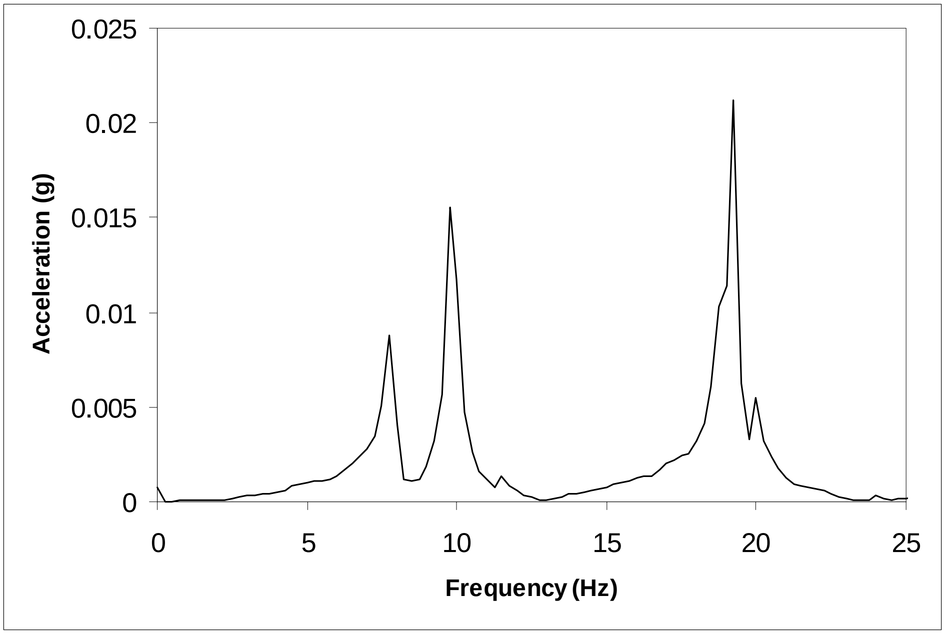

Figure C.17 – FRF Spectrum for Heel Drop Excitation for TCN 4

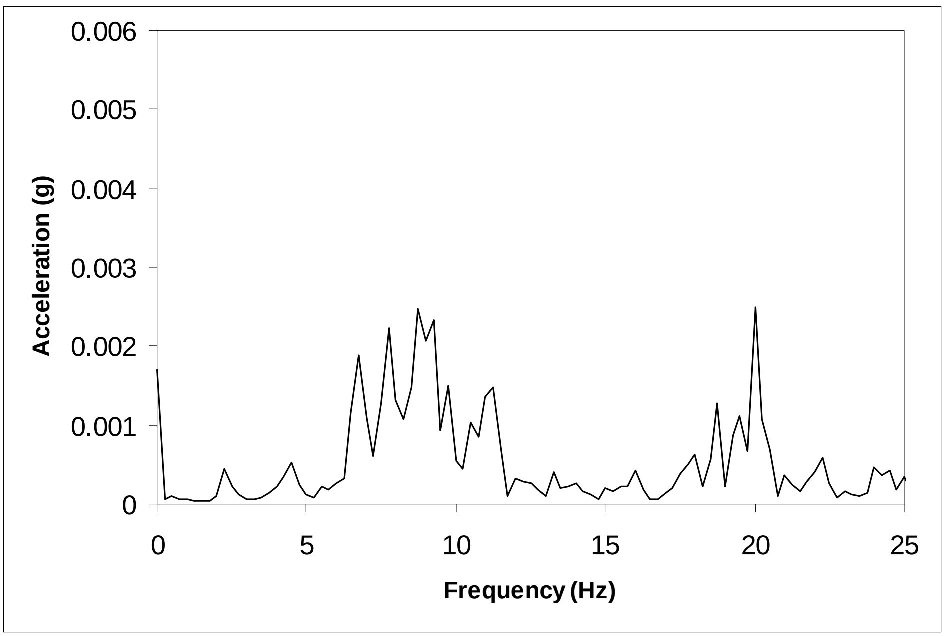

Figure C.18 – FRF Spectrum for Walking Parallel Excitation for TCN 4

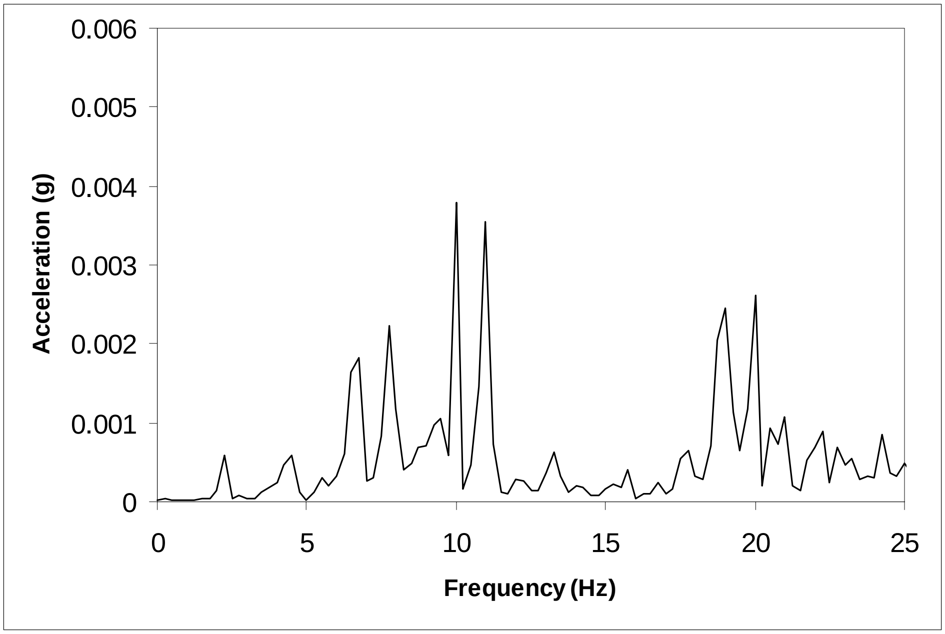

Figure C.19 – FRF Spectrum for Walking Perpendicular Excitation for TCN 4

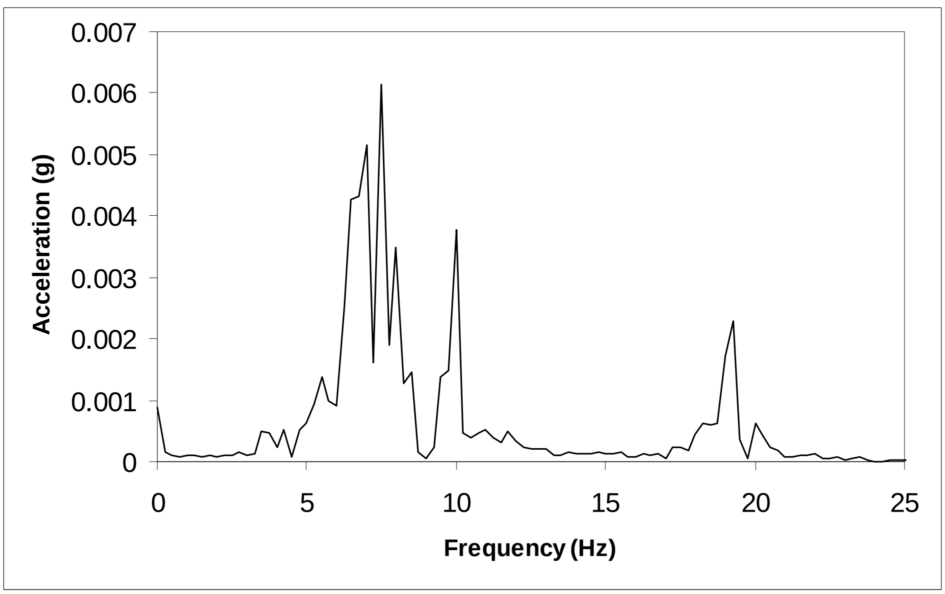

Figure C.20 – FRF Spectrum for Bouncing Excitation for TCN 4

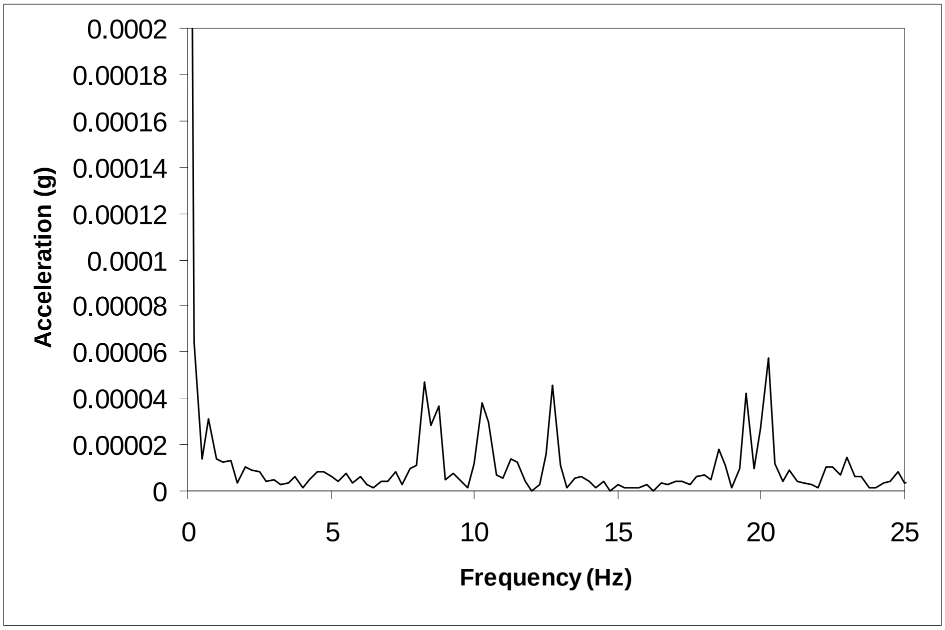

Figure C.21 – FRF Spectrum for Ambient Excitation for TCN 5

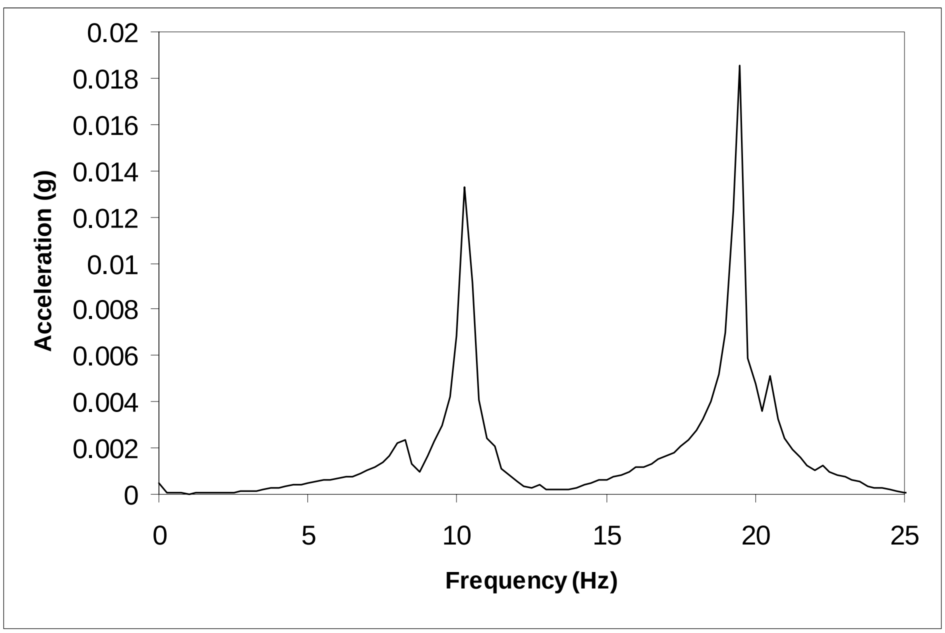

Figure C.22 – FRF Spectrum for Heel Drop Excitation for TCN 5

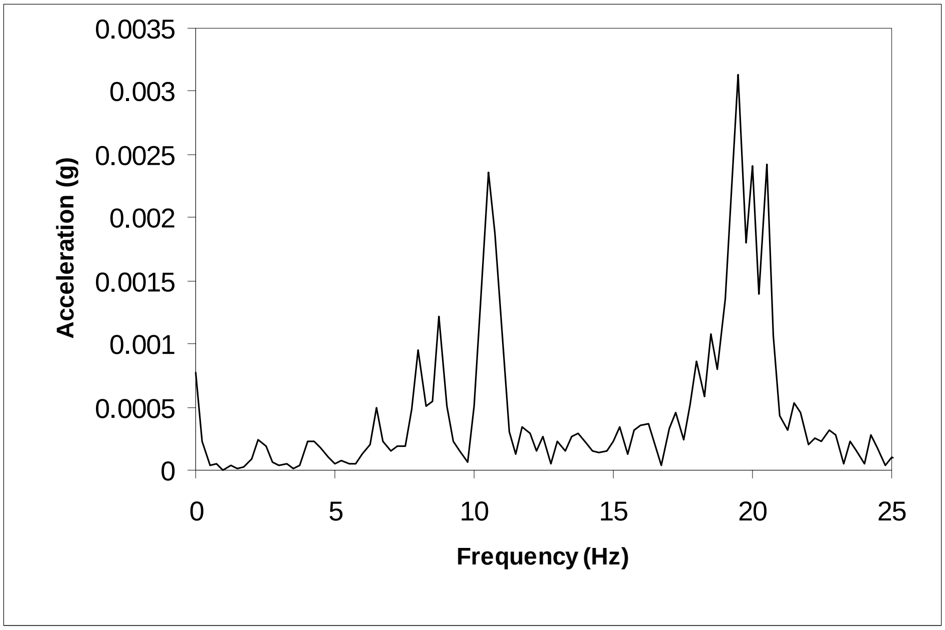

Figure C.23 – FRF Spectrum for Walking Parallel Excitation for TCN 5

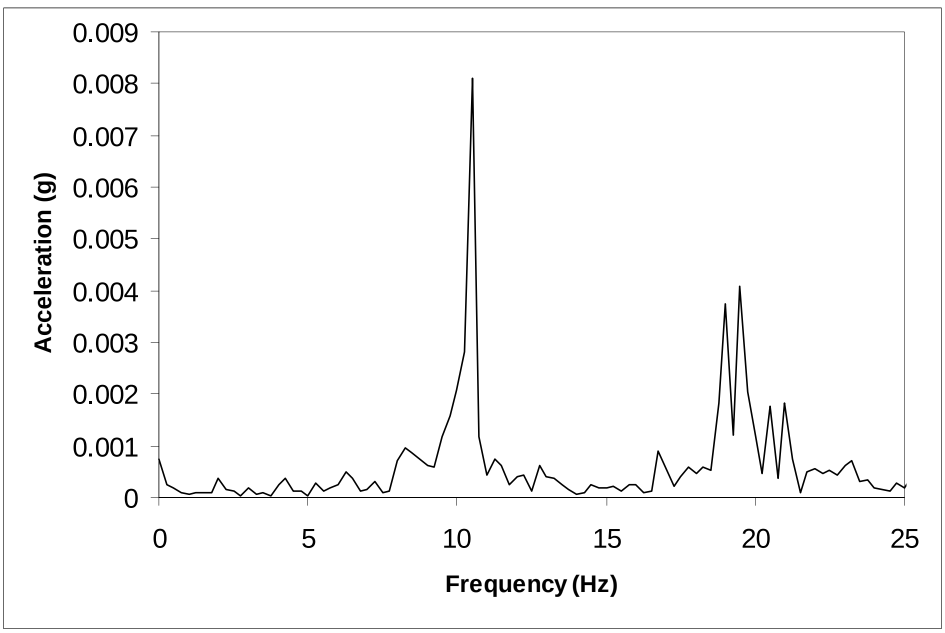

Figure C.24 – FRF Spectrum for Walking Perpendicular Excitation for TCN 5

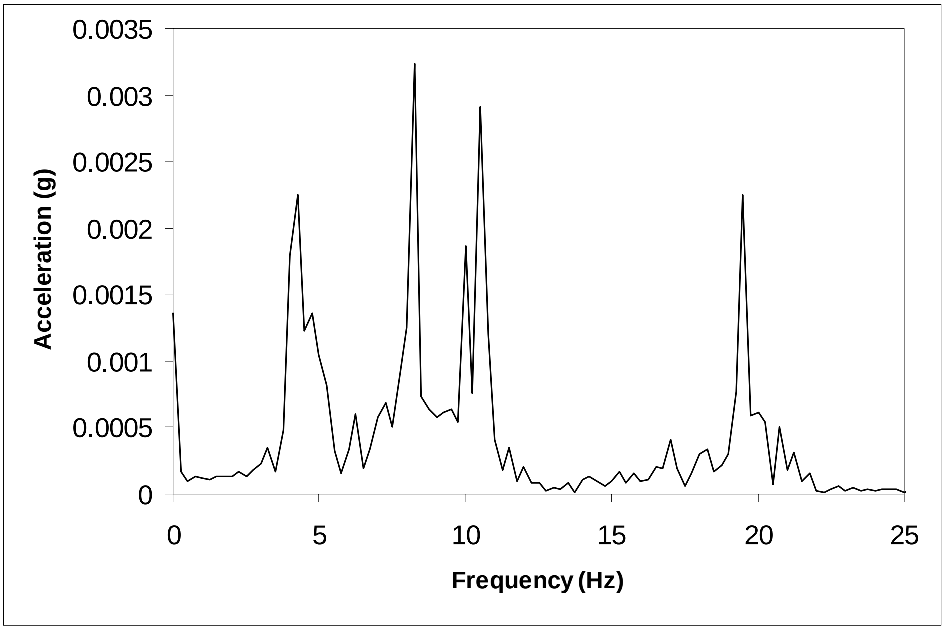

Figure C.25 – FRF Spectrum for Bouncing Excitation for TCN 5

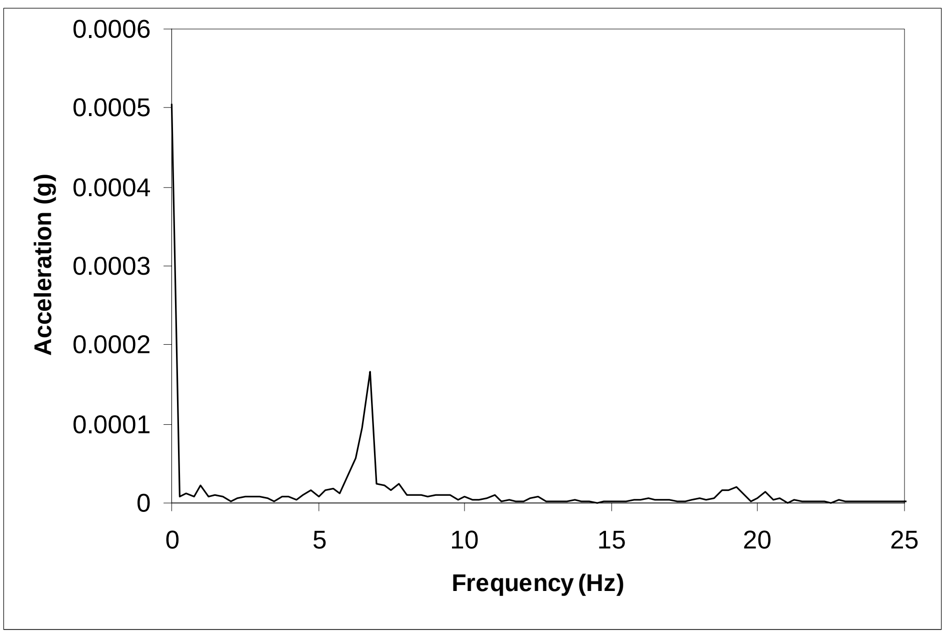

Figure C.26 – FRF Spectrum for Ambient Excitation for TCN 6

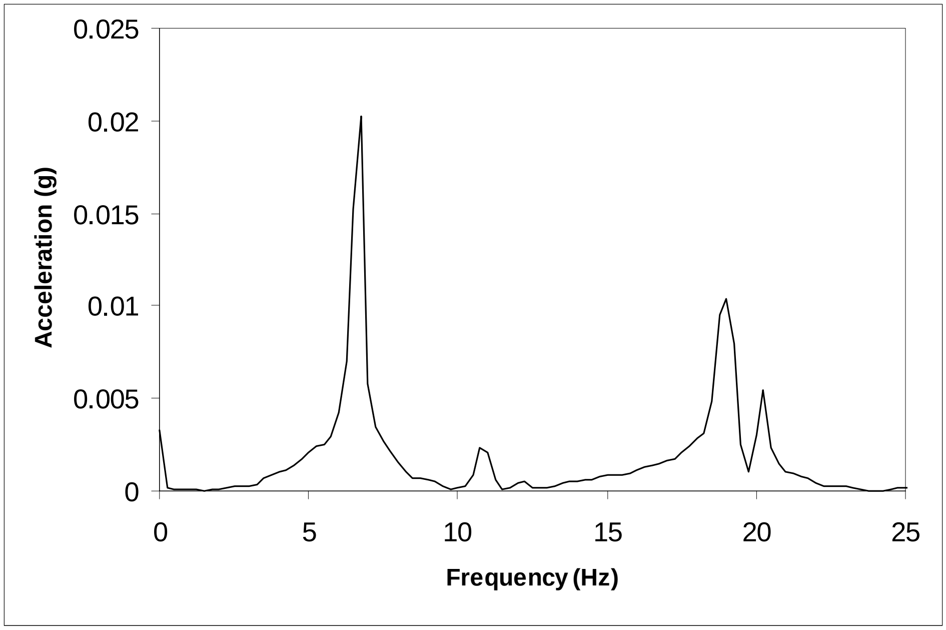

Figure C.27 – FRF Spectrum for Heel Drop Excitation for TCN 6

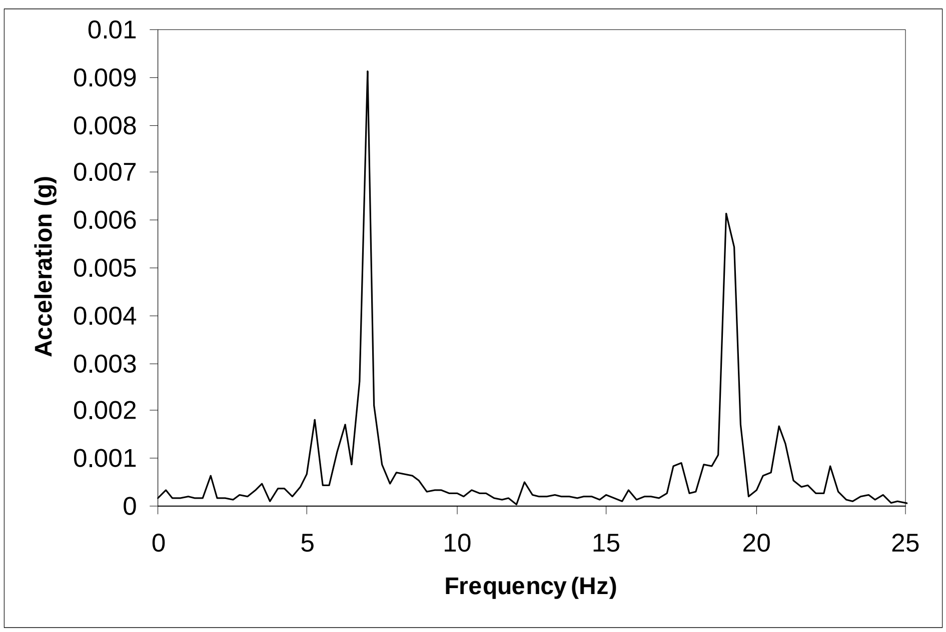

Figure C.28 – FRF Spectrum for Walking Parallel Excitation for TCN 6

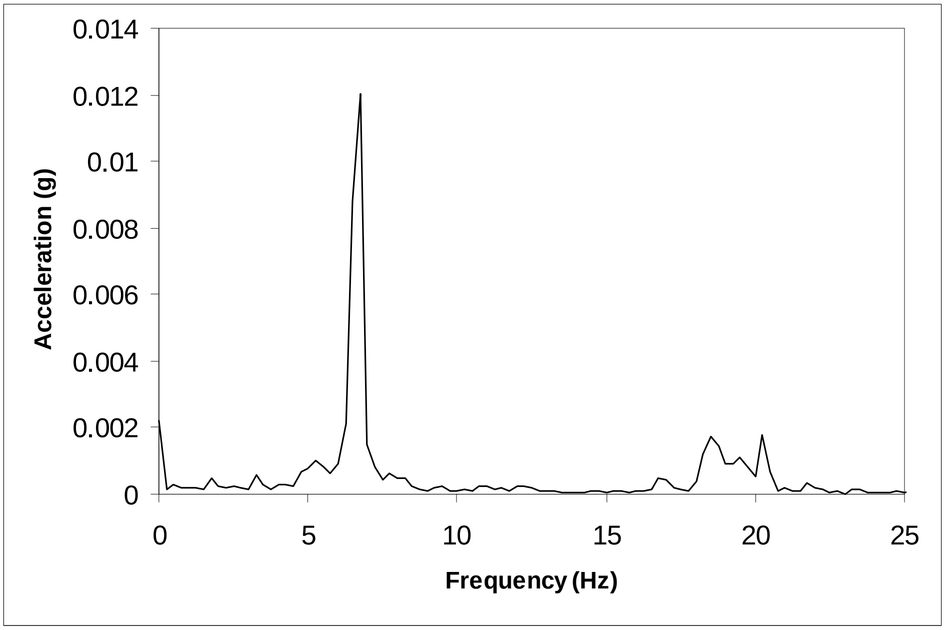

Figure C.29 – FRF Spectrum for Walking Perpendicular Excitation for TCN 6

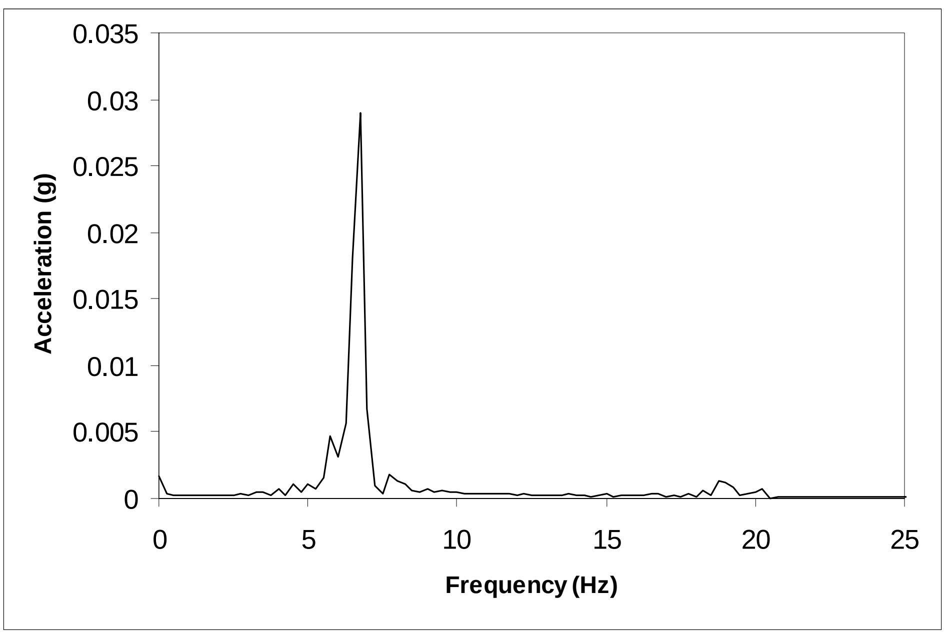

Figure C.30 – FRF Spectrum for Bouncing Excitation for TCN 6

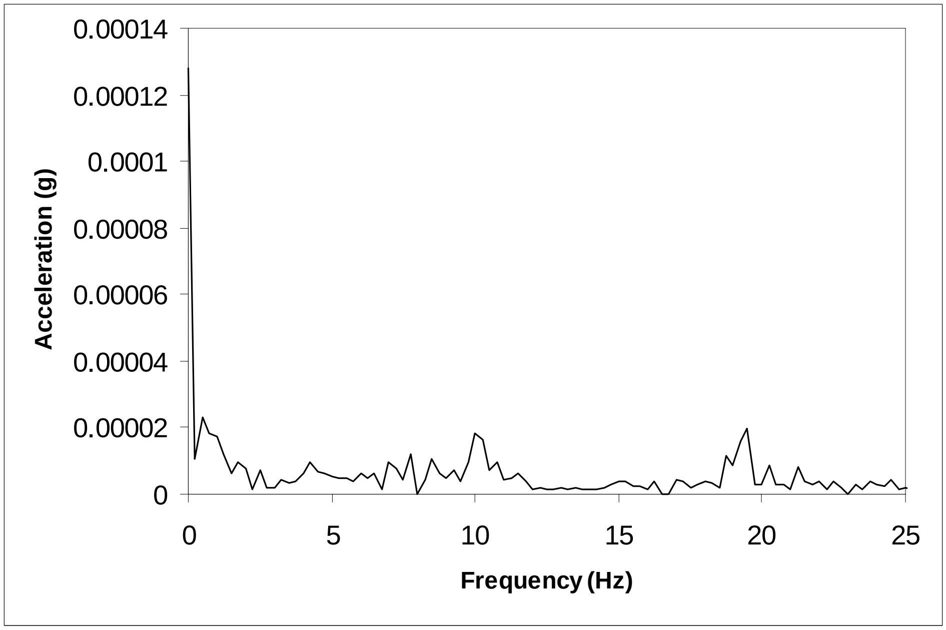

Figure C.31 – FRF Spectrum for Ambient Excitation for TCN 7

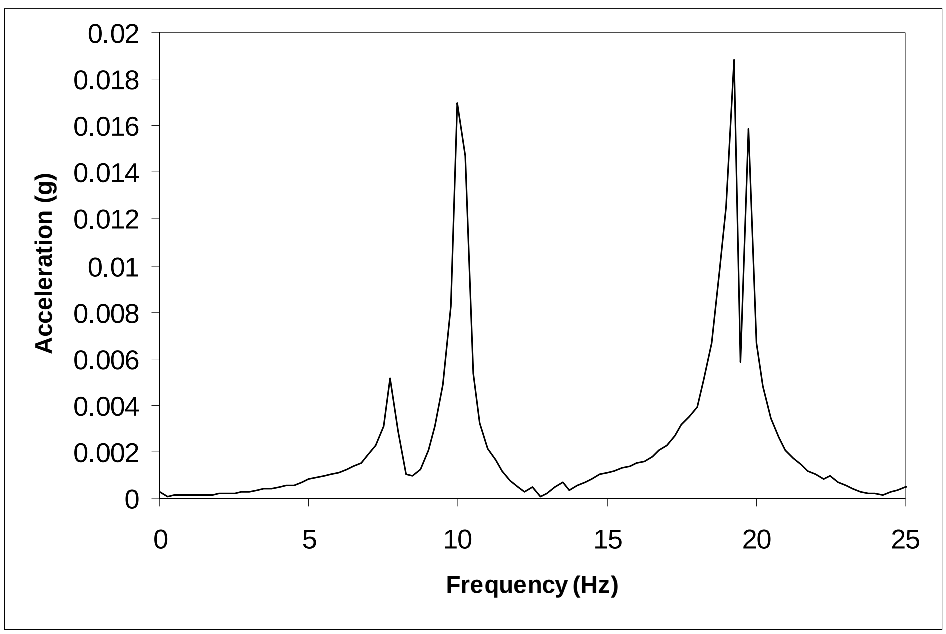

Figure C.32 – FRF Spectrum for Heel Drop Excitation for TCN 7

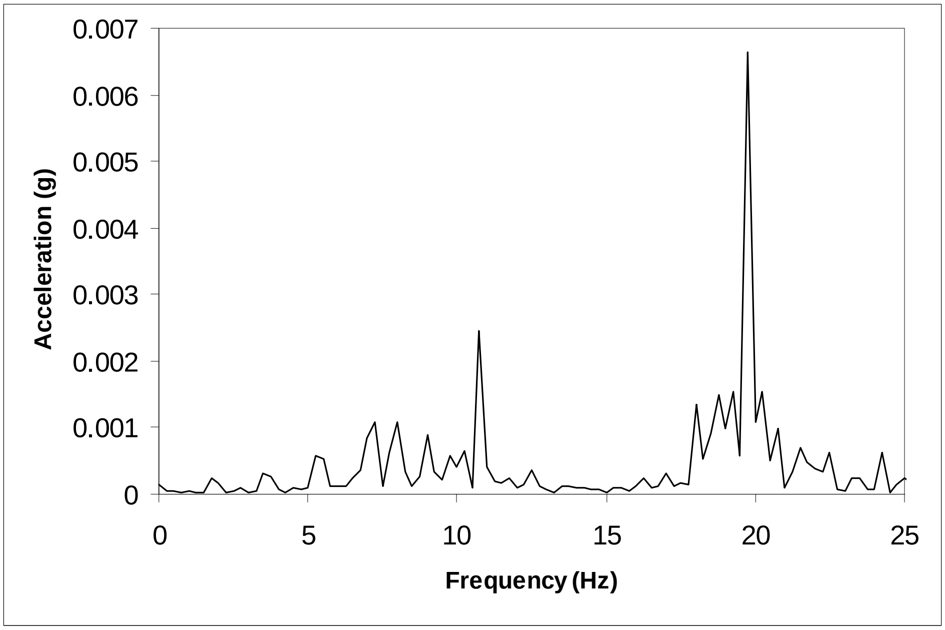

Figure C.33 – FRF Spectrum for Walking Parallel Excitation for TCN 7

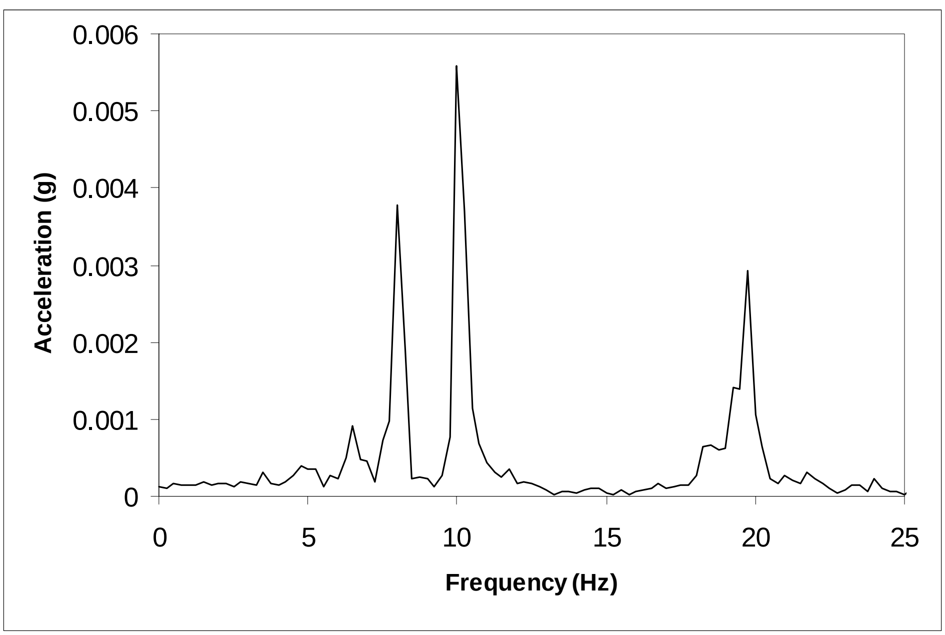

Figure C.34 – FRF Spectrum for Walking Perpendicular Excitation for TCN 7

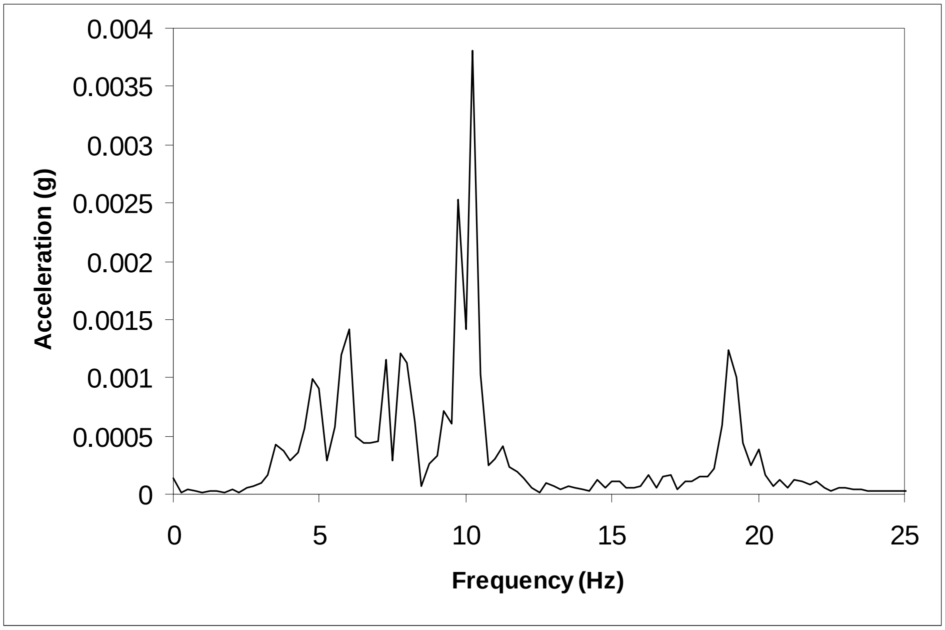

Figure C.35 – FRF Spectrum for Bouncing Excitation for TCN 7

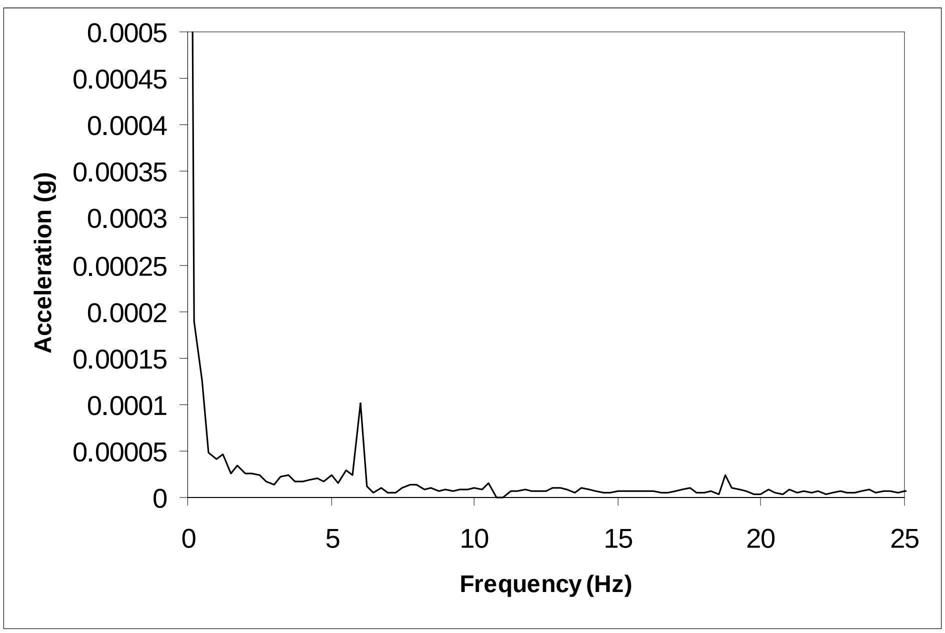

Figure C.36 – FRF Spectrum for Ambient Excitation for TCN 8

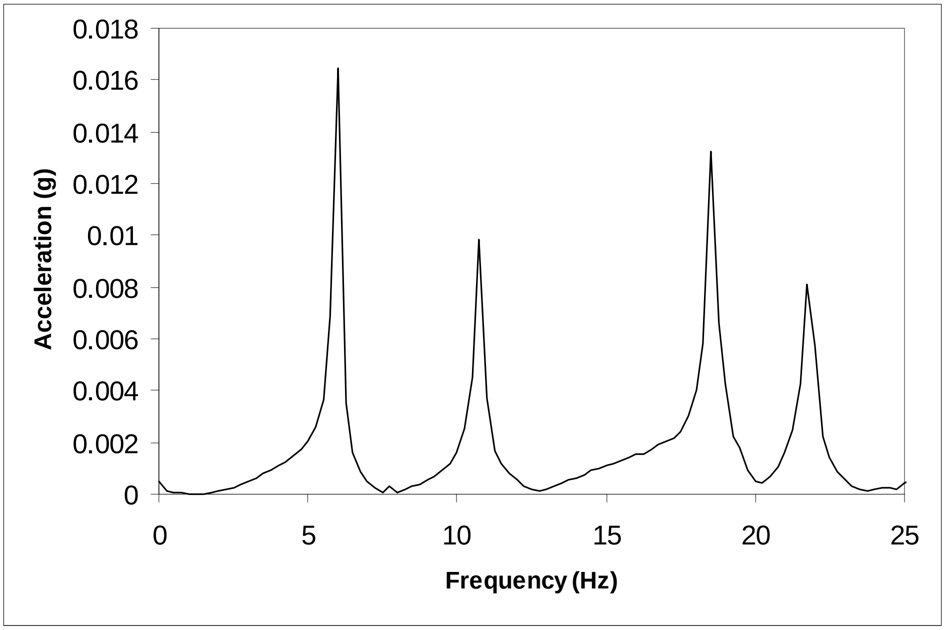

Figure C.37 – FRF Spectrum for Heel Drop Excitation for TCN 8

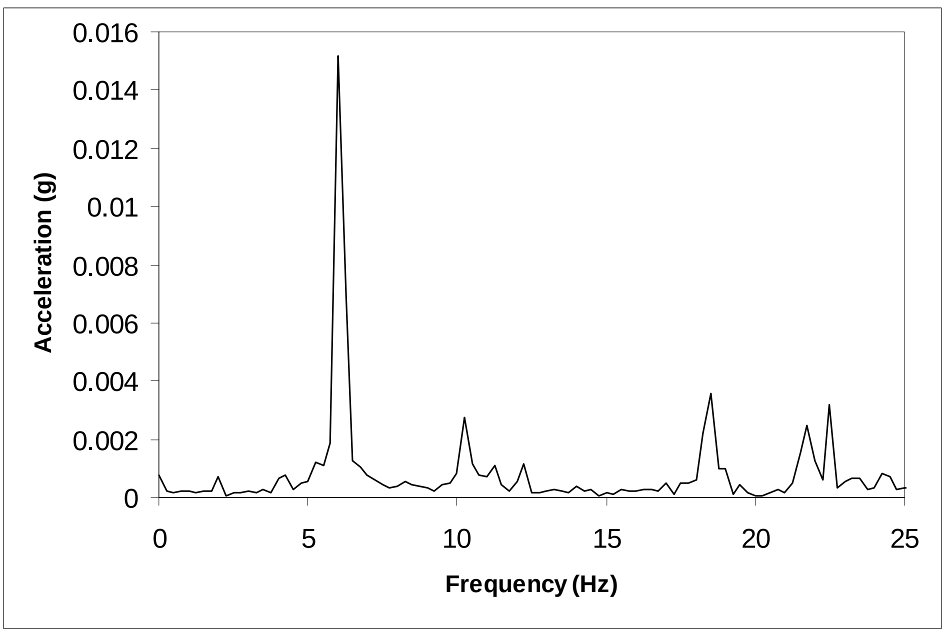

Figure C.38 – FRF Spectrum for Walking Parallel Excitation for TCN 8

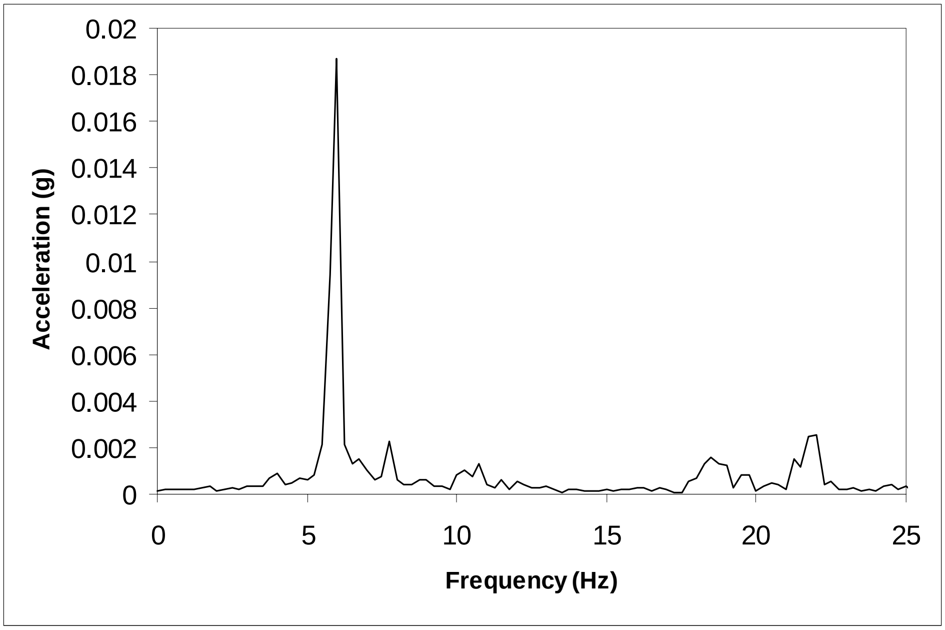

Figure C.39 – FRF Spectrum for Walking Perpendicular Excitation for TCN 8

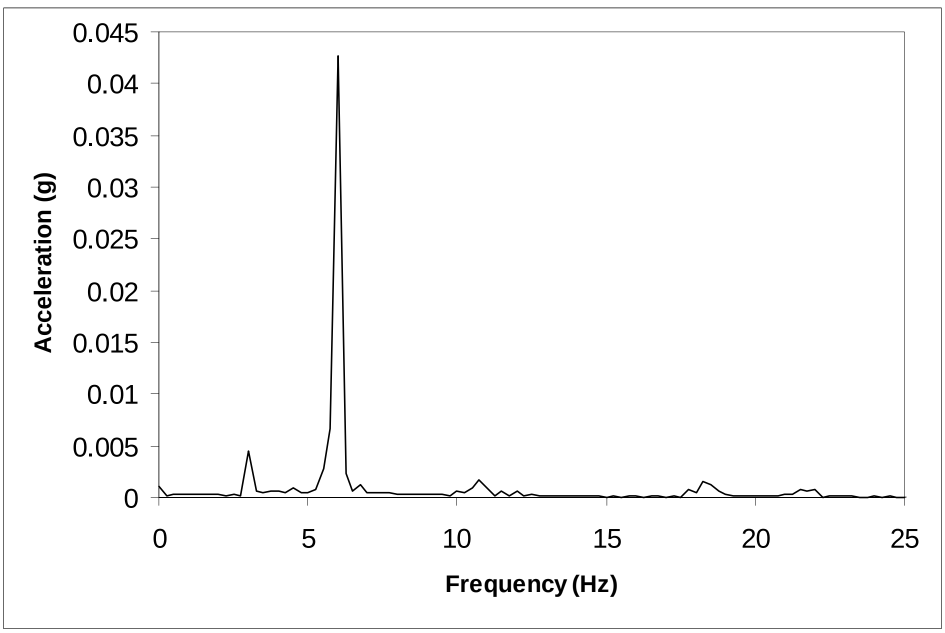

Figure C.40 – FRF Spectrum for Bouncing Excitation for TCN 8

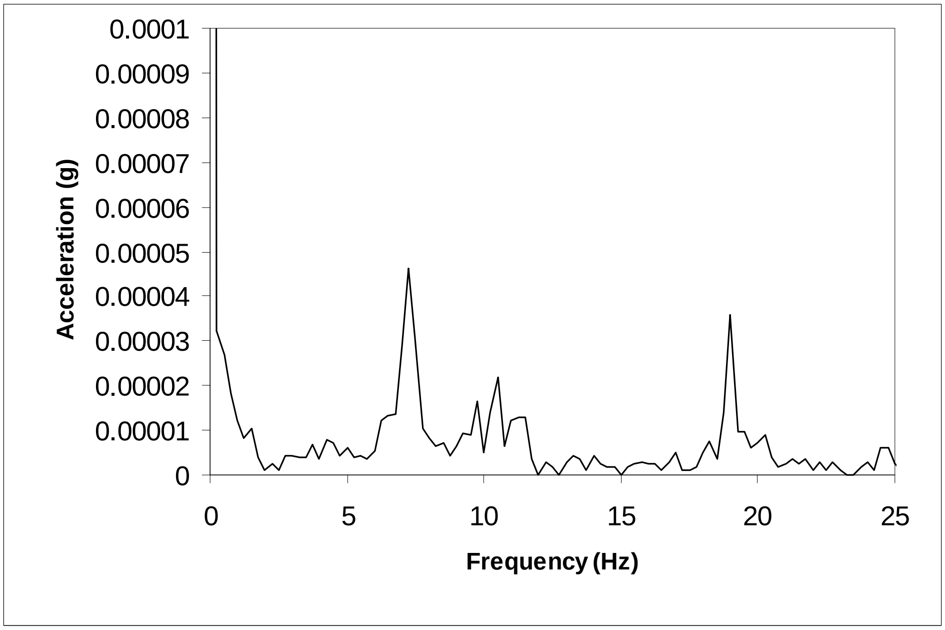

Figure C.41 – FRF Spectrum for Ambient Excitation for TCN 9

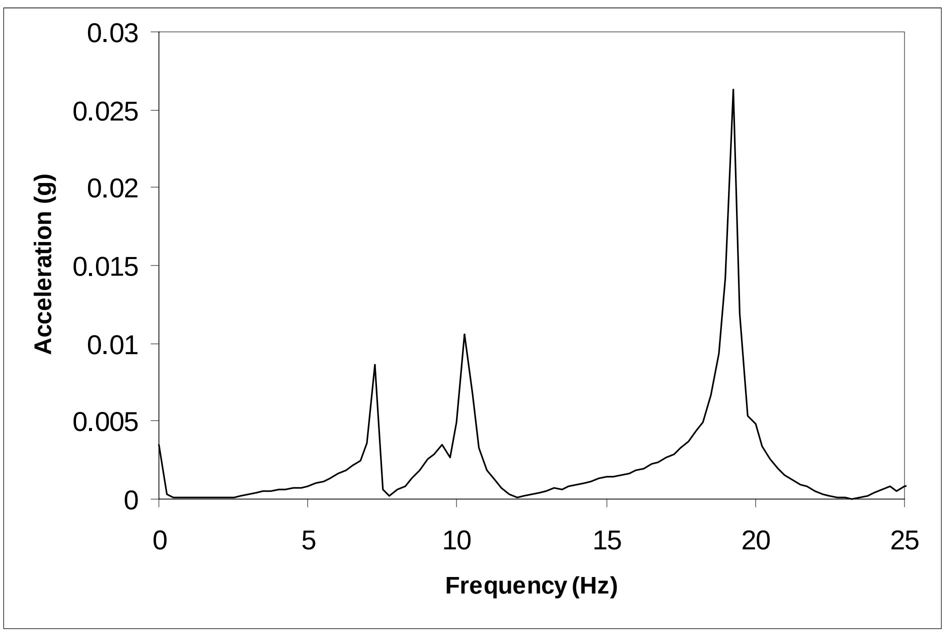

Figure C.42 – FRF Spectrum for Heel Drop Excitation for TCN 9

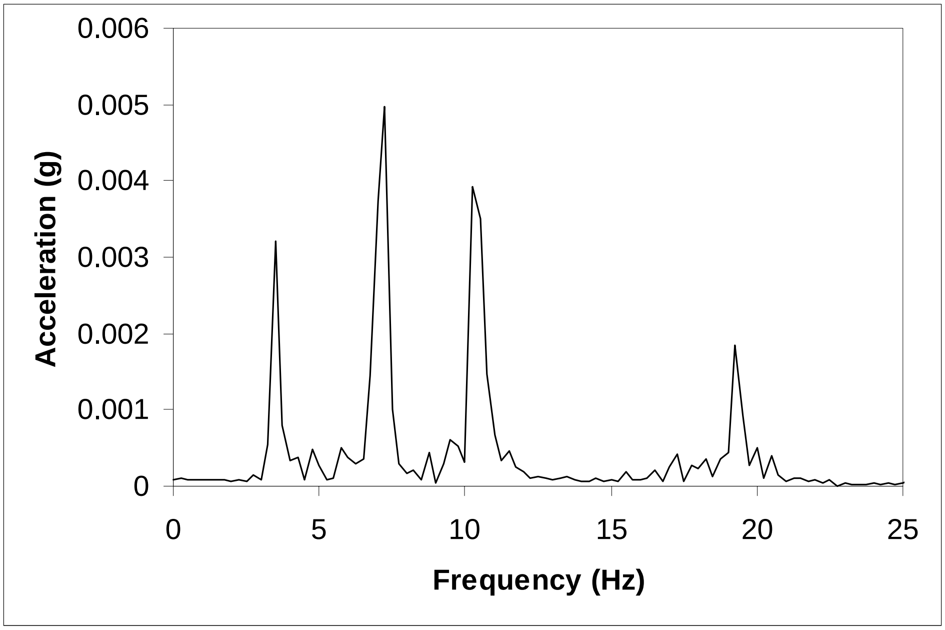

Figure C.43 – FRF Spectrum for Walking Parallel Excitation for TCN 9

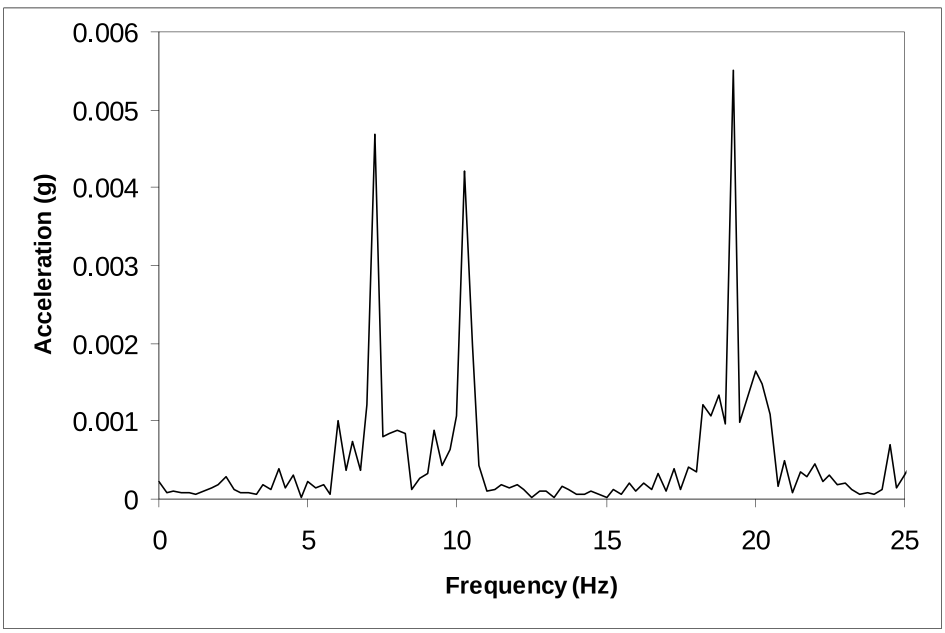

Figure C.44 – FRF Spectrum for Walking Perpendicular Excitation for TCN 9

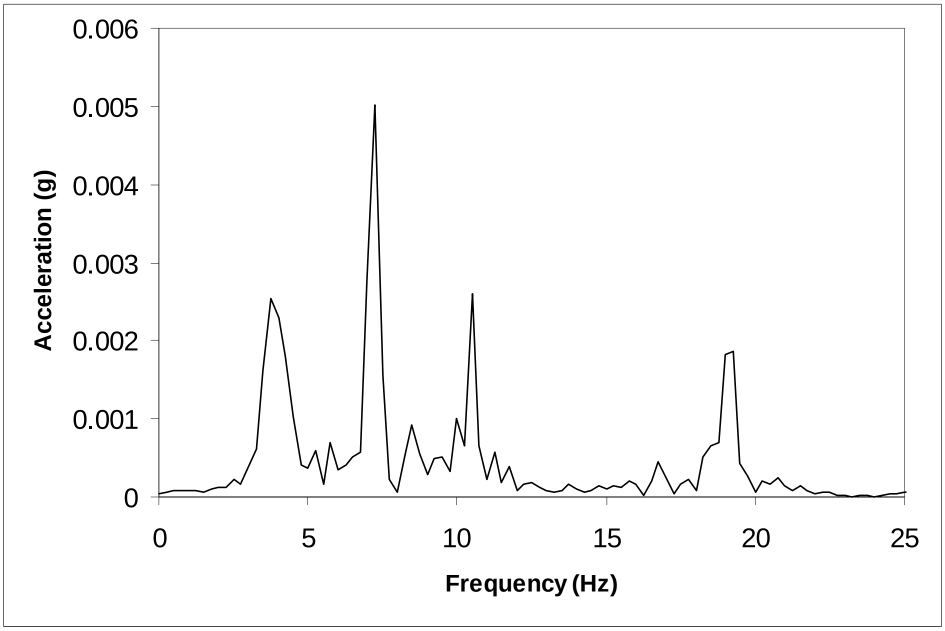

Figure C.45 – FRF Spectrum for Bouncing Excitation for TCN 9

VITA

Steven R. Alvis

Steven Robert Alvis was born June 16, 1977 in the Appalachia region of the United States in the city of Charleston, West Virginia. He graduated from Nitro High School in Nitro, WV in 1995. That summer, while waiting for college to start, he got a job working for the WV DOT doing road maintenance work which involved fun things like picking up road kill. After that summer with a first real work experience, he went to receive his BSCE degree from West Virginia Institute of Technology (which later became officially known as West Virginia University Institute of Technology). During his summers while enrolled in WV Tech, he participated in the co-op program for WVDOT doing various engineering things that never related to structures. Immediately following graduation in May 1999, he did bridge design work for a consulting company in Cross Lanes, WV known as E.L. Robinson Engineering Co. He then went on to pursue his MS degree in Structures at Virginia Polytechnic Institute and State University while working under Dr. Thomas Murray. During his stay in Blacksburg, he had a life-changing experience with God, which was the most notable and cherished event of his entire life. After his graduation, he plans to do connection design for Lynchburg Steel & Specialty Co. in Lynchburg, VA while daily pursuing a closer relationship with Jesus Christ.

Steven R. Alvis